UNIVERSITEIT VAN PRETORIA
UNIVERSITY OF PRETORIA
YUNIBESITHI YA PRETORIA

In vitro screening in cervical cancer cells of anti-cancer compounds derived from Cameroonian plants

By Angela Bona

Submitted in partial fulfilment of the requirements for the degree

MSc Genetics

Student Number: 14083117

Supervisor: Dr P Moela

Co-supervisor: Dr N October

In the Faculty of Natural & Agricultural Sciences

University of Pretoria

Pretoria

2023, 10 February

UNIVERSITEIT VAN PRETORIA
UNIVERSITY OF PRETORIA
YUNIBESITHI YA PRETORIA

Submission declaration

I, Angela Bona declare that this thesis/dissertation, which I hereby submit for the degree MSc Genetics at the University of Pretoria, is my own work and has not previously been submitted by me for a degree at this or any other tertiary institution.

Signed: 

Date: 10 February 2023

Summary

Cervical cancer is a global health challenge for women, especially in Africa, which is attributed to Human Papillomavirus (HPV) infections that are commonly mitigated by administration of HPV vaccines. Conventional treatment for advanced cervical cancers involves platinum-based chemotherapy and radiotherapy, many of which collaterally damage non-cancer cells. This warrants plants as an alternative source of novel potential pharmaceuticals with lower toxic side-effects in anti-cancer drug discovery. This motivates the aim of this research to screen 10 extracted compounds, including 3 novel compounds from various plants in Cameroon. Data regarding cell viability and cell death were obtained from various cell-based and sub-cellular assays revealing 3 novel compounds with cytotoxic and cancer-selective potentials. However, studies in additional cancer and non-cancer cell lines should be conducted before these compounds can be identified as effective leads in the expensive anti-cancer drug discovery process.

Table of Contents

List of figures

List of tables

Abbreviations

Abs -	Absorbance
AKT -	AKT serine/threonine kinase-1
APAF1 -	Apoptotic peptidase-activating factor-1
ASR -	Age-standardized rate
ATCC -	American Type Culture Collection
ATP -	Adenosine triphosphate
BAD -	BCL2-associated death promoter
BAK -	BCL2-associated agonist/killer-1
BARD-1 -	BRCA-1-associated RING domain protein-1
BAX -	BCL2-associated-X protein
BCL2 -	B-cell lymphoma-2 family protein
BCL2L -	BCL2-like protein-2
BCL2L10 -	BCL2-like protein-10
BCLX -	BCL2-like isoform X-1
BDA-366 -	BCL2-BH4 domain-antagonist-366
BH -	BCL2 homology domain/motif
BID -	BH3-interacting domain death agonist
BIM -	BCL2-like protein 11
BIR -	Baculovirus inhibitory apoptosis protein repeat domain
BIRC -	Baculovirus inhibitory apoptosis protein repeat-containing
BOK -	BCL2 ovarian killer
BRCA-1 -	*Breast cancer susceptibility gene-1*

BRCA-2 -	*Breast cancer susceptibility gene-2*
Ca^{2+} -	Calcium ions
CaSki -	Epidermoid cervical carcinoma cells
Caspase -	Cysteinyl, aspartate-specific protease
CI -	Cell index
CO_2 -	Carbon dioxide
CSCs -	Cancer stem cells
$CD4^+$ -	Cluster of differentiation-4 T-lymphocytes
CD-20 -	Cluster of differentiation antigen-20
cIAP1 -	Cellular inhibitory apoptosis protein-1
cIAP2 -	Cellular inhibitory apoptosis protein-2
CXCL-5 -	CXC motif ligand-5
DAMP -	Damage-associated molecular pattern
DCR1 -	Decoy receptor-1
DCR2 -	Decoy receptor-2
DD -	Death domain
DFFA -	*DNA fragmentation factor gene*
DFNA5 -	Deafness-associated tumour suppressor
DISC -	Death-inducing signalling complex
DMEM -	Dulbecco’s Modified Eagle’s Medium
DMSO -	Dimethyl sulfoxide
DNA -	Deoxyribonucleic acid
DSB -	DNA double-stranded break

BV6 -	Bivalent-6
E1 -	Early-1
E2 -	Early-2
E6 -	Early-6
E6AP -	E-6-associated protein
E7 -	*Early-7*
EDTA -	Ethylenediaminetetraacetic acid
E genes -	*Early genes*
EMEM -	Essential modified eagle’s medium
ER -	Estrogen receptor
FADD -	FAS-associated via death domain protein
FASL -	FAS cell surface death receptor -ligand
FASR -	FAS cell surface death receptor
FBS -	Foetal bovine serum
Fc -	Fragment crystallisable chain
FDA -	Food and Drug Administration
FITC -	Fluorescein isothiocyanate
GLOBOCAN -	Global Cancer
GPCR -	G-protein coupled receptor
HBA -	Hydrogen bond acceptor
HBD -	Hydrogen bond donor
HeLa -	Henrietta Lacks
HER-2 -	Human epidermal growth factor-2

HMGB1 - High mobility group box-1 protein

HPV - Human Papillomavirus

HR - Homologous recombination

HRT-A2 - Omi/high temperature requirement protein-A

IAP - Inhibitory apoptosis protein

IC_{50} - Half-maximal inhibitory concentration

IgG - Immunoglobulin G

IL-1 - Interleukin-1

IP3 - Inositol triphosphate-3

IR - Infra-red

L genes - *Late genes*

L1 - Late-1

L2 - Late-2

Log*P* - Octanol-water partition coefficient

Mab - Monoclonal antibody

MCF-7 - Michigan Cancer Foundation-7

MCL1 - Myeloid cell leukaemia protein-1

MDM2 - Murine double-minute-2 protein

MDM4 - Murine double-minute-4 protein

MLKL - Mixed lineage kinase domain-like protein

mTOR - Molecular target of rapamycin

MTT - 3-(4,5-dimethylthiazol-2-yl)-2,5-diphenyl tetrazolium bromide

MW - Molecular weight

NADH - Nicotinamide adenine dinucleotide

NSCLC - Non-small cell lung cancer

NMR - Nuclear magnetic resonance

NUMB - NUMB endocytic adapter protein

OMM - Outer mitochondrial membrane

OR - Oestrogen receptor

PALB2 - Partner and localizer of BRCA-2

PBS - Phosphate-buffered saline

PI - Propidium iodide

PI3K - Phosphatidylinositol-3 kinase

PMAIP1 - Phorbol-12-myristate-13-acetate-induced protein-1

PR - Progesterone receptor

PS - Phosphatidylserine

PUMA - Protein-53-upregulated modulator of apoptosis

QSAR - Quantitative structure-activity relationship

RCD - Regulated cell death

rhTRAIL - Recombinant human TNF related apoptosis-inducing ligand

RIPK1 - Receptor-interacting protein kinase-1

RNA - Ribonucleic acid

ROS - Reactive oxygen species

RTCA - Real-time cell analysis

RT-qPCR - Reverse transcriptase quantitative polymerase chain reaction

SANCR - South African National Cancer Registry

SD -	Standard deviation
SERM -	Selective estrogen receptor modulators
SI -	Selectivity index
SMAC -	Second mitochondrial activator of caspases
SMILES -	Simplified Molecular Input Line Entry System
tBID -	Truncated BH3-interacting domain death agonist
TM -	Transmembrane domain/motif
TNBC -	Triple-negative breast cancer
TNF -	Tumour necrosis factor
TNFα -	TNF-alpha
TNFRSF1A -	TNF-receptor superfamily member-1A
TNFRSF10A -	TNF-receptor superfamily member-10A
TNFRSF10B -	TNF-receptor superfamily member-10B
TPSA -	Topological polar surface area
TP53 -	Tumour protein-53
TRAs -	TNF-related apoptosis-inducing ligand-receptor agonists
TRADD -	TNFR1-associated via death domain protein
TRAIL -	TNF-related apoptosis-inducing ligand
TRAILR1 -	TNF-related apoptosis-inducing ligand receptor-1
TRAILR2 -	TNF-related apoptosis-inducing ligand receptor-2
UBC -	Ubiquitin-conjugating enzyme
USA -	United States of America
VEGF -	Vascular endothelial growth factor

VLP - Virus-like particles

XIAP - X-linked inhibitory apoptosis protein

βE - 17 beta (β)-estradiol hormone

Abstract

Cervical cancer is a public female health burden, especially in Africa, and is mainly caused by infection with HPV in which unvaccinated cases allow the development of malignancy and ultimately angiogenesis and metastasis. Apoptosis, which is often evaded in cancer, is a popular targeted mechanism of current and potential anti-cancer drugs. However, cytotoxic cervical cancer therapies, such as platinum-based chemo- and radiotherapy, also elicits non-selective and systemic toxicity and temporarily subdues advanced cancers into remission with unexpected relapse. In addition, treatments utilizing an apoptotic anti-cancer approach induce necrosis concomitantly which result in inflammatory side-effects. This necessitates the screening of alternative treatment regimens, such as plant secondary metabolites and their various combinations for discovery of new anti-cancer compounds or unprecedented anti-cancer potentials of old compounds. Therefore, compounds isolated from four Cameroonian plants, namely *Cassia arereh*, *Distemonanthus benthamianus*, *Echinops gracilis* and *Rhabdophyllum affine*, were screened for their individual cytotoxicities against cervical cancer cells. Compounds that showed sufficient anti-cancer and cancer-selective potentials were then further studied in combination. Initial screening revealed a terpenoid and flavonoid isolated from *C. arereh* (CAE21) and *E. gracilis* (EGF25), respectively. CAE21 and EGF25 induced strong apoptotic responses especially in combination with no necrotic response. In addition, CAE21 showed optimal oral bioavailability *in silico*, although EGF25 did not show the same drug-likability. CAE21 and EGF25 also demonstrated molecular bioactivities of 0.18 and 0.14 as GPCR and nuclear receptor ligands, respectively. Despite the demonstrated anti-cancer potential of CAE21 and EGF25, reproducible effects in more biological cancer models and further elucidation of apoptotic and molecular mechanisms are needed.

1 Introduction

Cervical cancer is a global-health issue affecting women and health care. To address this, clinicians have used various treatment strategies such as the combination of paclitaxel and platinum-based chemotherapy. Although platinum-based drugs remain the standard for cervical cancer treatment, this conventional chemotherapy still presents with off-target toxic side-effects, leading to a consideration of combining conventional chemotherapy with medicinal plant compounds since they are generally more tolerable and therefore present with less side effects.

However, research involving chemotherapy and plant medicine combinations is in the pre-clinical stages, especially combinations of pure natural compounds. This also warrants clinical study of plant secondary metabolites and their potential synergistic combinations, which could reduce the dosages needed when used together. This may also begin to reveal hidden holistic anti-cancer properties of the plants themselves when plant extracts containing multiple are consumed.

Therefore, this study aims to screen active compounds isolated from Cameroonian plants for cytotoxicity against an *in vitro* cervical cancer model. Cytotoxicity in cancer and non-cancer cells will also assess cancer cell selectivity of compounds. Compounds showing anti-cancer potential will be studied in combination for their down-stream apoptotic effects.

1.1 Cervical cancer

Cervical cancer is a malignant pathology that progresses in the inner- and outer epithelial linings of the cervix in the female reproductive system.[1] The endocervix is lined with columnar epithelial cells, whereas the ectocervix as well as its neuroendocrine glands are covered with squamous epithelium, which are often vulnerable to persistent HPV (Human Papillomavirus) infection that often progresses to cancer if left untreated.[1-2] Cervical carcinomas may remain *in situ* or invade tissues past their basal barrier in the absence of a treatment intervention.[1] These carcinomas exist in various histopathological forms, namely squamous carcinomas, adenocarcinomas, adenosquamous carcinomas and neuroendocrine malignancies.[1]

1.1.1 Cervical cancer epidemiology

According to Sung *et al*, cervical cancer was the fourth most prevalent malignant condition and cause of cancer-related mortality in women on a global scale.[3] Global cancer (GLOBOCAN) statistics calculated that 604 000 novel cases and 342 000 fatalities were reported globally in 2020.[3] In comparison to other regions of the world, Africa and Asia suffer the greatest prevalence and mortality rate with increased statistics in Southern Africa.[4] In particular, Swaziland had the highest incidence estimated during the GLOBOCAN consensus in 2018.[4] Southern Africa had a cervical cancer incidence rate of 36.4 per 100 000 people and fatality rate of 20.6 per 100 000 people annually.[3] This was the second highest incidence rate and third highest mortality rate per 100 000 people.[3]

Based on statistics from the South African National Cancer Registry (SANCR) in 2014, cervical cancer is the third most frequently diagnosed carcinoma, with an incidence age-standardized rate (ASR) of 22.56 per 100 000 women of all races.[5] The incidence ASR is the highest within the black female population group of South Africa (27.01 per 100 000 people), with coloured women ranking second (13.72 per 100 000 people), white females third (13.10 per 100 000 people) and Asian women fourth (9.98 per 100 000 people).[5] GLOBOCAN statistics collected in South Africa for 2018 suggests that cervical cancer incidence increased to 43.5 cases per 100 000 people with an ASR of 19.2 deaths per 100 000 people.[6]

1.1.2 Causes of cervical cancer

The majority of non-hereditary cases of cervical cancer in women are attributed to persistent infection with HPV.[1,7,8,9] However, not all HPV types cause malignancy.[1,8] HPV types 16, 18, 31, 33, 45, 52 and 58 are known to be the most carcinogenic, whereas types 6, 11 and 40 have very low carcinogenic potential and are considered low-risk.[1,8,10-11]

Other behavioural and environmental factors play a role in the aetiology of HPV infection and the development of cervical cancer.[1,12-14] Consumption of hormone contraceptives in young women is associated with premalignant cervical tumours and prolonged use increases the malignant potential of these lesions.[12] Oral contraceptives contain the 17 beta (β)-estradiol hormone (βE), which takes the endogenous form as found in the reproductive system.[15] Exogenous administration of βE increases the expression of *early-6* (*E6*) and *early-7* (*E7*) HPV oncogenes in cervical cancer cells transformed with HPV 16 and 18.[16] HPV 16 E6, E7 and HPV 18 E6 oncogenes also increase the expression of estrogen receptor-alpha (ERα) whereas E6 from HPV 16 and 18 up-regulate estrogen receptor-beta (ERβ).[16] Both E7 oncogenes from HPV 16 and 18 genomes promote the nuclear localization of estrogen receptors (ERs).[16] In addition, evidence suggests that a young age of becoming sexually active, usually under the age of 18, and having a multitude of coital partners increases the cervical cancer risk.[1,17] This is most likely due to an increased chance of HPV contraction as a sexually transmitted infection.[1]

Other lifestyle factors include primary and secondary tobacco smoking.[12,18] In a study of a population of Australian women aged 30-44 years, it was found that smoking 5 cigarettes per day increased the prevalence of benign cervical neoplasia with malignant potential.[12] Increasing usage to more than 5 cigarettes per day showed a stronger correlation to the progression from benign to invasive cervical tumours.[12] This is likely because of the immunosuppressive effect of tobacco smoking on cell-mediated immunity, which increases the susceptibility to HPV-infection of the cervical epithelium.[19-20] Evidence suggests that the specialized antigen-presenting Langerhans cells are mainly affected.[19]

1.1.3 HPV infection and cervical malignant transformation

HPV targets the basal epithelium tissue often during injury to the superficial epithelial layers in the uterine cervix.[10] HPV deoxyribonucleic acid (DNA) is transferred from virus capsid to host cell nucleus as free DNA molecules or episomal plasmids that can self-replicate.[10] However, the virus hijacks the host's replicative machinery during basal to squamous epithelial cell differentiation.[10] This normally terminates in cell aging or cell death, but during HPV infection, viral genes *E6* and *E7* encode proteins that continue the cell cycle and prevent cell death, allowing the production of thousands of HPV genomes.[10] HPV DNA begin to express late-1 (L1) and -2 (L2) genes that result in the capsid formation of HPV virions in the semi-differentiated cervical epithelium that once terminally differentiated, viruses are released and spread.[10] This cycle continues during general HPV pathogenicity of the cervical tissue.[9]

High-risk HPV episomally expresses more oncogenic forms of E6 and E7 that persistently inhibit the activities of important tumour suppressor proteins, namely tumour protein-53 (TP53) and retinoblastoma (RB) family proteins.[9] This permits progression of the cell cycle despite accumulation of many genetic mutations that ultimately leads to malignant transformation.[9] Viral integration in the host's genome may accompany episomal expression, which also results in the deletion or dysfunction of viral *early gene 1* (*E1*) and *2* (*E2*) that control E6 and E7 expression.[9] However, HPV type 16 cancer cell lines with sole viral episomal expression have been reported.[21]

1.1.4 HPV vaccines used to prevent cervical cancer

Due to the fact that cervical cancer is commonly caused by HPV infection, vaccination is a common preventative strategy.[1] The most recent marketed vaccines, Gardasil®, Gardasil9® and Cervarix™ were synthesized using L1 virus-like particles (VLP).[11] These are self-assembled viral capsules containing L1 proteins mainly produced in genetically-modified eukaryotes.[11,22] To achieve this, plasmid constructs containing the *L1* gene code are cloned and amplified in a vector organism, linearized using restriction enzyme technology and inserted into the genome of a competent organism, such as yeast.[22] L1-VLPs are not infectious as they do not contain the HPV genome.[11]

Different HPV types have different genotypes of *L1* genes, naturally containing capsid proteins specific to different low and high-risk HPVs allowing broad-spectrum coverage in multivalent vaccines.[23] For example, Cervarix™ was a bivalent vaccine that was designed with L1 VLPs from type 16 and type 18 HPVs.[11] Gardasil® and Gardasil9® have more broad-spectrum immunogenicity as they include L1 proteins from HPV 6, 11, 16 and 18 with Gardasil9® additionally including HPV 31, 33, 45, 52 and 58.[11] Gardasil® and Cervarix™ vaccines have been shown to illicit a strong memory B cell response and engagement of HPV-specific immunoglobulin G (IgG) antibodies.[24]

1.2 Cell death, cell aging and cancer

Cell death has many different forms with diverse regulatory mechanisms with intricate interconnection between their various pathways.[25] Cancer cells have evolved to evade cell death due to deregulated signalling from enhanced expression of oncogenic proteins or loss of tumour suppressor function.[26] As a result, defective cell death promotes increased tumour growth and resistance to the killing effect of anti-cancer therapy.[26]

There are other non-fatal cell fates that eventually lead to the cell's demise.[25] An example is the process of cell aging known as senescence, by which a cell loses its ability to reproduce yet remains metabolically and physiologically viable.[25] Senescence is characterized by increased cellular size, loss of cell growth and mitosis, damage by reactive oxygen species (ROS) and cumulative shortening of the chromatin ends (telomeres) after excessive cycles of DNA replication.[25] Senescent cells secrete pro-inflammatory chemo- and cytokines that recruit an immune response to remove aged cells to maintain tissue homeostasis and function.[25,27-28] Senescent cytokines recruit cluster of differentiation-4 ($CD4^+$) T-lymphocytes to mediate phagocytic removal of old cells by monocytes and/or tissue macrophages.[27] However, secretions from senescent cells may promote oncogenesis in pre-malignant tumours, especially if immune clearance is suppressed.[27]

1.2.1 Modes of cell death

Cell death occurs via diverse mechanisms, mainly summarized as regulated or non-regulated forms.[25] Regulated cell death (RCD) is initiated by cell signalling involving many molecules in and around the cell and can be modulated by exogenous drugs and genetic factors.[25] This is exploited in anti-cancer treatment to reduce neoplastic growth and sensitize resistant cancer cells to traditional therapy.[26,29] Many forms of RCD play a role in normal physiological processes, such as anatomical pre- and post-natal development as well as tissue homeostasis.[25,30-32] For example, the cells forming the inter-digital webs of mammalian embryos are removed by RCD.[30] Regulated modes of cell death also occur as a stress response to cellular insults.[25] In worst cases, cells are spontaneously killed before they even initiate a suicidal response by direct injury resulting in cell lysis and subsequent release of its contents.[25] This is known as accidental- or lytic cell death.[25]

Dying cells release a multitude of molecules, which may either exasperate or relieve diseases like cancer, in the tissue microenvironment.[25] Within the various types of cell death mechanisms, there are also several subtypes with characteristic molecular pathways such as apoptosis, necrosis, autophagy and necroptosis.[25] However, communicating molecules from one mode of cell death may exhibit cross-talk with another causing overlap between RCD and non-regulated cell death.[25]

1.2.1.1 Apoptosis

Apoptosis is a mode of programmed RCD orchestrated by protein-digesting enzymes called cysteinyl, aspartate-specific proteases (caspases).[33] Caspases are sequentially activated by auto-lytic cleavage of inactive precursor proteins, culminating in stimulation of effector proteases that disintegrate the cell from the inside.[26,34] Apoptosis follows rapid clearance of apoptotic cells, debris and pro-inflammatory substances by phagocytosis.[25,35] This surveillance mechanism is called efferocytosis and is signalled by the externalization of phosphatidylserine (PS) on the outer membrane of dying cells to aid phagocyte recognition.[25-26] However, if the rate of apoptosis far exceeds the rate of efferocytosis or if efferocytosis is absent, apoptosis will progress to more damaging forms of cell death.[34,36]

1.2.1.2 Autophagy

Autophagy is a RCD mechanism in which a cell digests itself to recycle nutrients during metabolic starvation.[25,37] This is initiated when normal proliferative activity is low.[38] Lysosomes are membrane enclosed “sacs” in the cell that contain digestive enzymes associated with the regulation of autophagy.[39] Lysosomal membranes fuse with a double-membranous vacuole known as the autophagosome, in which the contents are exposed to digestive enzymes namely hydrolases.[39] Hydrolases digest misfolded protein aggregates and defective organelles absorbed by the autophagosome.[39] Although autophagy reduces malignant cell numbers, it plays a contradictory role in the disease progression of cancer.[37-38] Some autophagic regulators act as tumour suppressors by repressing the effect of other enzymes on the expression of oncogenes and the activity of their products.[38] In contrast, autophagy may sustain cancer cell growth by recycling nutrients, such as amino acids, which feeds adjacent malignant cells.[37]

1.2.1.3 Necrosis

Necrosis, on its own, occurs due to severe cellular blows such as direct tissue injury, infection, extreme temperatures, glucose deprivation and intense loss of oxygen or hypoxia.[40-41] Whether passive or regulated, necrosis leads to cellular- and mitochondrial swelling, cell membrane lysis due to loss of membrane integrity and rupture of lysosomes causing all cellular contents to leak out into the microenvironment.[40] Usually cancer growth exceeds the rate at which blood vessels are synthesized towards areas of newly divided neoplastic cells (angiogenesis), causing a hypoxic microenvironment.[42] This induces necrosis and accelerates its pro-inflammatory repercussions.[42]

1.2.1.4 Necroptosis

Necroptosis shares morphological characteristics with necrosis as it also culminates in rupture of the plasma membrane.[43] However, it resembles apoptosis in its molecular mechanism, but occurs independently of caspases.[43] The signal transduction pathway in necroptosis relies on the phosphorylation of mixed lineage kinase domain-like (MLKL) protein by receptor-interacting protein kinase-1 (RIPK1).[44] MLKL is a pseudokinase that requires activation by RIPK1, sending MLKL to the inner layer of the cytoplasmic membrane where it disrupts the integrity of the lipid bilayer.[44] The downstream loss of membrane permeability results in the leakage of cytosolic molecules that initiate or potentiate inflammation in the extracellular space.[45]

Molecules released from necrotic or necroptotic cells are called damage-associated molecular patterns (DAMPs) and have the potential to elicit an inflammatory response that collaterally damage proximal cells.[25,33,46] An example of these DAMPs is high mobility group box-1 (HMGB1) nuclear protein which belongs to the high mobility group of proteins.[41,47-48] HMGB1 is a DNA-binding protein that organizes chromatin and regulates chromatin structure the transcription of genes involved in DNA repair, RNA transcription and telomere upkeep.[49] HMGB1-mobilization in response to tissue hypoxia increases mitochondrial replication, vascularisation and increased blood flow towards ischemic areas of carcinomas.[41,50] This enhances the metabolic, invasive and metastatic potential of malignant cells due to access to the circulatory system allowing migration to other organs of the body.[41]

1.2.2 Apoptosis and cancer

Apoptosis followed by efficient efferocytosis bypasses secondary necrosis and avoids its secondary inflammatory effects *in vivo*.[35-36] However, when HMGB1 is released from lysing cells it promotes cancer cell growth when released into the tumour microenvironment.[41] In contrast, apoptosis followed by efficient efferocytosis does not promote tumour angiogenesis unlike its lytic counter-part.[51] This is why apoptosis is the desired therapeutic mode of action against cancer cells.[35]

Apoptosis occurs in two ways, namely the intrinsic and extrinsic pathways.[52] The extrinsic pathway relies on ligands that interact with their receptors on the extracellular surface of the cell membrane.[52] This prompts the formation of a multi-protein complex that initiates a series of caspase activations.[52] The intrinsic pathway, also known as the mitochondrial-dependent pathway, is activated in response to internal stress stimuli and mainly involves modulators in the mitochondria.[52] Both pathways involve caspases that eventually result in the activation of the executioner caspases responsible for the morphological changes in the final phase of apoptosis.[52]

However, caspases need to be regulated so that healthy cells are not inappropriately killed.[26] Cancer cells hijack this mechanism to resist cell death.[26] Caspase suppressors include the inhibitory apoptosis proteins (IAPs) that block their proteolytic activity or promote their degradation.[26,53-54] IAPs act as E3 ligase enzymes that flag the caspases with ubiquitin, prompting their selective degradation in the proteosome when apoptosis is not needed.[54] IAPs are often over-active in breast and cervical cancers, promoting resistance to pro-apoptotic agents.[55-57]

1.2.2.1 Extrinsic Apoptosis

Extrinsic apoptotic signalling begins with extracellular ligand-receptor interactions.[52] The receptors involved belong to the tumour necrosis factor (TNF) superfamily and includes the FAS cell surface death receptor (FASR), TNF receptor superfamily member-1A (TNFRSF1A), 10A (TNFRSF10A) and 10B (TNFRSF10B), TNF-related apoptosis-inducing ligand receptor-1 (TRAILR1/DR4) and 2 (TRAILR2/DR5).[25,52] Transcription of TNF receptor genes are initiated by an important tumour suppressor, tumour protein-53 (TP53), activated during DNA damage signalling.[58-59] Loss of TP53 activity or steady-state levels is a prevalent oncogenic event in most malignancies.[59]

The FAS ligand (FASL) and TNF-related apoptosis-inducing ligand (TRAIL) induce death receptor signalling upon disturbances in the extracellular space.[25] The ligated FASR or TRAILRs engage their intracellular death domains with special adapter proteins that assemble to produce the death-inducing signalling complex (DISC).[25] However, TNF decoy receptors inhibit ligand-mediated apoptosis by sequestering TRAIL and FASL from DR4 and 5 without engaging downstream molecules due to lack of a death domain.[60] Ligand decoys, such as decoy receptor-1 (DCR1) and 2 (DCR2) are normally epigenetically inactivated.[60] When abnormally over-expressed in cancer, decoy receptors confer resistance to extrinsically-induced apoptosis.[60] Epigenetics is the upstream regulation of transcription by chemical modifications of DNA while preserving the genetic code.[61]

DISC processes caspase-8, which then up-regulates executioner caspase-3, 6 and 7 by proteolytic cleavage of their immature procaspases.[25-26] BH3-interacting domain death agonist (BID) is also cleaved by caspase-8, resulting in a truncated protein (tBID).[25] The protein, tBID, localizes in the mitochondria where it regulates molecules involved in intrinsic apoptosis.[25] This results in the co-activation of the intrinsic pathway, which occurs simultaneously to extrinsic apoptosis.[26]

1.2.2.2 Intrinsic Apoptosis

Intrinsic apoptosis occurs in response to several internal and external perturbations.[25] These include hypotrophy, hypoxia, deleterious DNA lesions, replication or mitotic stress, excess mitochondrial calcium ions (Ca^{2+}), endoplasmic reticulum stress, over-accumulation of ROS and oxidative damage to membranes.[25,52,62] Intrinsic apoptotic signalling mainly occurs in the mitochondria and is tightly regulated by a plethora of proteins.[25]

ROS-induced damage such as lipid peroxidation to the outer mitochondrial membrane (OMM) disrupts the membrane potential between the mitochondria and cytoplasm.[52] tBID positively regulates the B cell lymphoma-2 family protein (BCL2)-associated-X (BAX) and BCL2-associated agonist/killer-1 (BAK) proteins, which increase the permeability of the OMM.[25] This leads to the mitochondrial release of a special molecule that acts as an electron transporter involved in ATP synthesis for cellular respiration (cytochrome c).[25] Cytosolic cytochrome c then couples with apoptotic peptidase-activating factor-1 (APAF1), producing an activated complex called the apoptosome.[25,52] The apoptosome mediates the cleavage of procaspase-9, resulting in caspase-9-activation of the executioner caspase-3, 6 and 7.[26,52] During malignant development, caspase-3, 7 and 9 are disabled by a potent IAP known as X-linked IAP (XIAP).[63-64]

In the case of irreparable DNA damage, acetylation of TP53 prevents its proteosomal degradation, mediated by the oncogenic proteins murine double minute-2 (MDM2) and 4 (MDM4).[58,65-66] Acetylation is the process by which acetyltransferase enzymes add an acetyl group to specific residues of selected proteins.[67] Activated TP53 facilitates transcription of genes encoding BCL2 family proteins.[58] TP53 target genes include protein-53-upregulated modulator of apoptosis (PUMA) and BID.[58,68] PUMA and BID communicates with messengers in the mitochondria of the intrinsic pathway to further propagate cell death signalling.[58,68]

1.2.2.3 The execution phase of apoptosis

Activation of caspase-3, 6 and 7 prompts the common execution phase of apoptosis by cleaving many biological substrates.[26,52] One of the downstream effectors is the *DNA fragmentation factor gene* (*DFFA*) to which caspase-3 binds directly, initiating DNA fragmentation commonly observed in the nuclei of apoptotic cells.[52] Caspases are pleiotropic factors that promote an inflammatory microenvironment by inducing necrosis in other cells.[25,52] For example, caspase-3-mediated cleavage of the deafness-associated tumour suppressor (DFNA5) protein results in necrosis, although being initiated by apoptotic signalling.[34]

1.2.3 BCL2 family proteins and apoptosis regulation in cancer

The BCL2 family proteins are apoptotic regulators encompassing death-promoting and -suppressing modulators, closely associated with the mitochondrial pathway of apoptosis.[69] Pro-apoptotic proteins promote OMM permeability, allowing the release of cytochrome c required for apoptosome assembly.[69] On the other hand, anti-apoptotic proteins bind to and inhibit pro-apoptotic proteins, preventing permeabilization of the OMM.[26]

The function of BCL2 family modulators is determined by protein-protein interactions between four homologous regions of amino acid sequences known as BCL2 homology (BH) domains.[26] The content of BH motifs show similarities and differences between members and determines their functions.[26,69] BCL2 molecules are characterized into 3 separate classes according to the content of BH domains: multi-domain anti- and pro-apoptotic proteins as well as single domain pro-apoptotic proteins.[26] Multi-domain BCL2 members have a transmembrane domain at the end of their protein sequence (C-terminus).[26,69] This anchors the protein into the OMM with its globular peptides exposed in the cytoplasm.[69]

1.2.3.1 Pro-apoptotic BCL2 family proteins

Single domain pro-apoptotic regulators contain only one motif, namely the BH3 domain and are called BH3-only proteins.[26] BID, BCL2-like protein-11 (BIM), BCL2-associated death (BAD) promoter, PUMA and phorbol-12-myristate-13-acetate-induced protein-1 (PMAIP1; also known as NOXA) are BH3-only proteins.[26] The BH3 motif is responsible for the interaction and activation of apoptogenic multi- and single-domain proteins.[26,69] BH-3-only proteins lack a terminal TM domain and indirectly increase OMM permeabilization by upregulating its mutlidomain partners.[26] The BH3 motif also sequesters anti-apoptotic BCL2 proteins, liberating their counterparts to continue pro-apoptotic signalling.[69]

Multi-domain proteins contain BH motifs 1 to 3 and a TM region that form membrane pores to reduce the OMM integrity.[26,69] These encompass BAX, BAK and BCL2 ovarian killer (BOK) proteins.[26,69] BAK and BAX work to support excessive Ca^{2+} levels in the mitochondria, to further propagate intrinsic suicidal cues.[62] These apoptotic activators are also transcriptionally responsive to TP53 when incited by genotoxic stress, killing off genetically unstable lineages.[59] Inactivating mutations in *TP53* occur in majority of cancers and weaken tumour suppressor-mediated immunity against malignant transformation.[70]

1.2.3.2 Anti-apoptotic BCL2 family proteins

Pro-survival proteins contain motifs BH1 to 4 and repress apoptosis by direct inhibitory interactions with pro-apoptotic proteins via their BH3 binding domains.[26,69] Pro-survival BH1, 2 and 3 domains form a hydrophobic pocket that accommodates the BH3 motif from pro-apoptotic BCL2 modulators.[71] Moreover, anti-apoptosis BCL2 molecules prevent mitochondrial influx of Ca^{2+} due to activation of a calcium exporter, inositol triphosphate-3 (IP3) receptor that dilutes Ca^{2+} stores, bypassing intrinsic apoptosis.[62] Several pro-survival proteins have been identified, such as BCL2, BCL2-like isoform X-1 (BCLX), BCL2-like protein-2 (BCL2L/BCL-w), BCL2-like protein-10 (BCL2L10) and myeloid cell leukaemia protein-1 (MCL1).[26] Their activities grant cancer cells with the ability to evade apoptosis.[26]

Vast amounts of non-canonical regulators of apoptosis are still unexplored with novel molecules being continually identified.[69] The balance between the activities of anti-apoptotic and pro-apoptotic BCL2 proteins determines whether a cell dies or continues its cell cycle.[69] Cancer cells often have abnormally upregulated anti-apoptotic BCL2 proteins or down-regulated pro-apoptogenic proteins, potentiating malignancy and cancer therapeutic resistance.[69]

1.3 Pharmacological modulation of apoptosis in cancer treatment

A logical approach to anti-cancer treatment includes the pharmacological increase in activity of pro-apoptotic proteins and/or decrease in activity of anti-apoptotic proteins.[69] However, the feasibility of apoptosis-targeted pharmaceuticals is complicated by the molecular vastness and intra-tumour heterogeneity based on differences in expression patterns of apoptotic regulators.[72] Thus neoplastic cells harbour differential degrees of malignant potential and variable sensitivities to apoptosis-inducing treatment.[72]

Anti-cancer drugs consist of various compounds that modulate BCL2 family proteins, IAPs, extrinsic ligands and receptors.[66] Anti-malignant drugs additionally suppress oncogenic disruption of tumour suppressors, which indirectly promotes apoptosis.[66] Pharmacological intervention aims to strengthen or restore apoptotic responses to ultimately effectively reduce malignant cell numbers or eradicate tumours.[66] To promote successful tumour regression in a clinical context, combinations of apoptosis-inducing agents are used.[66]

1.3.1.1 Inhibition of anti-apoptotic BCL2 family proteins

Xenobiotics, such as small molecule repressors of pro-survival BCL2 proteins, block interactions of their BH domains with pro-apoptotic family members.[66] BCL2 and BCLX are inhibited by a selective interaction with the BH3 domain of pro-apoptotic BH-3-only proteins, reproduced by a class of drugs known as BH-3-mimetics.[69] Hydrophobic amino acids of the BH3 motif fit into a hydrophobic pocket of pro-survival BCL2 family proteins.[69] This facilitates stable binding as non-polar residues adhere more strongly to each other than to intracellular water molecules.[69,73] This conceals the anti-apoptotic BCL2 interface, preventing their inhibitory interactions with BAK and BAX.[69]

The most characterized BH3-mimetics include venetoclax (ABT-199), ABT-737 and navitoclax (ABT-263), which have been clinically examined as anti-cancer interventions.[74-75] Navitoclax and venetoclax repress anti-apoptotic BCL2 regulators BCL2, BCLX and BCL2L, although venetoclax binds more strongly to BCLX and BCL2L.[74-75] Navitoclax has also been used as a MCL1 antagonist to sensitize TNBC cells to other death-inducing agents.[76] Patients with recurring chronic lymphocytic leukaemia have benefited from individual navitoclax treatment and in combination with a monoclonal antibody (MAB).[77-78] An example of a MAB includes rituximab, which induces B-lymphocytic death via specific induction of cell surface antigen CD-20.[79]

In addition, pro-survival BCL2 proteins are repressed by small molecules, namely BH4 antagonists that bind to the BH4 domain.[80] BH4 domain-antagonist-366 (BDA-366) is a BH4 antagonist of BCL2 that was tested in lung cancer cell lines.[80] BDA-366's interaction with the BH4 domain incites a conformational change in BCL2, hindering its suppression of IP3 receptors and enhancing Ca^{2+}-mediated apoptosis.[80] BDA-366 also facilitates the exposure of the BH3 motif, turning anti-apoptotic BCL2 into activators that promote the function of BAX.[80] Evidently, BDA-366 effectively combats cancer insensitivity to other death-inducers caused by BCL2 overactivity.[80]

1.3.1.2 Repression of IAPs using SMAC-mimetics

IAPs are naturally inhibited by second mitochondrial activator of caspases (SMAC) residing in the mitochondria[26,53] Like BH-mimetics, hydrophobic residues of SMAC selectively bind to the baculovirus IAP repeat (BIR) domains of IAPs.[53] These BIR domains sequester caspase enzymes, conferring insensitivity to TNF-mediated apoptosis.[53,81] Interaction between SMAC and IAPs are imitated by small molecules called SMAC-mimetics.[53]

SMAC-mimetics are designed to target XIAP, cellular IAP-1 (cIAP1) and 2 (cIAP2), although more potent on cIAP1 and cIAP2.[53,82] cIAP1 and cIAP2 antagonists have the ability to induce IAP ubiquitination, promoting their proteosomal degradation.[53] SMAC-mimetics also competitively inhibit cIAP-mediated degradation of necroptotic RIPK-1, restoring alternative pathways of cell death.[53] Competitive inhibition implies that a binding site in cIAP1 or 2 is shared between small molecules and RIPK-1.[82] This suggests that increasing concentrations SMAC-mimetics prevent RIPK-1 degradation more effectively.[82] However, non-canonical signalling may enhance cIAP2 activity in response to decreasing levels of cIAP1 expression induced by IAP antagonists.[82] As a result up-regulated cIAP2 further promotes resistance to TNF-alpha (TNFα)-mediated apoptosis.[82]

TL-32711 and bivalent-6 (BV6) inhibit XIAP, cIAP1, cIAP2 and promote proteosomal degradation of cIAP1 and 2, restoring caspase activity.[83-84] In this way, SMAC-mimetics aid caspase-8 activation, potentiating extrinsic apoptotic signalling by TNF superfamily of ligands.[83-84] BV6 additionally mediates the auto-activation of caspase-9, expanding apoptotic signalling via the intrinsic pathway.[84]

1.3.1.3 Suppression of the MDM2 oncoprotein

MDM2 is the most commonly over-expressed proto-oncogene in cancer yet causes a similar phenotype to a deleterious TP53 mutation.[66] MDM2 is a cellular TP53 inhibitor that increases its nuclear export, inhibits TP53-dependent transcription of apoptotic genes and reduces TP53 stability.[66] Moreover, its homologue, MDM4 associates with MDM2, forming a heterodimer that anchors MDM2 binding and mediates post-translational TP53 ubiquitination for proteosomal degradation.[85-86]

MDM2 antagonists interfere with the interaction between MDM2 and TP53, restoring TP53-induced transcription of apoptotic genes, such as *PUMA*, *BID*, *BAK* and *caspase-3*.[58,66,68,87] Nutlin-3 is a small MDM2 antagonists derived from imidazoline organic molecules and was used in multiple anti-cancer drug studies.[87] This is an efficacious sensitization agent for the chemotherapeutic drug cisplatin in nasopharyngeal, ovarian and prostate cancer cell lines.[88-90] Another MDM2 inhibitor, G-613 (also known as 5-chloro-4′,5′-diphenyl-3′-(4-(2-(piperidin-1-yl) ethoxy) benzoyl) spiro[indoline-3,2′-pyrrolidin]-2-one) showed anti-cancer activity in ER+ breast cancer cells.[91]

1.3.1.4 Induction of TRAILR-mediated extrinsic apoptosis

TRAIL interacts with both TRAILR1 and TRAILR2 receptors in TRAILR-positive carcinomas and elicits apoptosis in TP53-deficient cancers to address therapeutic resistance due to loss of TP53.[92] TRAIL-induced apoptosis exhibits selective cytotoxicity to malignant cell lines as opposed to benign cells, revealing a promising treatment modality.[93] Ligand-receptor binding is reproduced by TRAIL-receptor agonists (TRAs) such as bacterial-synthesized TRAIL (recombinant human (rh)TRAIL).[92,94] Dulanermin is an rhTRAIL molecule that showed short-term efficacy alone and in various chemotherapeutic combinations in patients with non-small cell lung cancer (NSCLC).[95] However, chemotherapeutic combinations with dulanermin as a first-line therapy did not improve overall survival.[95] Irrespectively, the use of rhTRAIL is limited by its short half-life and lack of potency due to TRAILR competition by decoy receptors.[92,96]

Recombinant TRAIL biologics have undergone several enhancements, one of which involves TRAILs that recognize TRAILR2.[92,97] This design is composed of numerous multimeric TRAILR-interactive peptides linked to a molecular scaffold.[97] Presence of more than one receptor-binding site engages more receptors at single molecular level and stabilizes TRAILR2 ligation.[97] Increased binding sites resulted in superior apoptotic effects in colorectal, lung and T-lymphocyte cancer cell lines [97] MEDI-3039 is a TRAILR2 agonist constructed with a fibronectin type III protein scaffold and four TRAILR-binding domains, demonstrating impressive potency in breast cancer *in vivo*.[98]

1.3.2 Cervical cancer drugs promoting apoptosis

Chemotherapeutics cisplatin and paclitaxel are the most efficacious treatments currently used for cervical cancer.[99] Paclitaxel as a monotherapy improves overall patient survival, but potentiates drug response and longevity when administered concomitantly with cisplatin.[99] In addition, cisplatin combined with topotecan showed enhanced clinical endpoints, but exhibited strong adverse side effects.[99] To address these setbacks, further research focused on targeted therapies for cervical cancer in patients that were previously treated with chemotherapy.[99]

Navitoclax has been analysed in cervical cancer cell lines in combination with a MCL1-specific inhibitor (A-1210477), revealing a synergistic relationship.[56] Resistance of cervical cancer cell lines to navitoclax is frequently attributed to up-regulation of MCL1.[56] Therefore selective repression of MCL1 is a logical approach to increase navitoclax efficacy.[56] However, inhibition of other pro-survival BCL2 proteins by navitoclax also sensitized cervical cancer cells to A-1210477.[56] The synergy between navitoclax and A-1210477 is thus supported by the sensitization properties of these drugs on each other.[56] Co-treatment in non-cancerous cells resulted in lower cytotoxicity than in cancer cells.[56] This suggests that cervical cancer cells are naturally more responsive to the combination of navitoclax and A-1210477, indicating *in vivo* toxicological efficacy for pre-clinical studies.[56]

An early event in cervical carcinogenesis involves deletion of decoy receptor genes, *DCR1* and *2*, coincidentally removing linked tumour suppressor genes.[60] Despite this trade-off, it creates a vulnerability to TRAIL-induced apoptosis.[60] Based on an *in vitro* study, decreased expression of DCR1 or DCR2 sufficiently sensitized cervical cancer cell lines to rhTRAIL-mediated apoptosis.[60] In contrast, cervical cancer cells expressing HPV oncoprotein E-6 are insensitive to TRAIL-activated apoptosis.[100] E-6 associates with the E-6-associated protein (E6AP) that contains E3-ubiquitin ligase activity and promotes proteosomal degradation of TP53.[100] This blocks transcription of TNF family genes including *TRAIL*, *TRAILR1* and *TRAILR2*.[58,100] These effects were reversed by an anti-diabetic medicine (ciglitazone) that has been repurposed as an anti-cancer drug, resulting in the additional up-regulation of caspases and BID.[100] Furthermore, ciglitazone successfully perturbed the growth of cervical cancer implants in mice, showing promising potential in a clinical setting.[100]

Despite constant advances in anti-cancer therapeutics, malignancies possess a vast array of deregulated apoptotic proteins as well as genetic instability.[26] This suggests intact mechanisms of therapeutic resistance and frequent acquisition of new mechanisms.[92] Consequently, extrinsic apoptotic signals are disconnected from downstream and/or intrinsic signals which prevent the execution phase of programmed cell death.[26,92] Furthermore, lack of tumour vascularisation due to exceeding malignant proliferation reduces the targeted delivery of therapeutic substances to the tumour.[42]

1.3.3 Chemotherapeutic combinations in cervical cancer treatments

Paclitaxel, a widely-used drug discovered from plants, with cisplatin is a standard drug combination used in cervical cancer care in patients without prior platinum-based chemotherapy.[101] The paclitaxel-cisplatin regimen had improved survival outcome compared to carboplatin-paclitaxel combination in an open-label randomized phase III clinical trial.[101] However, the carboplatin-based regimen improved outcomes in patients with a history of platinum-based chemotherapy.[101] Cediranib is a synthetic tyrosine kinase inhibitor of vascular endothelial growth factor (VEGF) which plays a role in angiogenesis in cervical cancer progression as its normal function.[102] Therefore, targeted VEGF inhibition is also effective when used in combination with paclitaxel-carboplatin regimens.[103] However this comes at a cost of increased adverse side effects such as bowel irritation, hypertension and decline of neutrophil lymphocytes with fever.[103]

To address the potentially increased toxic events, more preclinical studies of plant-based chemotherapeutic combinations are being studied.[104] A recent example includes *in vitro* effects of alkaloids extracted from *Piper nigrum* (*P. nigrum*) plants in improving response to paclitaxel in cervical cancer cells.[105] The main isolated compound piperine sensitized paclitaxel-resistant cells via inhibiting the effects of MCL1 and phosphorylated AKT serine/threonine kinase-1 (AKT).[105] In addition, two saponin triterpenoids extracted from roots of *Radix Bupleuri* (*R. Bupleuri*) used in Chinese herbal medicine have potentiated cisplatin cytotoxicity in *in vitro* cervical cancer cells.[106] Saponins, namely saikosaponin-a and saikosaponin-d resulted in increased superoxide and hydrogen peroxide accumulation in co-treatments with cisplatin, revealing a ROS-mediated apoptotic response.[106] Apart from combination treatments with paclitaxel, literature regarding pure plant-based drug combinations are limited.[104] This further motivates the current study of sole plant-derived compounds and their combinations as additional therapeutic strategies in cervical cancer treatment.[104]

1.4 Drug discovery and plant-derived drugs for cervical cancer

The general pharmaceutical approach begins by identifying and evaluating a molecular target strongly associated with a specific cancer.[107] Compounds or whole compound libraries are extensively screened *in silico* and to generate potential "hits".[107-108] However, a huge population of compounds will not reach their biological targets intact, having poor pharmacokinetics *in vivo*. [109] Lipinski's rule of 5 is used to throw out compounds that have unfavourable bioavailability when absorbed from the digestive tract.[109] Orally bioavailable drugs often have a molecular weight (MW) ≤ 500 g/mol, octanol-water partition coefficient (log*P*) ≤ 5, hydrogen bond donors (HBDs) ≤ 5 and hydrogen bond acceptors (HBAs) ≤ 10. [109] Log*P* is a value expressing the ability of a molecule to passively permeate the lipid cell membrane while also being able to partially dissolve in water allowing absorption from the digestive tract into the circulation where it can be distributed to cellular targets. [110-111] Additional molecular properties include topological polar surface area (TPSA) and number of rotatable bonds (nrot). [109,112-113] TPSA is the sum of atomical surface areas of polar atoms (i.e. oxygen and nitrogen) and nrot is the number of free, non-cyclical single bonds in a compound with non-terminal constituents other than hydrogen.[112-113]

Computational analysis of quantitative structure-activity relationships (QSARs) may also be used to predict and categorize compounds based on their influence on biological targets before validating them by biological screening.[114] Pharmacological modulation of common protein drug targets such as receptors (i.e. G-protein coupled receptors (GPCRs) and nuclear receptors), enzymes (i.e. kinases and proteases) and ion channels show promising anti-cancer advantages.[115-121] Potential leads are assessed and re-assessed in animal models to produce effective and safe candidates and to confirm efficacy.[122] Candidate drugs enter the clinical phase, in which drugs must surpass three phases of clinical trials.[122] Drugs showing satisfactory efficacy and safety profiles in humans during all clinical phases are applied to the Food and Drug Administration (FDA) for approval.[122] Sometimes drugs with high adverse side-effects require post-approval to clarify safety for commercial use to the public.[122] Overall anti-cancer drug discovery is a financially-heavy process that can take up to 15 years from bench-top to bedside.[107] Alternatively, existing FDA-approved drugs used to treat a different disease are repurposed to cervical cancer, skipping the early preclinical stages.[104]

Plants produce diverse compounds (i.e. phyto-chemicals) which are the source of 49% of FDA-approved drugs entering the market from years 1981 to 2014.[123] Most plant-derived anti-cancer drugs encompass secondary metabolites produced as by-products of biochemical pathways.[124] Major classes of medicinal secondary phyto-metabolites include phenolics, alkaloids and terpenoids.[124-125] Phenols are composed of hydroxylated aromatic rings in which flavonoids form part of this group.[126] Alkaloids are biologically synthesized from amino acids, therefore containing non-protein nitrogen atoms.[126] Terpenoids are biosynthesized from acetate precursors via the mevalonic acid pathway.[126] Abundant anti-cancer molecules and even several chemotherapeutic drugs were originally isolated from plants.[124]

Some of the most famous plant-derived anti-cancer drugs include vincristine, paclitaxel, curcumin and betulinic acid.[124] Furthermore, vincristine and paclitaxel are clinically available for the treatment of cancer while curcumin and betulinic acid are currently under clinical study.[124] Vincristine is an alkaloid that exerts its anti-proliferative effects by disrupting microtubule progression during mitosis.[124] It was first isolated from *Catharanthus roseus* shrubs.[124] Paclitaxel is a terpenoid with similar anti-mitotic activity and was initially found in the bark of the *Taxus brevifolia* (*T. brevifolia*) tree (commonly known as Pacific yew).[124] Curcumin is a phenolic compound extracted from the turmeric plant (*Curcuma longa* (*C. longa*)) and is been used in traditional Chinese herbal medicine for centuries.[124] Lastly, betulinic acid is also a terpenoid, initially obtained from extracts of the herb *Gratiola officinalis* (*G. officinalis*).[124] Despite specific origins, these compounds have now been extracted from a variety of other botanical sources.[124]

Several studies have validated the anti-proliferative effects of betulinic acid, curcumin and paclitaxel in cervical cancer.[124] Based on pre-clinical studies, curcumin and betulinic acid have demonstrated various anti-proliferative modes of action, inducing apoptosis by mediating endoplasmic reticulum and mitochondrial stress responses.[127-130] The negative side effects of paclitaxel led to the design of semi-synthetic paclitaxel-analogues, such as docetaxel, with enhanced bioavailability, anti-cancer activity and reduced systemic cytotoxicity.[124]

Certain plant metabolites have been shown to directly interact with apoptotic regulators.[124-125] For example, betulinic acid was observed to up-regulate BAX, caspase-8, 3 and 9 while inhibiting BCL2 in ovarian carcinoma cells.[131] In addition, gossypol (AT-101) induces cell cycle arrest and directly represses anti-apoptotic BCL2 family members, acting as a natural BH-3-mimetic.[75] Plant metabolites have also been used in combination with apoptosis-targeted agents *in vitro*.[125,132] Synergistic cytotoxicity was observed when BCL2 repressor, ABT-737 and chalcones were each used as a co-treatment in a breast cancer cell line.[132]

Indiscriminate toxic side-effects in off-target cells pose a problem in cancer chemotherapies, demanding more tolerable alternatives.[124] Therefore, secondary plant metabolites have paved the way for anti-cancer drug discovery in the pipeline of many pharmaceutical products.[124] Whether directly derived from nature or used as a backbone in semi-synthetic drugs, phyto-chemicals warrant very useful leads to more efficacious cell-killing or palliative drugs.[124]

Recently, Nwodo *et al*, documented the identification of 400 African plant-derived compounds with *in vitro* anti-cancer properties in a broad variety of cell lines.[125] Most of these identified phyto-compounds were isolated from various plant species belonging to the Rutaceae family located in Cameroon.[125] The Rutaceae family of plants are the natural source of many citrus fruits and produce many biologically active phenolic molecules.[133] Phyto-chemicals of African ethno-botanical sources have shown cytotoxicity in several *in vitro* cancer cell lines, such as cervical cancer cells.[125] Cervical cancer cell lines were sensitive to 2′,4′-dihydroxy-3′,6′dimethoxychalcone (from *Polygonum limbatum* (*P. limbatum*)), ent-trachyloban-3beta-ol (from *Croton zambesicus* (*C. zambesicus*)) and the crude alkaloidal extracts of *Erythrina abyssinica* (*E. abyssinica*).[134-136]

1.4.1 Other plant compounds from medicinal African plants

Cameroon is a country of rich flora biodiversity, providing many opportunities for discovery of anti-cancer compounds.[137] Traditional medicine has claimed that many plant extracts possess healing qualities that deserve further investigation to identify more efficacious alternatives for the treatment of cervical cancer.[137] Therefore, this study will focus on the plant-derived compounds isolated from 4 Cameroonian plants, namely *Cassia arereh* (*C*. *arereh*), *Distemonanthus benthamianus* (*D*. *benthamianus*), *Echinops gracilis* (*E*. *gracilis*) and *Rhabdophyllum affine* (*R*. *affine*).[138]

C.arereh has been used in African-traditional medicine for treatment of intestinal infections, diarrhoea, malarial- and skin infections with known anti-bacterial activities against *Escherechia coli* (*E. coli*), *Klebsiella pneumoniae* (*K. pneumoniae*) and *Staphylococcus aureus* (*S. aureus*),[139] Pentacyclic triterpenoids betulinaldehyde and betulinic acid (also used in this study, **figure 5**), with anti-microbial effects against *Pseudomonas aeruginosa* (*P. aeruginosa*) and *Haemophilus influenza* (*H. influenza*) and *K. pneumoniae* bacteria, were also isolated by Missi, *at al*.[138] There is very limited literature regarding the anti-cancer effects of pure compounds from *C. arereh*, warranting its source in this study.

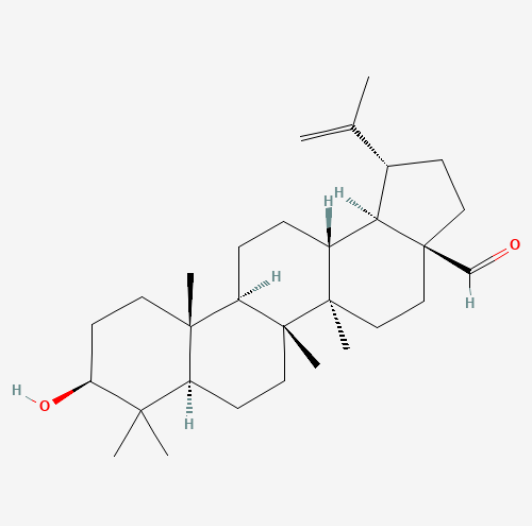

Figure 1: Molecular structure of betulinaldehyde provided from the Pubchem database.[140]

D. benthamianus (**figure 1**) is a medicinal source for treatment of colonic infection and associated gastrointestinal conditions in Western Cameroon.[141-142] This is because of its anti-inflammatory, anti-oxidant and immunomodulatory effects.[142] Methanolic extracts of *D. benthamianus* revealed therapeutic effects against gastric ulcers in male rats.[142] The therapeutic effects were narrowed down to the presence of gallic acid in the extract, which disrupts function of voltage-regulated calcium channels and cholinergic receptors. [142-143] Gallic acid (**figure 2**) was extracted and studied by Marte, *et al*.[142]

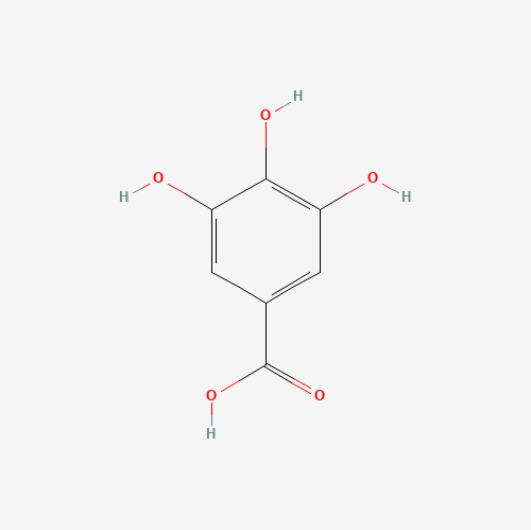

Figure 2: Molecular structure of gallic acid provided from the Pubchem database.[144]

Extracts prepared from the aerial sections of *E. gracilis* plants possess therapeutic qualities against bacterial infections caused by *E. coli*, *P. aeruginosa* and *K. pneumonia*.[145] In addition, the *E. gracilis* extract also showed anti-oxidant activities.[145] The extract contained flavonoids apigenin-7-O-(4″-feruloyl)-β-D-glucoside, apigenin-7-O-(4″-trans-p-hydroxycinnamoyl)-β-D-glucoside (also used in this study, **figure 7**) and apigenin-7-O-glucoside (also used in this study, **figure 7**) isolated by Weyepe Lah, *et al*.[145] General medicinal purposes of the *Echinops* genus include treatment of sexually transmitted infections, fever, sepsis, typhoid fever, respiratory conditions, pain of the teeth and ears.[146]

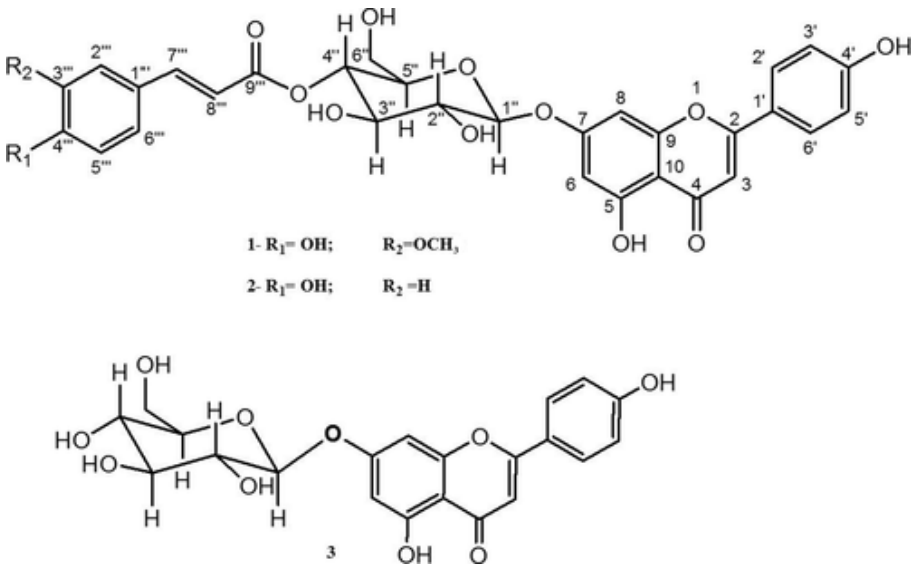

Figure 3: Backbone molecular structures of apigenin-7-O-(4″-feruloyl)-β-D-glucoside (R1-OH; R2-OCH_3), apigenin-7-O-(4″-trans-p-hydroxycinnamoyl)-β-D-glucoside (R1-OH; R2-H) and apigenin-7-O-glucoside (bottom).[147]

Plants belonging to the *Rhabdophyllum* genus are used as African herbal medicines to treat pelvic pathologies, pain in ribs and fatigue.[148] In addition, *Rhabdophyllum* have been used as an aphrodisiac.[148] Due to lack of literature about the therapeutic uses of *R.affine*, anti-bacterial effects of various extracts of *Rhabdophyllum arnoldianum* (*R. arnoldianum*) are reported against gram positive bacterial species.[148] These include *S. aureus*, *Enterococcus faecalis* (*E. faecalis*), *Bacillus cereus* (*B. cereus*) and *Bacillus subtilis* (*B. subtilis*).[148] Compounds listed in **figure 4** were isolated from *R. arnoldianum* extracts by Mbing, *et al.*[148] However none of these compounds revealed anti-microbial qualities individually.[148]

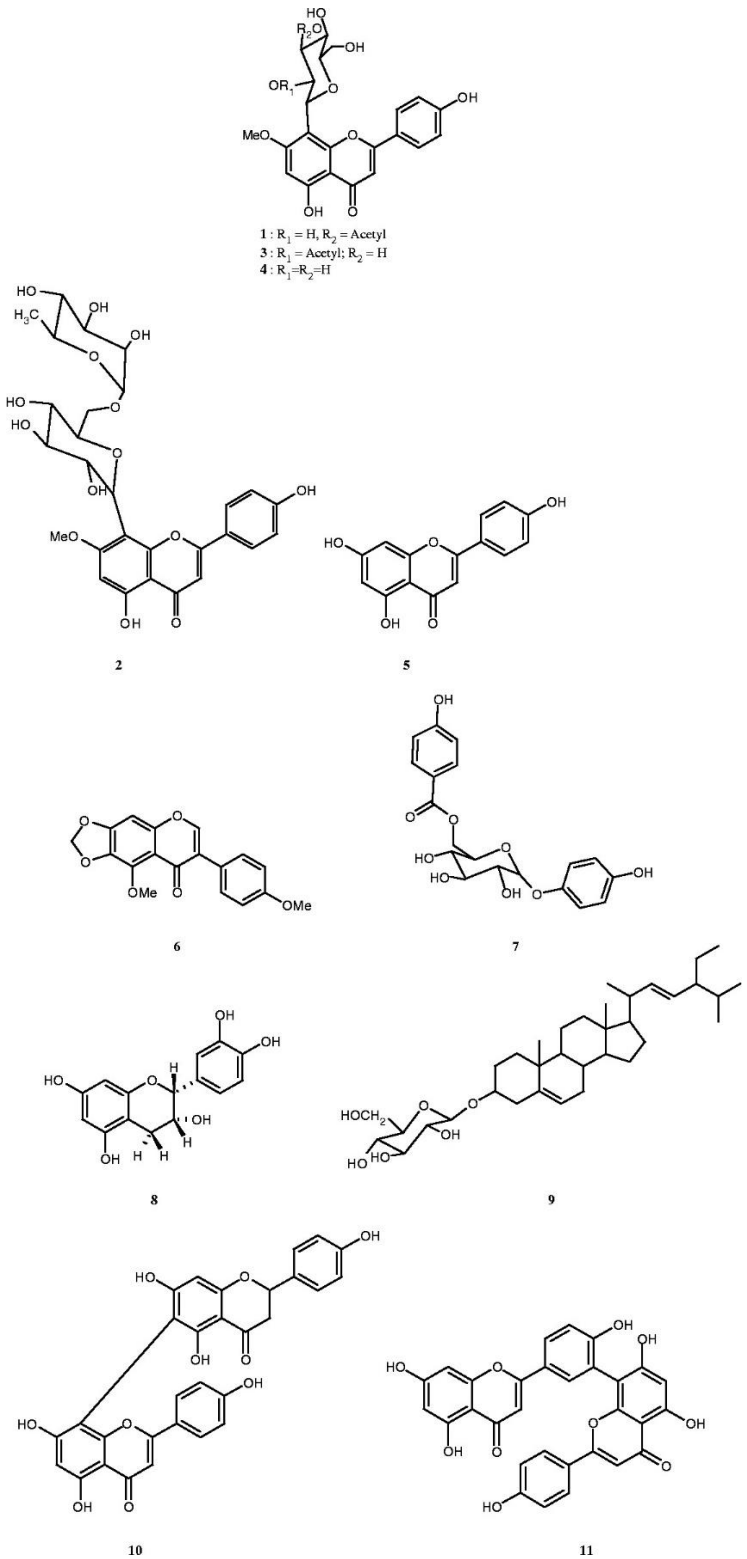

Figure 4: Structures of compounds isolated from *R. arnoldianum, namely* arnoldioside A (1), arnoldioside B (2), 2″-O-acetyl-7-O-methylvitexin (3), 7-O-methylvitexin (4), apigenin (5), 4′,5-dimethoxy-6,7-methylenedioxyisoflavone (6), lanceoloside A (7), epicatechin (8), 3-β-O-d-glucopyranosyl-β-sistosterol (9), rhusflavone (10) and amentoflavone (11).[149] Compounds 1, 3 and 4 share the same carbon ring structure with different side chains as indicated.

2 Aim and Objectives

2.1 Aim

To screen the potential anti-cancer effects of Cameroonian medicinal plant-derived compounds and assess the individual and combined cytotoxic effects of the most potent compounds in cervical cancer cells

2.2 Objectives

2.2.1 Objective 1

1.1 To determine the half-maximal inhibitory concentration (IC_{50}), selectivity index (SI) of each compound and assess the cytotoxicity of the most bioactive compounds at various fractions of their respective IC_{50} doses individually and in combination by:

- 3-(4,5-dimethylthiazol-2-yl)-2,5-diphenyl tetrazolium bromide (MTT) assay for assessment of cytotoxicity, IC_{50} and SI
- xCelligence Real-time Cell Analysis (RTCA) of cytotoxicity as well as additional IC_{50} and SI values

2.2.2 Objective 2

To quantify the distribution of cells in different modes of cell death in response to half the IC_{50} doses of bioactive compounds alone and in combination via:

- Annexin-V and propidium iodide (PI) staining of externalized PS and nuclear DNA quantified by flow cytometry

2.2.3 Objective 3

To quantify the oral drug-likability of compounds based on Lipinski's rule of 5 as well as the predicted bioactivity against classes of protein targets by:

- *In silico* analysis using Molinspiration v2021.10 online software

3 Materials and Methods

3.1 Cell cultures

The effects of the plant-based compounds were studied in commercial adherent cervical cancer cell lines *in vitro*. Cervical cancer cell lines included Henrietta Lacks-(HeLa) and epidermoid cervical carcinoma (CaSki) cells which were provided by the National Institute of Biomedical Innovation, Health, and Nutrition (Osaka, Japan). HeLa and CaSki cells are both HPV-positive.[150] HeLa cells were first isolated from the cervical carcinoma of Henrietta Lacks, an African-American 31-year old female in 1951.[151] CaSki cells were originally derived from the cervical epidermoid metastatic lesion in the small bowel mesentery of a 40-year old Caucasian women.[152-153] These cell lines resemble HPV-transformed cells of an advanced cervical carcinoma *in vitro* that is a useful model of the disease.[152] Vero cell lines were used as a non-cancer kidney epithelial cells derived from the African Green Monkey or *Cercopithecus aethiops* (*C. aethiops*) which was provided from the American Type Culture Collection (ATCC) (Manassas, United States of America (USA)).

3.1.1 Cell culture reagents

Dulbecco's Modified Eagle's Medium (DMEM) (with phenol red, 4 mM, L-Glutamate, 4.5 g/L glucose and sodium pyruvate), 500 mL foetal bovine serum (FBS), 1- and 10X phosphate-buffered saline (PBS) (without calcium and magnesium), penicillin-streptomycin (([+] 10, 000 Units/mL, penicillin, [+] 10, 000 ug/mL, streptomycin)), amphotericin B (25ug/mL) and trypsin-ethylenediaminetetraacetic acid (EDTA) (0.25% (1x) with 0.1% EDTA) were supplied from Dithlano Biotechnology (PTY) LTD (Midrand, SA). Dimethyl sulfoxide (DMSO) and trypan blue was supplied from Sigma-Aldrich (St Louis, USA). These reagents were used for the cell culture maintenance protocol, based on the methods described by Kutwin *et al* and Bowey-Dellinger *et al*.[154-155]

3.1.2 General cell culture maintenance

HeLa and Vero cells were cultured in DMEM prepared with 10% FBS, 1% antibiotics (penicillin and streptomycin) and 1% amphotericin B. All cells were incubated in a humidified air-jacketed incubator (Stericycle, Plymouth, USA) at 37°C with 5% carbon dioxide (CO_2). Cell culture media is replaced regularly, and cells routinely passaged every three to four days, cryo-preserved or seeded for experiments whenever reaching above a confluency of 70%. Cells are cultured in 25 cm^2 (T-25) cell culture flasks and examined during trypsinization and general upkeep using an inverted light microscope. All cell culture techniques are performed under sterile conditions in a laminar flow hood.

3.1.3 Cell counting and seeding for experiments

Prior to seeding, cells are stained with trypan blue, transferred into a haemocytometer and counted in four quadrants in each counting chamber. Trypan blue dye stains intracellular contents and were used to distinguish live and dead cells.[156] Dead cells stain positive with trypan blue as their membranes break, whereas live cells stain negative as their membranes are intact.[156] Cell aliquots of 100 µL were prepared with 400 µL 0.4% trypan blue solution using a dilution factor of 5. The average number of cells counted in the counting chambers were calculated and the cell density was determined using the following formula:

$$Cell\ density\ per\ ml = average\ cell\ number \times dilution\ factor \times 10^4$$

The seeding density will determine the volume of cell suspension to seed according to recommendations for cell lines and analytical glassware of various formats. After seeding, cells were allowed to attach for 24 hours before treatment with phyto-compounds.

3.2 Phyto-compounds and controls used for screening

3.2.1 Compounds and compound preparation

The plants, *C.arereh*, *D.benthamianus*, *E.gracilis* and *R.affine*, were harvested and processed in Cameroon and their compounds (**table 1**) were isolated at the University of Yaoundé in collaboration with the Department of Chemistry at the University of Pretoria. These plant-derived compounds were used to investigate their anti-proliferative activities in cervical cell lines. Air-dried plant material was subject to maceration, extraction in methanol (MeOH), filtration and concentration to yield crude extracts.[157] Extracts were then partitioned, solubilized in 2:8 MeOH:H_2O solvent and repetitively separated into various organic extracts.[157] Compounds were isolated using flash or normal silica column chromatography.[157] Compound structures were identified using nuclear magnetic resonance (NMR), infra-red (IR) and mass spectrophotometry.[138,145,157] One mg of powdered compounds were dissolved in 100% DMSO which was diluted at the final concentration and used as a vehicle for each compound as it promotes intracellular movement of the compounds.[158] CAE21 (cassiaramine; **figure 5**), DBF4 (distemonanthoside; **figure 6**) and EGF25 (Apigenin-7-O-[4″-(3‴-methoxy-4‴-hydroxycinnamoyl)-β-D-glucoside]; **figure 7**) are newly isolated and undescribed phyto-compounds.[138]

Table 1: List of plant secondary-metabolites for anti-cancer screening in cancer cell lines. *Compounds with newly identified structures.

Code	Compounds	Plant source	Compound classification
CAE1	Catechin	*C. arereh*	Phenolic
CAE3	Betulinic acid		Triterpenoid
CAE5	Lupeol		Triterpenoid
CAE8	Ceanothic acid		Sesquiterpenoid
CAE21*	Cassiaramine		Triterpenoid
DBF4*	Distemonanthoside	*D. benthamianus*	Flavonoid
EGF4	Apigenin-7-”-(4″-trans-*p*-hydroxycinnamoyl)-*β*-*D*-glucoside	*E. gracilis*	Flavonoid
EGF25*	Apigenin-7-*O*-[4″-(3‴-methoxy-4‴-hydroxycinnamoyl)-*β*-*D*-glucoside]		Flavonoid
EGF36	Apigenin-7-*O*-glucoside		Flavonoid
RAR2	Serotobenine	*R. affine*	Alkaloid

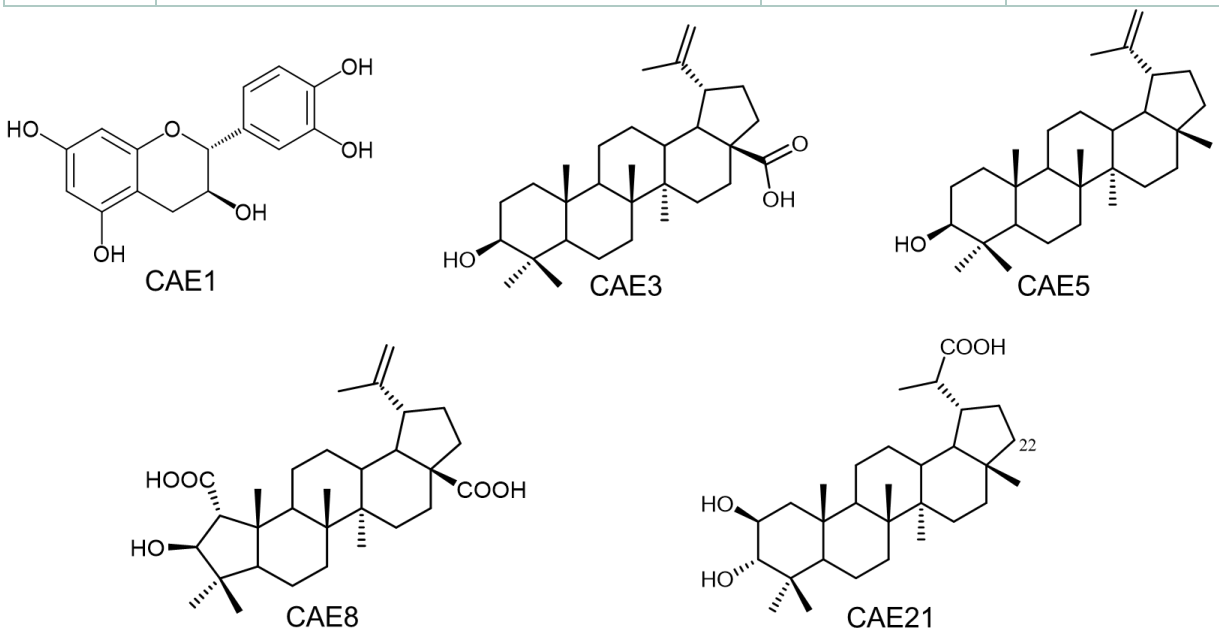

Figure 5: Flavonoids and terpenes isolated from *C.arereh* stem bark.

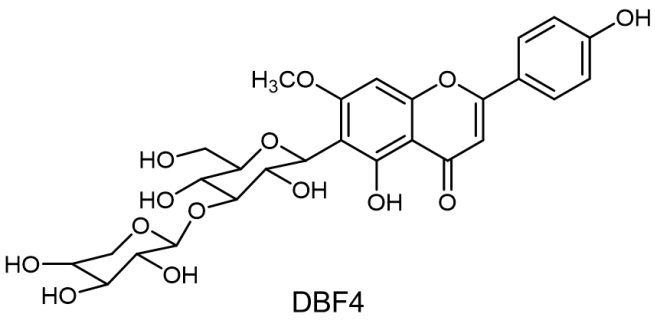

Figure 6: Flavonoid isolated from *D. benthamianus*.

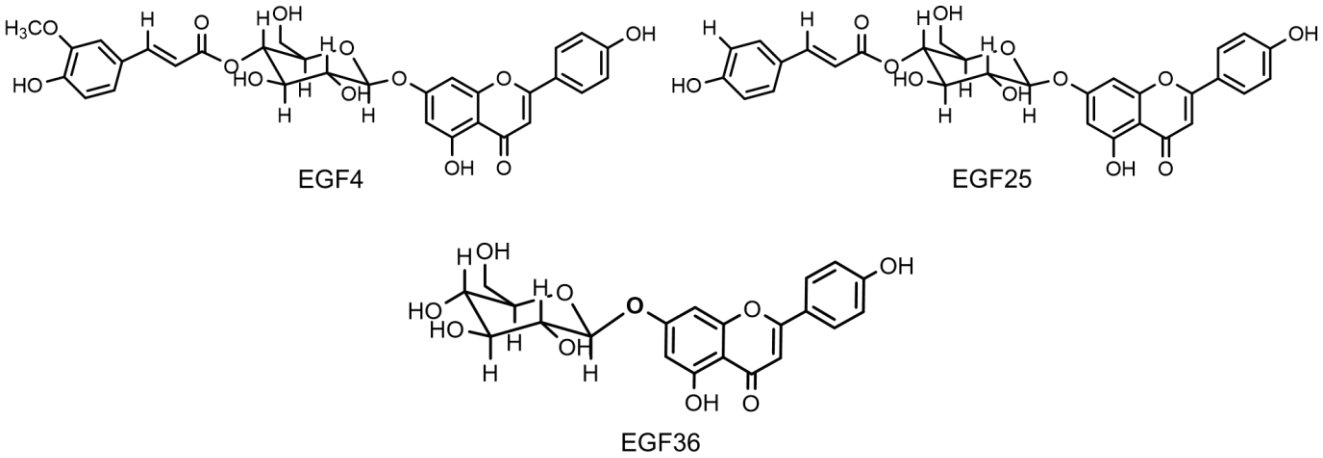

Figure 7: Flavonoids isolated from *E. gracilis*.

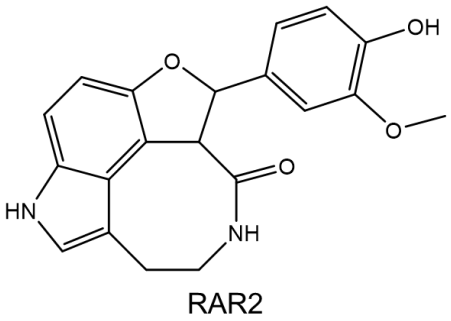

Figure 8: Pentacyclic indole alkaloid isolated from *R. affine*.

3.2.2 Controls

The 0.1% DMSO dissolved in medium was used as a vehicle control to address potential effects of the drug solvent on cells. A negative control included DMEM without any cells or untreated cervical cancer cells. Cells treated with camptothecin were used as a positive control.

Camptothecin is an alkaloid that was originally isolated from the bark of the *Camptotheca acuminata* tree from China.[159-160] It was chosen as a positive control because it is an powerful plant-based anti-cancer drug which was FDA-approved in the 1970s.[161] Camptothecin's anti-cancer mode of action is that it inhibits topoisomerase I enzyme in mammalian cells. [161-162] Topoisomerase I normally relieves chromatin supercoiling by introducing reversible single- and double-strand DNA breaks, uncoiling the DNA and resealing the loose ends.[163] Camptothecin specifically targets the resealing step of topoisomerase I[162], leaving permanent breaks that culminates in cell death and ceasing DNA replication required for cancer cell survival.[161] (S)-(+)-Camptothecin was supplied from Sigma Aldrich (St Louis, USA).

3.3 Cell viability analyses

An MTT cell viability and RTCA assays were conducted to determine cytotoxicity and the real-time cell index of compounds, Therefore, results obtained from cytotoxicity analyses were used to assess the ability of the phyto-metabolites to kill cancer cells. The cytotoxicity and selectivity endpoints were also used as guidance in selection of which compounds to use for downstream experiments and further analyse the mechanisms of cytotoxicity.

3.3.1 MTT Cell Proliferation Assay

3.3.1.1 Principle

MTT is a popular yellow tetrazolium salt used for cell growth assays and was superior when compared to other tetrazolium salts by Mosmann in 1983.[164] The positive charge of the MTT tetrazole ring assists its movement across the cytoplasmic and mitochondrial membranes inside the cell.[165] MTT is then cleaved by oxidoreductase enzymes, mostly mitochondrial nicotinamide adenine dinucleotide (NADH) and partially by intracellular succinate dehydrogenase.[165] The colorimetric product of MTT cleavage is insoluble purple formazan, which is solubilized by additional agents such as DMSO or alcohols.[165] Therefore the NADH-reduction of MTT allows the quantitative and qualitative analysis of metabolic activity, which indirectly represents cell viability.[165] Solubilized formazan can be measured spectrophotometrically as the colorimetric indicator produces an absorbance. The absorbance can be read at a wavelength of 560 nm.[164]

Many *in vitro* cell viability assays performed by different investigators have shown notably variable results, due to chance variation in the number of mitochondria and abundance of intracellular dehydrogenase enzymes across different cells in culture.[166] Therefore pre-optimization of certain factors, such as cell density, drug treatment and MTT incubation periods are recommended to improve replicability and reproducibility of bioassays in drug discovery.[166]

3.3.1.2 Reagents

MTT (Thermo Fisher, Waltham, USA) was used to analyse the cytotoxicity of the compounds on HeLa cells. The MTT reagent is available in a yellow powdered format which was prepared according to a recipe as described by Mosmann in 1983.[164]

3.3.1.3 General MTT colorimetric assay and cell viability calculation

HeLa (10 000 cells/well), Vero (10 000 cells/well) and CaSki (12 000/well) cells were seeded in 96-well plates and incubated for 24 hours to allow for cell attachment. CAE21 and EGF25 were used to treat cells for 24 hours and CAE1, CAE3, CAE5, CAE8, DBF4, EGF4, EGF36 and RAR2 for 48-hour treatments. All compounds were treated in various concentrations of 0, 5, 25, 50, 75 and 100 µM. Compound treatments of 0 µM contained only 0.1% DMSO which was also used as a negative control. CaSki cells, however, were subject to treatments of CAE1, CAE3, CAE5, CAE8, DBF 4, EGF4 and EGF36, but not RAR2, at 0 – 100 µM with reduced final DMSO concentrations to eliminate background solvent effects.

After treatment, 20 µL of 5 mg/ml MTT solution prepared in 1x PBS was added to each well and incubated for 4 hours at 37 °C. Media containing MTT was discarded and the resultant formazan product was solubilized in 200 µL 99.9% (v/v) DMSO. The absorbance of the solubilized formazan was then measured by spectrophotometry using the SpectraMax® Paradigm® multi-mode microplate reader (Molecular Devices, San Jose, USA). Microplates were scanned at a wavelength of 570 nm and background absorbance at 670 nm was subtracted from the former. Cell viability percentages were calculated from absorbances (Abs) using the following formula:

$$\%\ Cell\ viability = \frac{Abs(_{treated\ cells}) - Abs(_{blank})}{Abs(_{untreated\ cells}) - Abs(_{blank})} \times 100$$

3.3.1.4 *IC_{50} determination and compound selection for downstream studies*

The average cell viability percentages were summarized in bar charts with error bars using GraphPad Prism. Average cell viability data were also normalized according to the lowest and highest values which were used as the 0 % and 100 % references on the y-axis and the concentrations on the x-axis (0 – 100 µM) were logarithmically transformed. The actual dose-response curves for each compound treatment were co-plotted with their respective lines of best-fit from which their logIC_{50}, IC_{50} and R^2 values were determined using the GraphPad non-linear regression analyses. The R^2 values indicate the quality of fit of the actual dose-response curve to the line of best-fit. This is represented as a value between 0 and 1 with 0 being the worst fit and 1 being the best fit. The IC_{50} dose is the concentration at which a compound results in 50 % cell viability in which highly cytotoxic compounds have low IC_{50} values.

The determined IC_{50} values were then compared to reported IC_{50} data of similar compounds as well as recommendations from literature based on selection criteria used in the NCI-60 drug screens which are also described by Boik.[167] Compounds with IC_{50} concentrations below 50.00 µM were selected as anti-cancer compounds to be assessed by downstream studies. The SI values were calculated according to the formula below in which Vero cells were used as a non-cancer cell line. Compounds were considered sufficiently cancer cell-selective if their SI values were above 2, which was also used in research conducted by Artun, *et al*.[168]

$$SI = \frac{IC_{50}\ in\ Vero\ cells}{IC_{50}\ in\ cancer\ cells}$$

3.3.1.5 *Additional cell viability studies*

HeLa (10 000 cells/well) and Vero (10 000 cells/well) cells were seeded at in 96-well plates and co-treated at various fractions (0.06x, 0.13x, 0.25x, 0.50x and 1.00x) of the IC_{50} of the 2 most bioactive compounds. HeLa cells seeded at 8 000 cells/well were also treated at individual and combined CAE21 and EGF25 IC_{50} fractions 20.0 and 22.5 µM to confirm cell response to the fractioned IC_{50} doses.

3.3.2 xCelligence real-time cell analysis

3.3.2.1 Principle

xCELLigence™ systems employ RTCA technology that live-tracks the electrical dynamics in biological samples.[169] The path through which electrons move is altered in the presence of adherent cells, a phenomenon known as cell impedance.[169] xCELLigence packages includes microtiter E-plates containing microelectrodes at the base of its wells that can monitor cells during the treatment protocol.[169] This apparatus is connected to a power source and biosensor that measures changes in cell impedance when an electrical current is applied.[169] The RTCA sends data to a computer, allowing convenient real-time analysis of cell impedance.[169] This is converted to a value referred to as the cell index (CI) which indicates changes in cell attachment, growth and viability.[169] Increasing CI values are interpreted as increased cell proliferation and decreasing CI values indicate decreased cell proliferation.[169] RTCA is preferred over traditional cell assays as it is more sensitive and does not require dyes or substrates to quantify cell growth, reducing accidental contamination and saving time.[169]

3.3.2.2 Materials

The xCELLigence™ RTCA system was used to measure real-time time-dependent effects of compounds on cervical cancer cell growth and adherence. The xCELLigence™ products include a wireless RTCA instrument, software component and disposable 16-well E-plates (ACEA Biosciences, Inc, San Diego, USA).

3.3.2.3 Technique

HeLa (8 000 cells/well), Vero (10 000 cells/well) and CaSki (12 000 cells/well) cells were seeded in 16-well DP E-plates at a maximum volume of 200 µL DMEM. Before seeding, background impedance was measured before addition of cells which were incubated for 24 hours to allow for cell adherence. Cell-free medium and untreated cells were used as background- and negative controls during real-time analysis. Before treatment, the CI values were captured at 0 minutes (T = 0) to use as a normalization time point. Individual and combined treatments of 40.0 µM CAE21 and 45.0 µM EGF25 for 24 hours were assessed in HeLa and Vero cells. 25 µM Camptothecin was used as a positive control. 2.1 and 3.5 % DMSO were used as vehicle controls of EGF25 alone and combined with CAE21.

Additional cytotoxic assessments were conducted in which HeLa, Vero and CaSki cells were subject to individual RAR2 treatments at 5, 25, 50, 75, 100 and 150 µM for 48 hours. CI dose-response curves were generated from CI values attained every 15 minutes in HeLa and Vero cells. CI data was normalized according to T=0 according to which additional logarithmic dose-response curves were plotted and RAR2 IC_{50} doses were determined 24- and 48 hours post-treatment in HeLa, Vero and CaSki cells. MS excel was used for statistical analysis of independent repeated experiments.

3.4 Cell death analysis

3.4.1 Annexin-V-FITC/PI staining

3.4.1.1 Principle

A flow cytometer analyses multiple features and optical properties of individual cells that is quantified based on light signals deflected off stained or fluorescent cellular components.[170] Cells in suspension are arranged into single-file that then pass through a focused laser beam that illuminates the constituents of cells.[170] Bypassed and deflected photons travel in straight and perpendicular directions, resulting in forward and side-scatter perceived by photodetectors.[170] Forward-scattered light is used to measure the size of cells and side-scattered light determines the abundance of cellular components.[170] This machine is designed to allow the analysis of one cell at a time, accurately monitoring cell membrane integrity at the single-cell level.[170]

Apoptosis can be distinguished from other modes of cell death, using Annexin-V staining.[171] Annexin-V binds to externalized PS of pre-mortem apoptotic cells that result from PS-flips in the initial phase of apoptosis. [171] In contrast, necrosis may also be identified using intracellular dyes such as PI.[171] PI specifically stains DNA and RNA which occurs in necrotic cells due to a deteriorating nuclear membrane.[171] However, 2-D cell culture systems do not include phagocytes, therefore post-mortem apoptotic/necrotic cells will present with both Annexin-V and PI stains.[170-171] Many scientific products consist of Annexin-V linked to fluorescein isothiocyanate (FITC).[170] FITC emits fluorescence when excited by argon lasers that strengthen light signals and enhances the sensitivity of this technique.[170]

3.4.1.2 Reagents

Annexin V-FITC Apoptosis Detection Kit I (BD Pharmingen, Franklin Lakes, USA) was used. The staining package includes a 10 x Annexin V-binding buffer and an Annexin-V-FITC and PI dyes. 1 x Annexin V-binding buffer was prepared in 1 x PBS.

3.4.1.3 Technique

The Annexin-V-FITC and PI staining method was based on the manufacturer's instructions. HeLa cells were seeded at 150 000 cells per well in 6-well plates and incubated for 24 hours for cell attachment. Cells were then exposed to individual- and co-treatments of C21 and E25 for 24 hours. 0.1% DMSO was used as a negative control and 25 µM camptothecin as a positive control. DMSO dissolved in medium at concentrations of 1.4%, 2.1% and 3.5% were also used as vehicle controls for the C21 and E25 individual and co-treatments. After treatment for 24 hours, medium in the untreated samples was discarded to exclude dead cells and the cells washed with warm 1 x PBS. Media in the treated samples were transferred to 15 mL centrifuge tubes. Cells from all samples were trypsinizied, resuspended and transferred into their corresponding centrifuge tubes. Detached cells were centrifuged at 1 500 x g for 5 minutes and the supernatant was discarded. After washing the pellet with cold 1 x PBS, cells were centrifuged again at 1 500 x g for 5 minutes. The supernatant was discarded and the pelleted cells were resuspended in 1 x Annexin V buffer. 100 µL cells were then transferred into 1.5 mL reaction tubes. Cells were stained with ice cold 5 µL Annexin V-FITC and PI, vortexed lightly and incubated in the dark for 15 minutes at room temperature. Stained cells were then resuspended in 400 µL cold 1 x Annexin V-FITC binding buffer. Cell suspensions were then analysed individually using a CytoFlex flow cytometer (Beckman Coulter, Brea, USA). Apoptotic and necrotic cell populations were identified and quantified using the Kaluza Analysis 2.1.2 software.

3.5 *In silico* analysis of oral pharmacokinetics and bioactivity prediction of molecular targets

3.5.1 Pharmacokinetic analysis based on compounds' molecular properties

3.5.1.1 Procedure

Compounds with previously known structures were entered using the Simplified Molecular Input Line Entry System (SMILES) and novel compounds (i.e. CAE21, EGF25 and DBF4) were drawn using the JSME Molecular Editor v2013-03-19 embedded into the Molinspiration software (https://www.molinspiration.com). The editor also generates SMILES for drawn structures. Molecular properties according to the structure were calculated and compared to the parameters of the Lipinski's rule of 5.

3.5.2 Bioactivity prediction of molecular targets of compounds

3.5.2.1 Procedure

The JSME Molecular Editor v2013-03-19 on the Molinspiration online software was used to draw compounds directly or by using SMILES. The bioactivity score of each compound was calculated to predict compound activity against 6 pharmacological classes based on their respective biological targets. These are namely GPCR ligands, ion channel modulator, kinase inhibitor, nuclear receptor ligand, protease inhibitor and enzyme inhibitor. Scores are determined by evaluating bioactive and non-active QSARs from a database of thousands of compounds using Bayesian statistics (https://www.molinspiration.com).

3.6 Statistical analysis

Data from two or three experimental replicates were averaged and represented as the mean ± standard deviation (SD). Dose-response curves from average cell viability data were generated and individual compound IC_{50} doses were determined by non-linear regression using the GraphPad Prism 9 software. For combination treatments, a student's t test was used for statistical analyses where comparisons with the negative control resulting in p values < 0.05 were considered significant. Microsoft (MS) Excel was used to analyse and generate graphical representations of data from combination treatments.

4 Results

4.1 Cytotoxicity and cancer selectivity of plant-based compounds

Compounds administered for 24 hours, namely CAE21 and EGF25, produced model-fitted dose response curves in HeLa cells with R^2 values of 0.98 and 0.94, respectively (**figure 9** and **figure 10**). CAE21 (**figure 9**) revealed sufficient cytotoxicity with an IC_{50} of 42.94 µM (**table 2**) after 24-hours in HeLa cells, which was slightly more potent than EGF25 (IC_{50} = 44.65 µM; **figure 10**)**.** Vero cells were more sensitive to CAE21 and EGF25, resulting in IC_{50} values of 38.51 and 28.54 µM, respectively. However, both CAE21 and EGF25 were less potent than 24-hour treatments of camptothecin (positive control) in HeLa (IC_{50} = 31.72 µM) and Vero (IC_{50} = 4.54 µM) cells. Other terpenoids (**table 4**) and flavonoids (**table 5**) in literature were also shown for comparison and later discussion (p61).

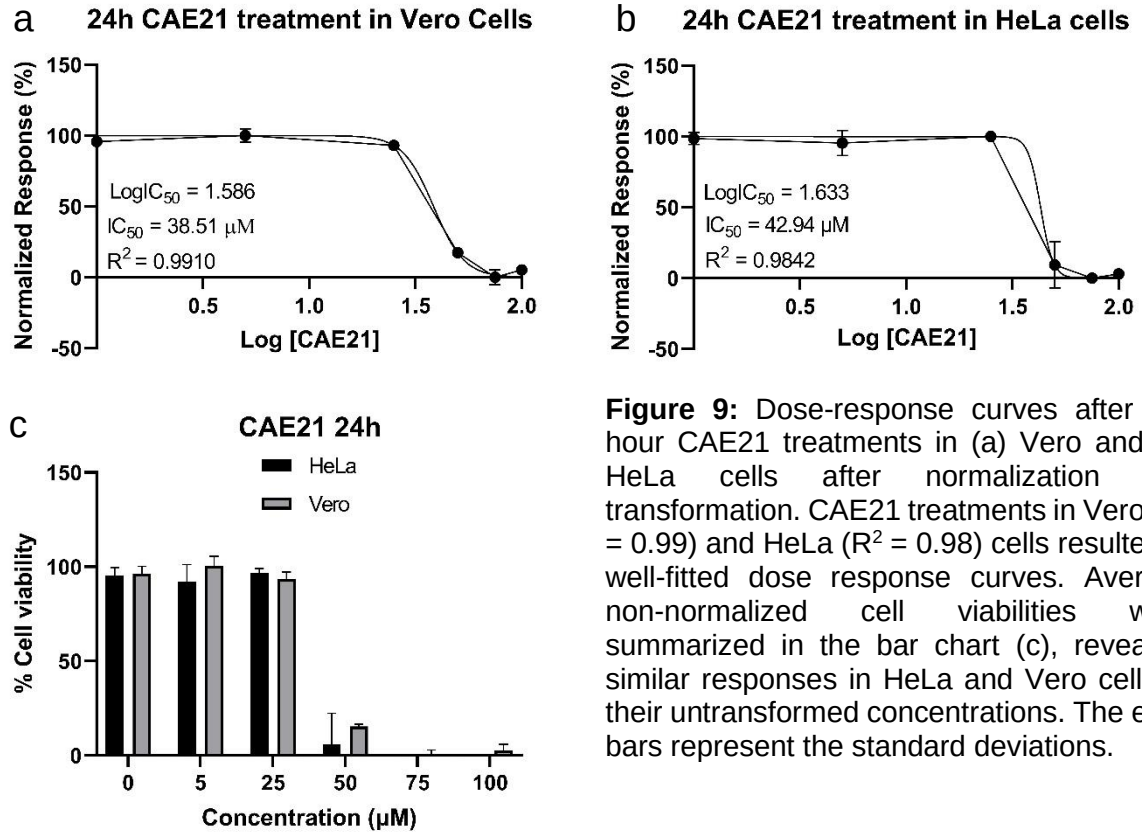

Figure 9: Dose-response curves after 24-hour CAE21 treatments in (a) Vero and (b) HeLa cells after normalization and transformation. CAE21 treatments in Vero (R^2 = 0.99) and HeLa (R^2 = 0.98) cells resulted in well-fitted dose response curves. Average non-normalized cell viabilities were summarized in the bar chart (c), revealing similar responses in HeLa and Vero cells at their untransformed concentrations. The error bars represent the standard deviations.

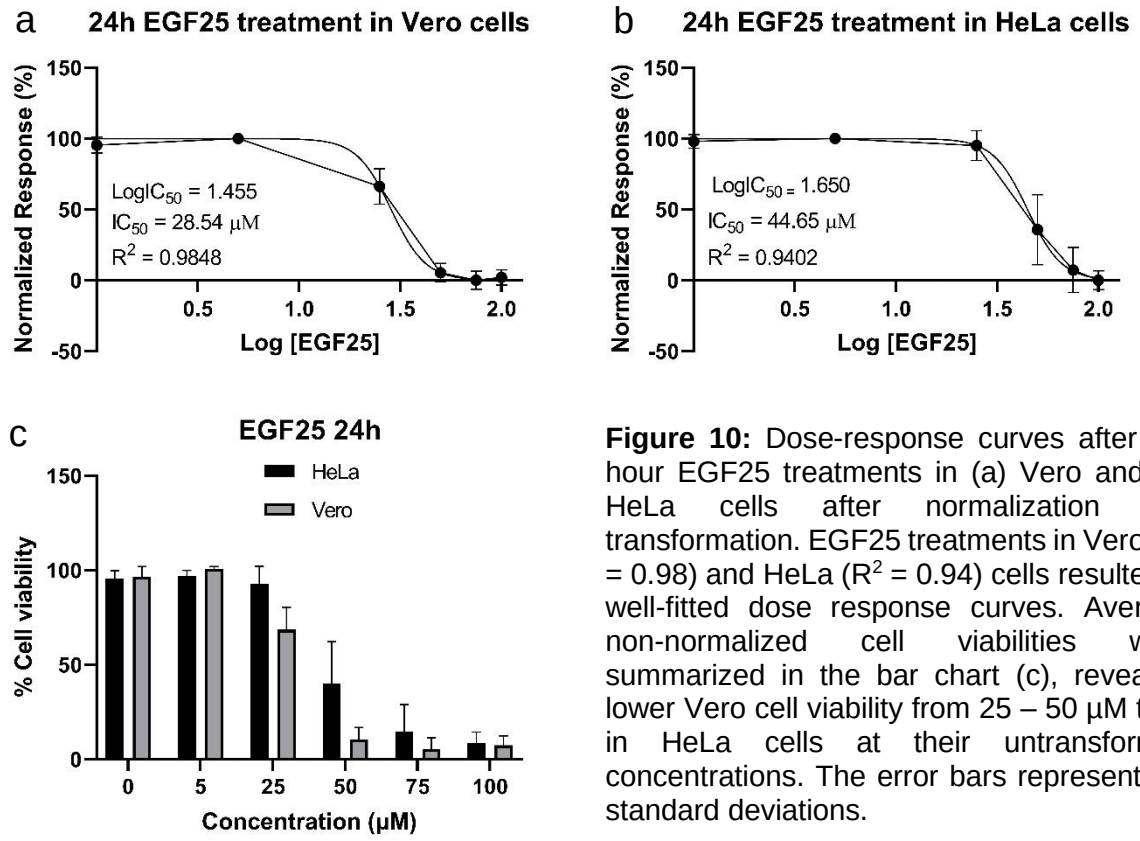

Figure 10: Dose-response curves after 24-hour EGF25 treatments in (a) Vero and (b) HeLa cells after normalization and transformation. EGF25 treatments in Vero (R^2 = 0.98) and HeLa (R^2 = 0.94) cells resulted in well-fitted dose response curves. Average non-normalized cell viabilities were summarized in the bar chart (c), revealing lower Vero cell viability from 25 – 50 µM than in HeLa cells at their untransformed concentrations. The error bars represent the standard deviations.

Table 2: IC_{50} concentrations of compounds CAE21 and EGF25 in Vero and HeLa cells after 24-hour treatments. The IC_{50} of camptothecin was determined by the same means as the other compounds and a 24-hour treatment of camptothecin used as a positive control. SI are shown in the last column in which SI values ≥ 2 were considered sufficiently selective of HeLa cells compared to Vero cells.[168]

Compounds	IC_{50} (µM) in Vero cells	IC_{50} (µM) in HeLa cells	HeLa cell selectivity (SI_{HeLa})
CAE21	38.51	42.94	0.90
EGF25	28.54	44.65	0.64
Camptothecin	4.54	21.72	0.21

CAE21 and EGF25 (**table 2**) revealed notable anti-cancer effects in HeLa cells as they revealed IC_{50} doses below, but close to 50.00 µM. However, these compounds exhibited stronger cytotoxicity in the non-cancer Vero cells, resulting in low cancer cell selectivity of CAE21 (SI = 0.90) and EGF25 (SI = 0.64). According to Boik, bioactive compounds (exhibiting IC_{50} doses between 1 and 50 µM) have potential synergism when used in combination.[167]

Regression analyses of 48-hour treatments of cells revealed CAE1 (**figure 11**) as the most cytotoxic compound to HeLa cells with an IC_{50} concentration of 2.24 µM (**table 3**). This was more potent than the 48-hour treatment of camptothecin in HeLa cells (IC_{50} = 7.77 µM). CAE1 (IC_{50} = 18.25 µM), CAE3 (IC_{50} = 0.15 µM; **figure 12**), CAE8 (IC_{50} = 6.29 µM; **figure 14**) and EGF36 (IC_{50} = 21.37 µM; **figure 17**) also revealed sufficient cytotoxicities (i.e. IC_{50} < 50 µM) in CaSki cells after 48-hours, in which CAE3 was the most potent. However, only CAE3 revealed higher cytotoxicity than camptothecin (IC_{50} = 3.76 µM) amongst the 48-hour treatments in CaSki cells. Vero cells were also sensitive to CAE1 (IC_{50} = 27.59 µM) and camptothecin (IC_{50} = 3.96 µM) after 48-hour treatments. Compounds CAE5 (**figure 13**), DBF4 (**figure 15**), EGF4 (**figure 16**) and RAR2 (**figure 18**) revealed weak HeLa, CaSki and Vero cytotoxicities (IC_{50} > 50 µM) after 48-hour treatments.

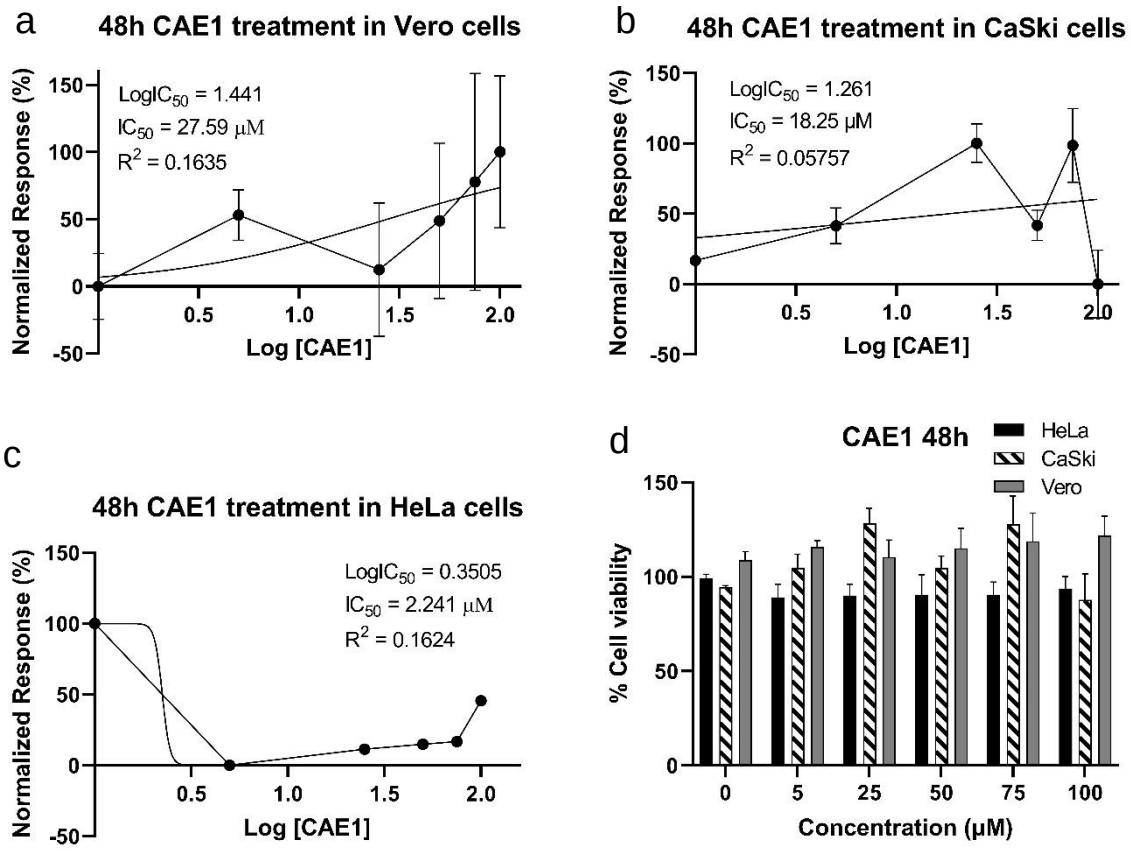

Figure 11: Dose-response curves after 48h-hour CAE1 treatments in (a) Vero and (b) CaSki and (c) HeLa cells after normalization and transformation. CAE1 treatments in Vero (R^2 = 0.16), CaSki (R^2 = 0.06) and HeLa (R^2 = 0.16) cells resulted in poorly fitted dose-response curves. Average non-normalized cell viabilities were summarized in the bar chart (d), revealing lowest HeLa cell viability at 25 and 75 µM than in Vero cells at their untransformed concentrations. The error bars represent the standard deviations.

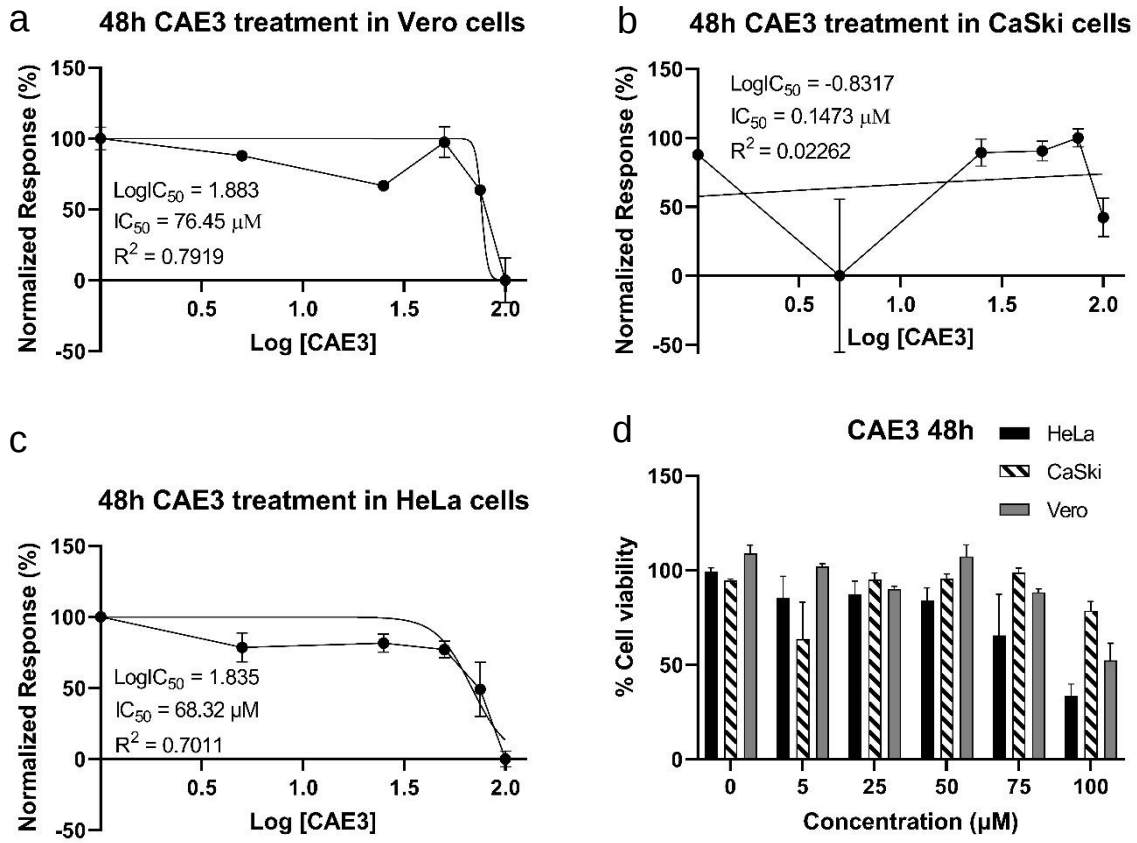

Figure 12: Dose-response curves after 48-hour CAE3 treatments in (a) Vero and (b) HeLa cells after normalization and transformation. CAE3 treatments in Vero (R^2 = 0.79) and HeLa (R^2 = 0.70) cells resulted in well-fitted dose response curves, whereas it was poorly fitted in CaSki cells (R^2 = 0.02). Average non-normalized cell viabilities were summarized in the bar chart (d), revealing similar responses in Vero, CaSki and HeLa cells at all their untransformed concentrations except at 100 µM where HeLa cell viability was lowest. The error bars represent the standard deviations.

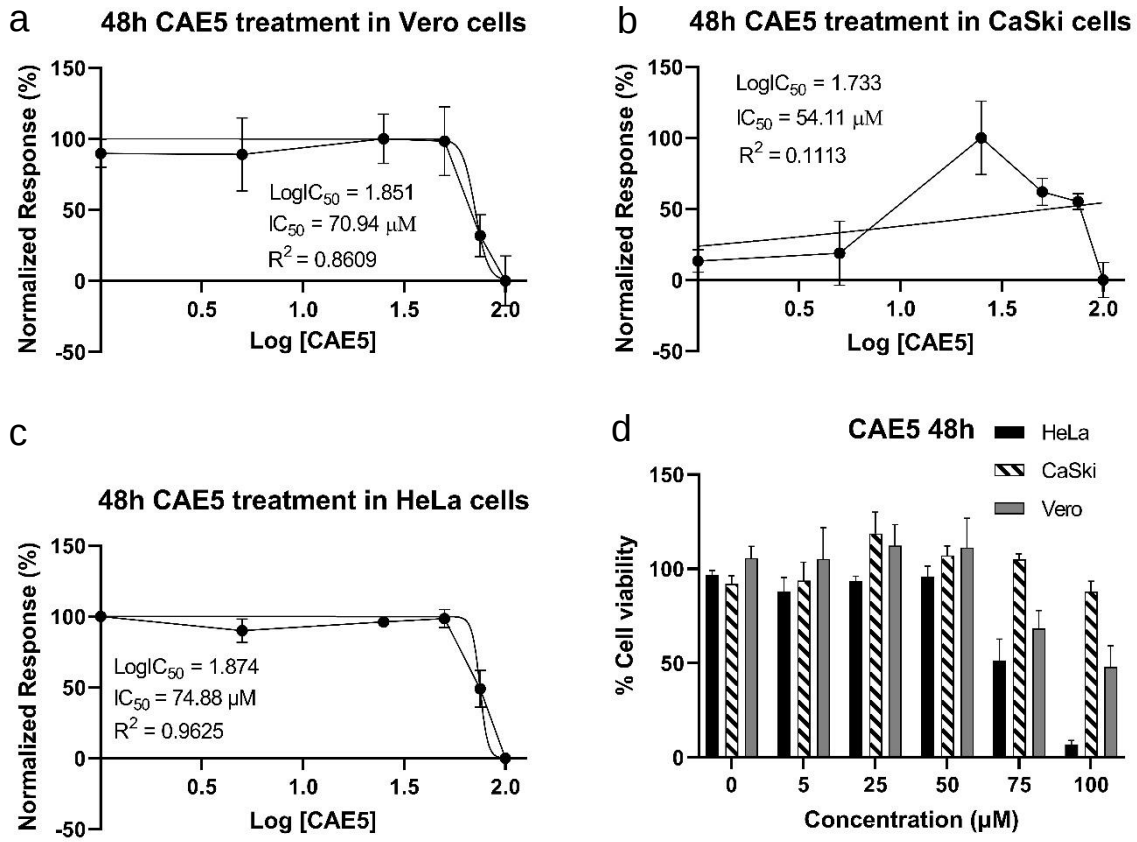

Figure 13: Dose-response curves after 48-hour CAE5 treatments in (a) Vero, (b) CaSki and (c) HeLa cells after normalization and transformation. CAE5 treatments in Vero (R^2 = 0.86) and HeLa (R^2 = 0.96) cells resulted in well-fitted dose response curves, whereas it was poorly fitted in CaSki cells (R^2 = 0.11). Average non-normalized cell viabilities were summarized in the bar chart (d), revealing lower cell viabilities in HeLa cells compared to CaSki cells at untransformed concentrations 75 and 100 µM. The error bars represent the standard deviations.

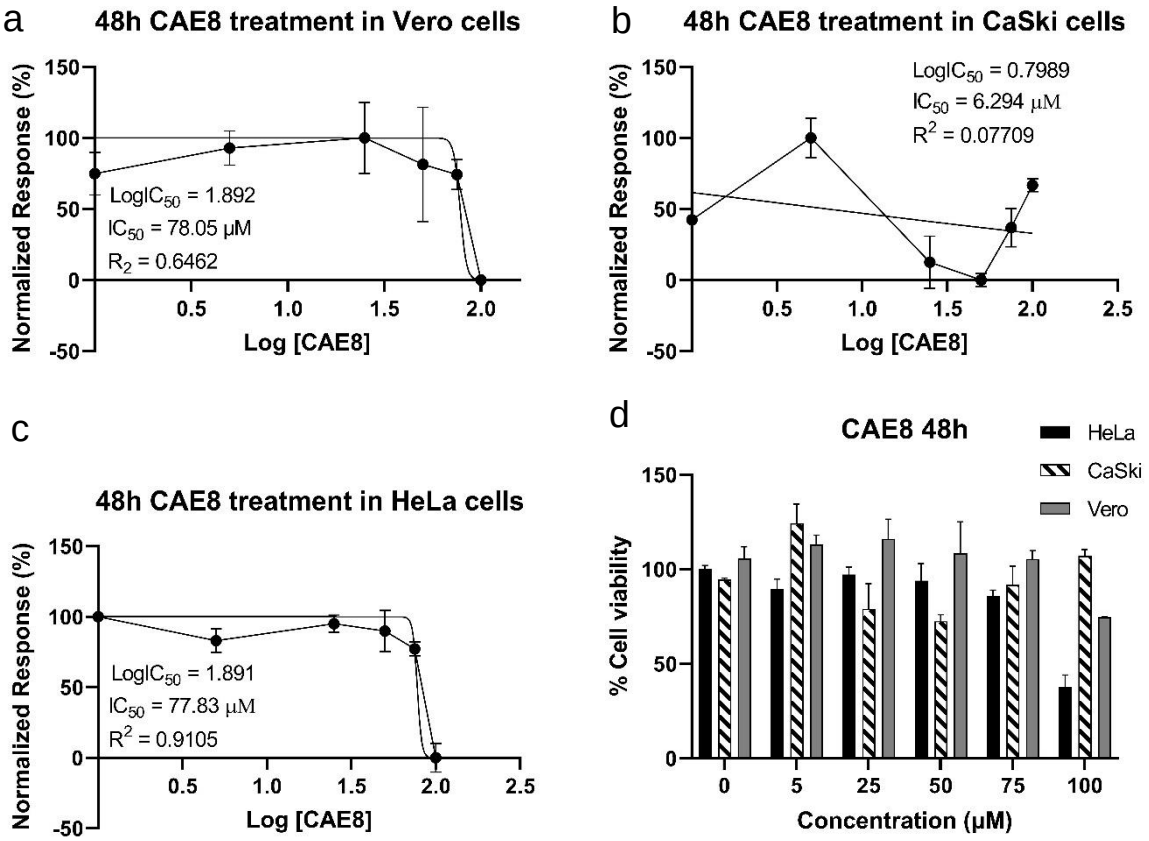

Figure 14: Dose-response curves after 48-hour CAE8 treatments in (a) Vero, (b) CaSki and (c) HeLa cells after normalization and transformation. CAE8 treatments in Vero (R^2 = 0.65) and HeLa (R^2 = 0.91) cells resulted in well-fitted dose response curves, whereas it was poorly fitted in CaSki cells (R^2 = 0.08). Average non-normalized cell viabilities were summarized in the bar chart (d), revealing lower cell viability in HeLa cells than CaSki cells at untransformed concentration 100 µM. In contrast, CaSki cell viability was lowest at 25 and 50 µM. The error bars represent the standard deviations.

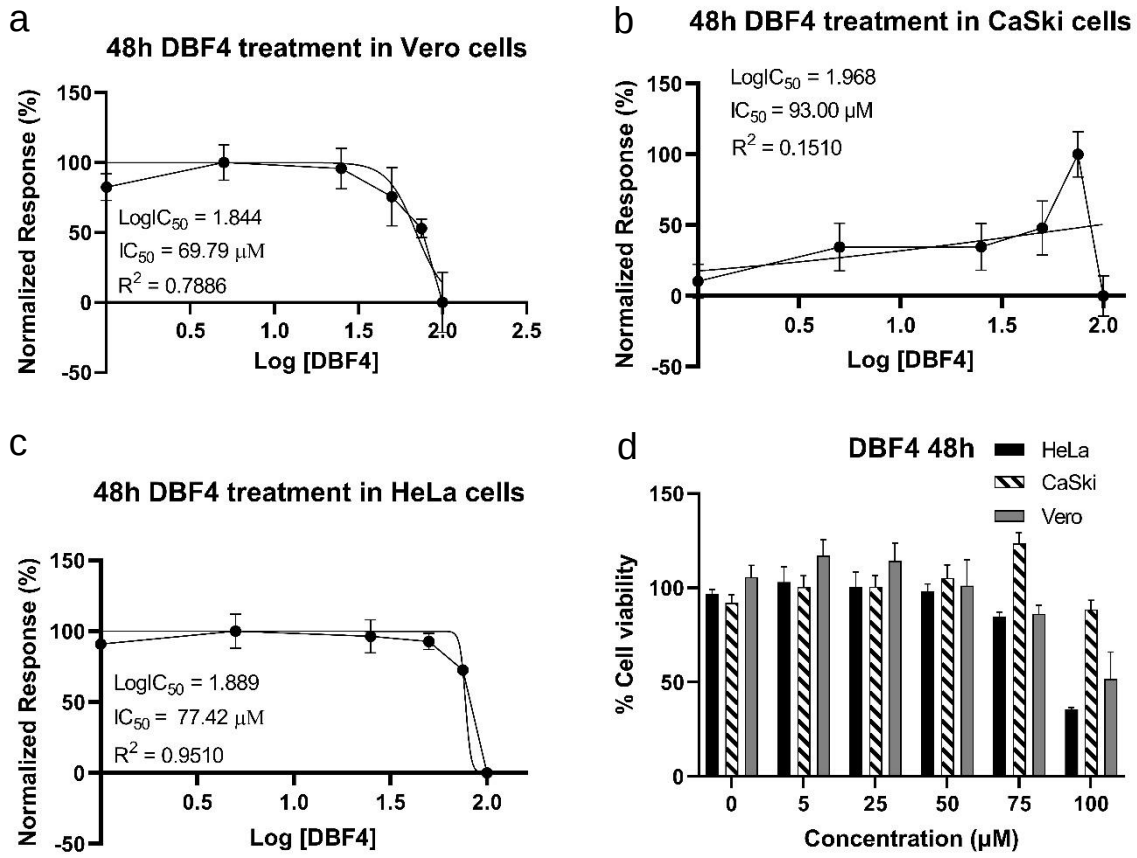

Figure 15: Dose-response curves after 48-hour DBF4 treatments in (a) Vero, (b) CaSki and (c) HeLa cells after normalization and transformation. DBF4 treatments in Vero (R^2 = 0.79) and HeLa (R^2 = 0.95) cells resulted in well-fitted dose response curves, whereas it was poorly fitted in CaSki cells (R^2 = 0.15). Average non-normalized cell viabilities were summarized in the bar chart (d), revealing lower HeLa cell viabilities than in CaSki cells at untransformed concentrations of 75 and 100 µM. The error bars represent the standard deviations.

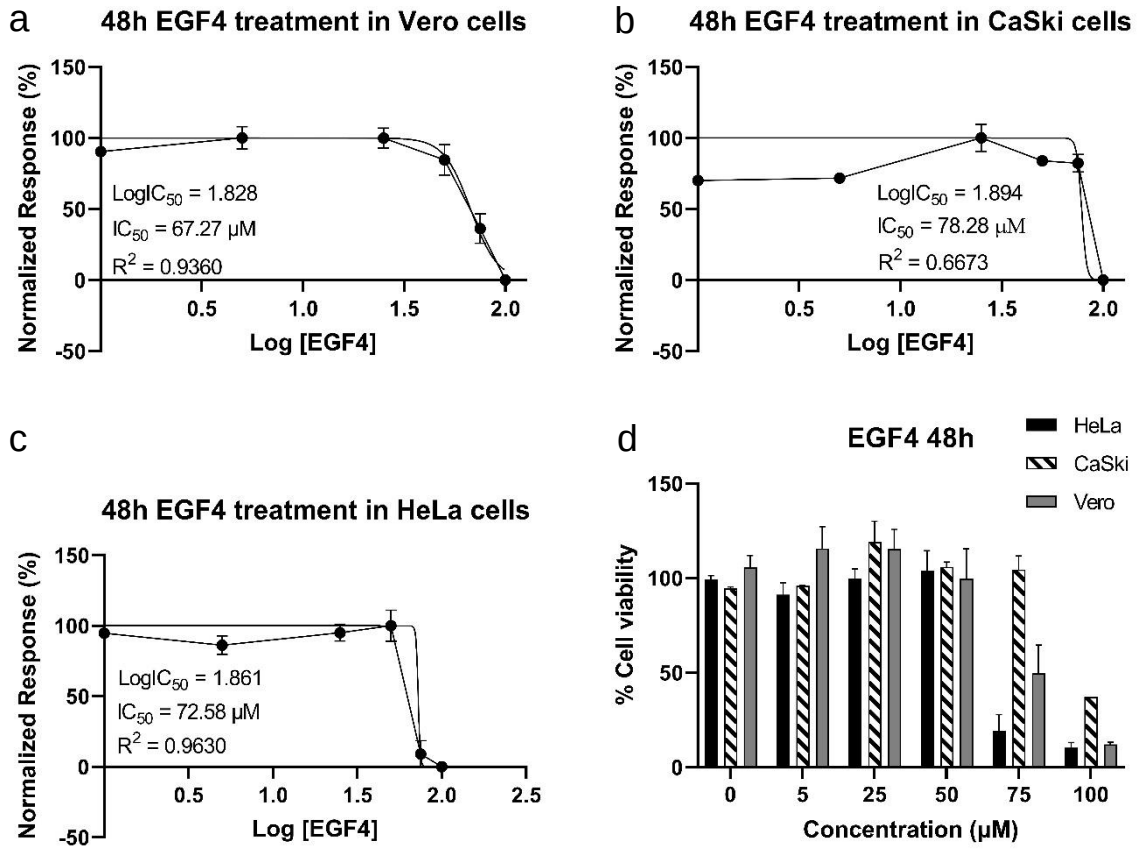

Figure 16: Dose-response curves after 48-hour EGF4 treatments in (a) Vero, (b) CaSki and (c) HeLa cells after normalization and transformation. EGF4 treatments in Vero (R^2 = 0.94), CaSki (R^2 = 0.67) and HeLa (R^2 = 0.96) cells resulted in well-fitted dose response curves. Average non-normalized cell viabilities were summarized in the bar chart (d), revealing notably lower HeLa cell viabilities at untransformed concentrations of 75 and 100 µM compared to CaSki cells. The error bars represent the standard deviations.

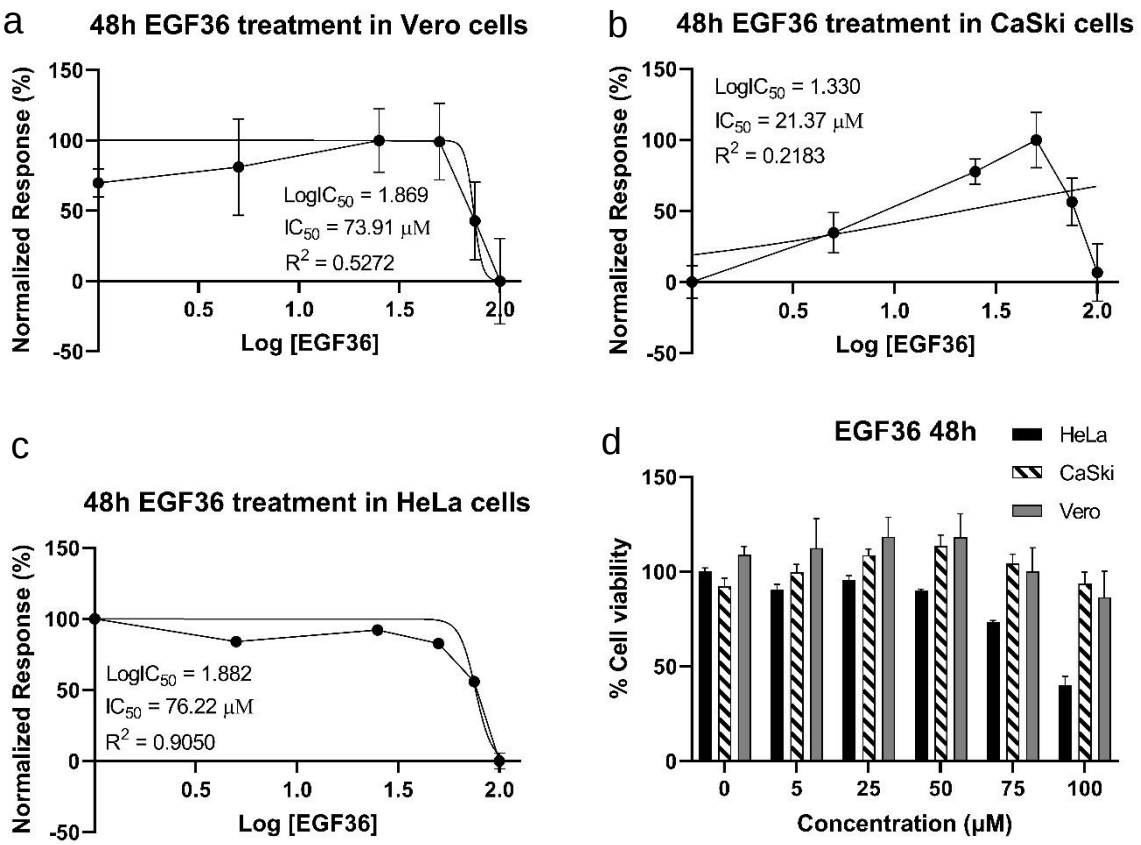

Figure 17: Dose-response curves after 48-hour EGF36 treatments in (a) Vero, (b) CaSki and (c) HeLa cells after normalization and transformation. EGF36 treatments in Vero cells (R^2 = 0.53) yielded a moderately-fitted curve, but a poor fit in CaSki cells (R^2 = 0.22). Dose-response in HeLa cells (R^2 = 0.96) resulted in a well-fitted curve. Average non-normalized cell viabilities were summarized in the bar chart (d), revealing the lowest HeLa cell viability at untransformed concentrations of 50 to 100 µM. The error bars represent the standard deviations.

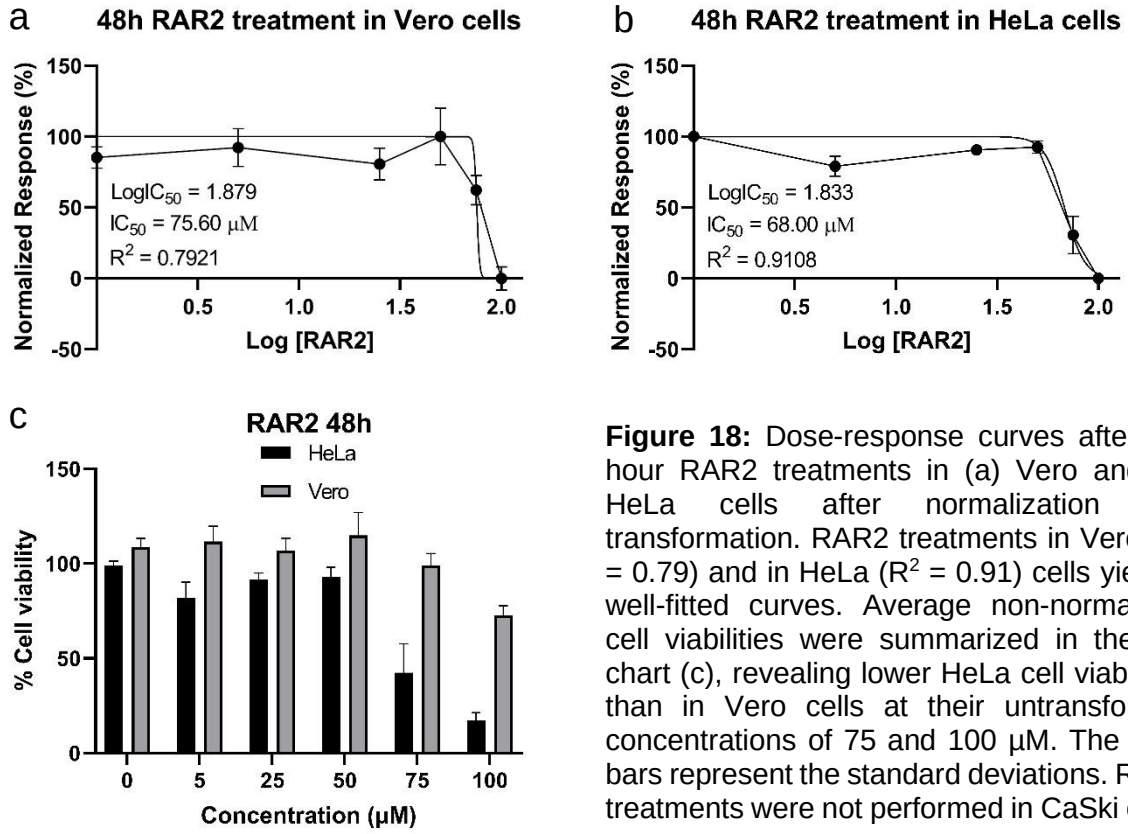

Figure 18: Dose-response curves after 48-hour RAR2 treatments in (a) Vero and (b) HeLa cells after normalization and transformation. RAR2 treatments in Vero (R^2 = 0.79) and in HeLa (R^2 = 0.91) cells yielded well-fitted curves. Average non-normalized cell viabilities were summarized in the bar chart (c), revealing lower HeLa cell viabilities than in Vero cells at their untransformed concentrations of 75 and 100 µM. The error bars represent the standard deviations. RAR2 treatments were not performed in CaSki cells.

Table 3: IC_{50} concentrations in Vero, HeLa and CaSki cells after 48-hour treatments determined by MTT. Only compounds CAE1, CAE3, CAE5, CAE8, DBF4, EGF4, EGF36 and RAR2 were used for 24-hour treatments. A 48-hour treatment of camptothecin was used as a positive control. *RAR2 IC_{50} values were determined during RTCA experiments only as limited compound prevented additional MTT experiments in CaSki.

Compounds	IC_{50} (µM) in Vero cells	IC_{50} (µM) in HeLa cells	IC_{50} (µM) in CaSki cells	HeLa cell selectivity (SI_{HeLa})	CaSki cell selectivity (SI_{CaSki})
CAE1	27.59	2.24	18.25	12.32	1.51
CAE3	76.45	68.32	0.15	1.12	509.67
CAE5	70.94	74.88	54.11	0.95	1.31
CAE8	78.05	77.83	6.29	1.00	12.41
DBF4	69.79	77.42	93.00	0.90	0.75
EGF4	67.27	72.58	78.28	0.93	0.86
EGF36	73.91	76.22	21.37	0.97	3.46
RAR2	75.60	68.00	No data*	1.11	N/A
Camptothecin	3.96	7.77	3.76	0.51	1.05

CAE1 cancer cell selectivity was observed as sufficient (SI > 2), higher than 48-hour camptothecin treatments (SI_{HeLa} = 0.51) and the highest in HeLa cells (SI_{HeLa} = 12.32) because its IC_{50} was more than twice the potency as in Vero cells (**table 3**). CAE3 (SI_{CaSki} = 509.67), CAE8 (SI_{CaSki} = 12.41) and EGF36 (SI_{CaSki} = 3.46) also exhibited higher CaSki cell selectivities than camptothecin (SI_{CaSki} = 1.05) after 48 hours. However, CAE1 did not produce well-fitted dose-response curves in HeLa nor CaSki cells with low R^2 values of 0.16 and 0.05. This was also the case for CAE3 (R^2 = 0.02), CAE8 (R^2 = 0.07) and EGF36 (R^2 = 0.22) dose-response curves after 48-hour treatments in CaSki cells.

Other terpenoid and flavonoid compounds from previous studies in literature revealed micromolar IC_{50} concentrations ranging from 1.40 µM to 130.00 µM. The terpenoids all revealed sufficient cytotoxicities (IC_{50} < 50 µM) in colon, cervical, breast, lung, pancreatic- and neuron cancer cells (**table 4**). However, only 3 of the reported flavonoids (i.e. 4 H-1-benzopyran-4-one,2-(4-hydroxyphenyl)-3,7-dihydroxy-5-methoxy-8-[5-methyl-2-(1-methylethenyl)-4-hexenyl] and ferulic acid) revealed IC_{50} values more potent than 50 µM in lung, colon and cervical cancer cells *in vitro* (**table 5**). The remaining flavonoids demonstrated inactive cytotoxicity against cervical cancer cells (IC_{50} > 50 µM).

Table 4: IC_{50} data of known triterpenoids from literature from various human cancer cell lines. Micromolar IC_{50} data with numbered references are described.

Compound name	IC_{50} dose (µM)	Cell line
Ursolic acid	24.00[172]	HCT-116 Colorectal cells
Maslinic acid	41.00[172]	HCT-116 Colorectal cells
Betulinic acid	3.95[173]	A-431 cervical carcinoma
	30.42[174]	HeLa cells
Lupeol	2.32[175]	MCF-7
	4.47[175]	MDA-MB-231
	10.20[175]	HeLa
Hederagenin	44.50[176]	A-549 lung cancer
	30.78[176]	HeLa
	31.40[176]	PANC-1 pancreatic cancer cells
	23.10[176]	SH-SY5Y neuroblastoma

Table 5: IC_{50} data of known flavonoids in various human cancer cell lines from literature. Micromolar IC_{50} data with numbered references are described.

Compound name	IC_{50} dose (µM)	Cell line
2′-hydroxyl neophellamuretin	56.10[177]	HeLa
2″-O-rhamnosylswertisin	69.00[177]	
4 H-1-benzopyran-4-one,2-(4-hydroxyphenyl)-3,7-dihydroxy-5-methoxy-8-[5-methyl-2-(1-methylethenyl)-4-hexenyl]	3.60[178]	A-549 lung cancer
	1.40[178]	HCT-116
Ferulic acid	14.00 – 16.00[179]	HeLa
		CaSki
Gallic acid	60.00 - 80.00[180]	HeLa
	90.00[180]	C33A
	110.00 - 130.00[180]	SiHa

4.2 Additive cytotoxicity of CAE21 and EGF25 in combination

CAE21 and EGF25 resulted in additive cytotoxic effects when treated in combination at their halved (20.00 µM and 22.50 µM) and full (40.00 µM and 45.00 µM) rounded IC_{50} doses (**figure 19**). However, the combined toxicity of the 20.0 µM CAE21 and EGF25 22.5 µM co-treatments were not reproduced in HeLa cells. Semi-quantitative RTCA revealed a rapid decrease in cell index in HeLa and Vero (**figure 20**) cells within the first hour of individual and combined EGF25 and CAE21 treatment. Similar results were observed for the camptothecin (CMT) control, although HeLa cells were notably less sensitive than Vero cells.

DMSO controls, 2.10% and 3.50% also revealed similar responses to CAE21 and EGF25 in HeLa and Vero cells. Unfortunately, primary stocks of CAE21 and EGF25 compound preparations were limited, and additional stocks could not be prepared with reduced DMSO concentrations. Therefore, compound dilutions of RAR2 were later prepared with DMSO concentrations < 1% (**figure 22**).

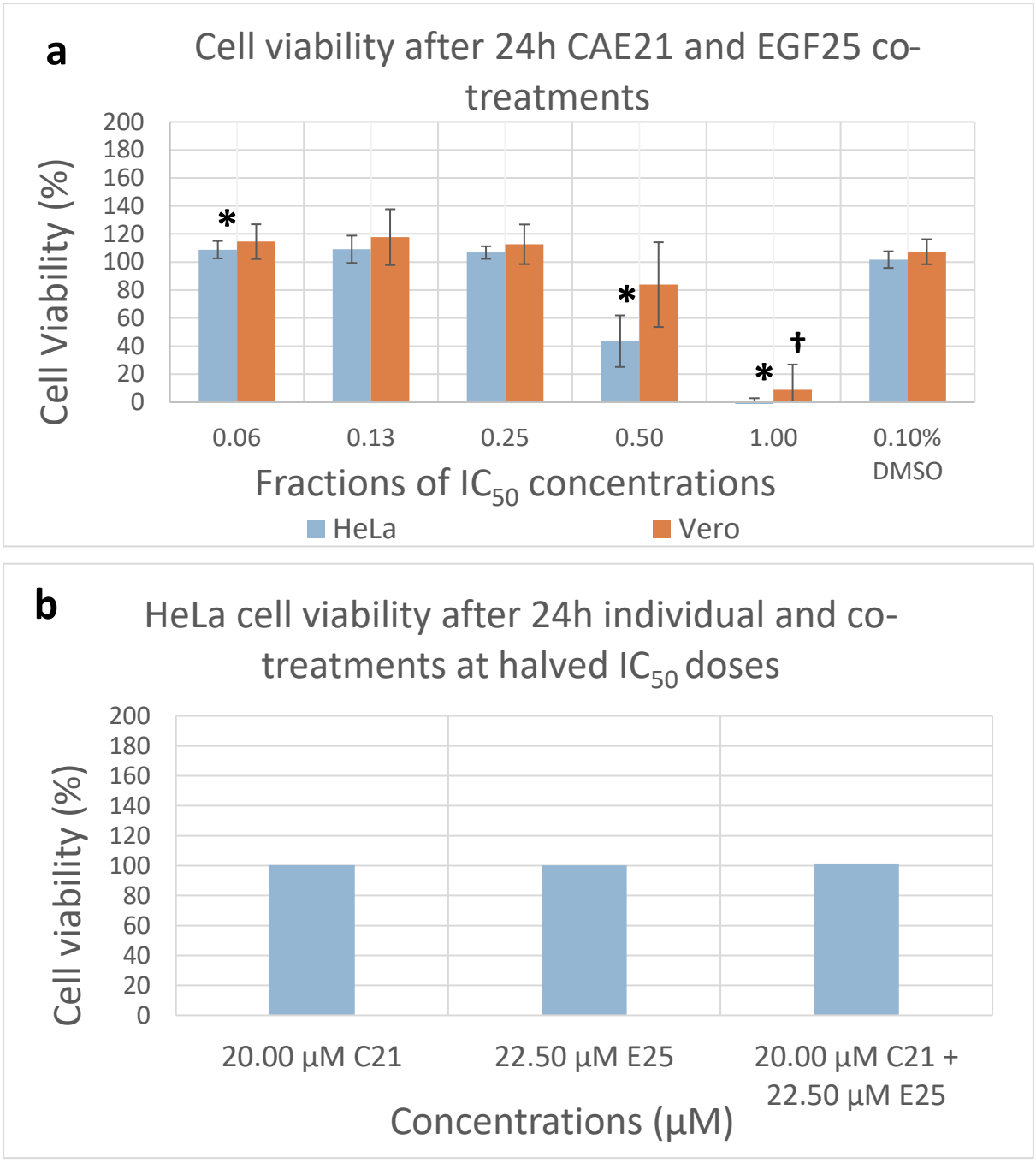

Figure 19: Cell viabilities in response to combined 24h treatments of CAE21 and EGF25 in HeLa and Vero cells (a) and confirmatory individual and co-treatments in HeLa cells alone (b). 0.50x the IC_{50} of CAE21 (20.00 µM) and EGF25 (22.50 µM) yielded significant additive effects compared to 0.1% DMSO in HeLa cells (*). These were inconsistent with the confirmatory CAE21 and EGF25 co-treatment (bottom), in which no notable differences were shown between individual and combined experiments. Statistically significant differences from DMSO in both HeLa and Vero cells (†) were also observed at 1.00x IC_{50} of CAE21 (40.00 µM) and EGF25 (45.00 µM).

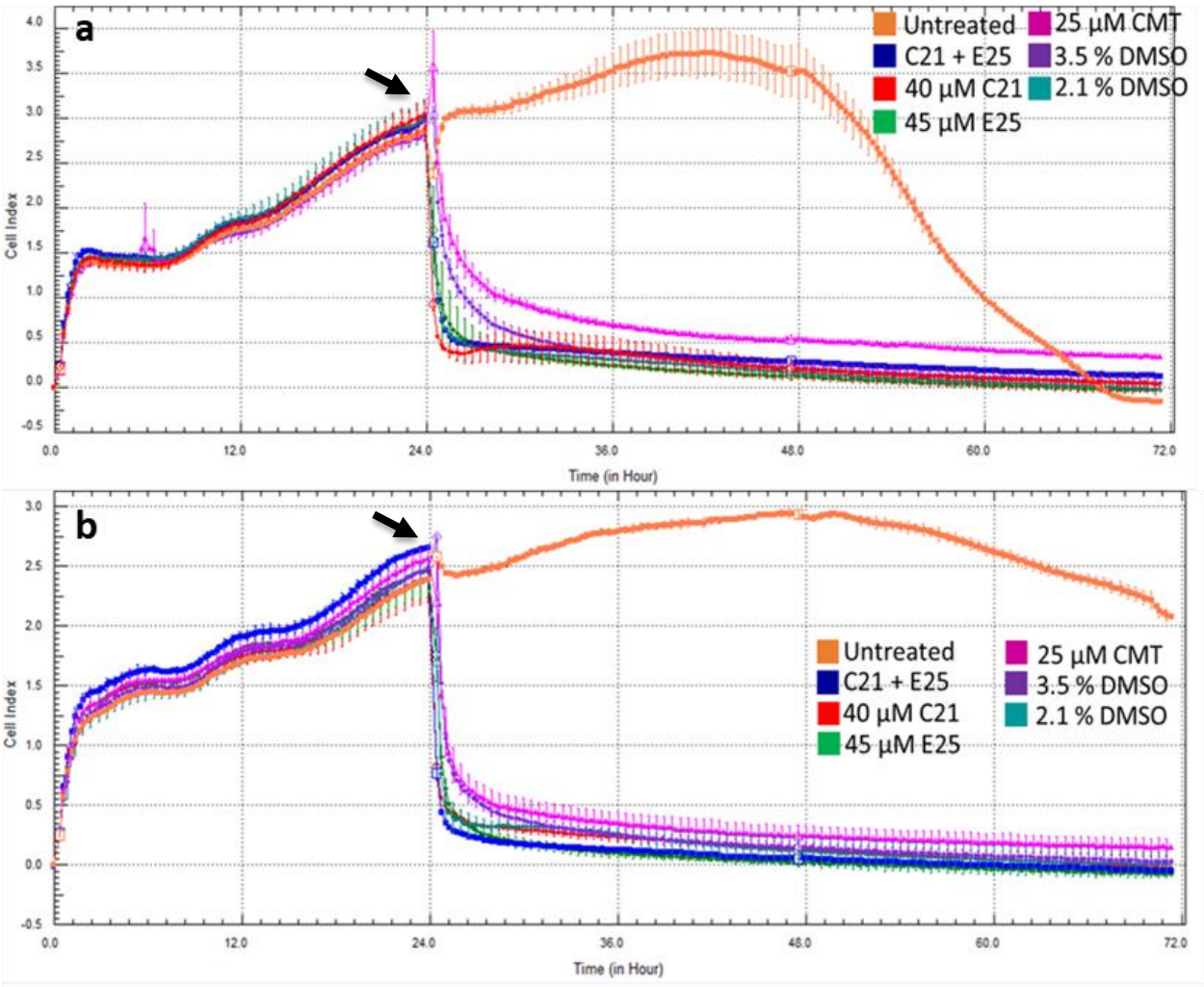

Figure 20: Cell index (CI) curves after 24h individual and combined treatments of 40.00 µM CAE21 (C21) and 45.00 µM EGF25 (E25) in HeLa (a) and Vero (b) cells. Average CI values obtained at 15-minute intervals for 72 hours were plotted using the RTCA DP software. 3.50% , 2.10% DMSO and 25 µM CMT (Camptothecin) were used as vehicle- and positive controls, respectively. Error bars in each curve indicate the standard deviations. CAE21 and EGF25 yielded similar cell death activity when each treated alone and in combination. However, the cytotoxicity of the DMSO solvents became notable during this experiment at 3.50% (combined CAE21 and EGF25 solvent) and 2.10% (E25 solvent) v/v concentrations. These were also similar to CAE21 and EGF25 individual and co-treatments, suggesting solvent interaction with cells. The black arrows indicate the time of treatment which was 24 hours after seeding (0 hours). CMT, Camptothecin.

4.3 Cell death responses to CAE21 and EGF25 co-treatments

HeLa cells were subject to individual and combined treatments of CAE21 (40.0 µM) and EGF25 (45.0 µM) at their full IC_{50} concentrations for 24 hours. Combined treatments induced apoptosis (sum of early and late) in 99.95 % (97.09 % + 2.86 %) of cells, with no necrotic cells (**figure 21**). This apoptotic population was additively more than the individual treatments of CAE21 and EGF25 which only resulted in total apoptosis of 63.51 % and 67.79 %.

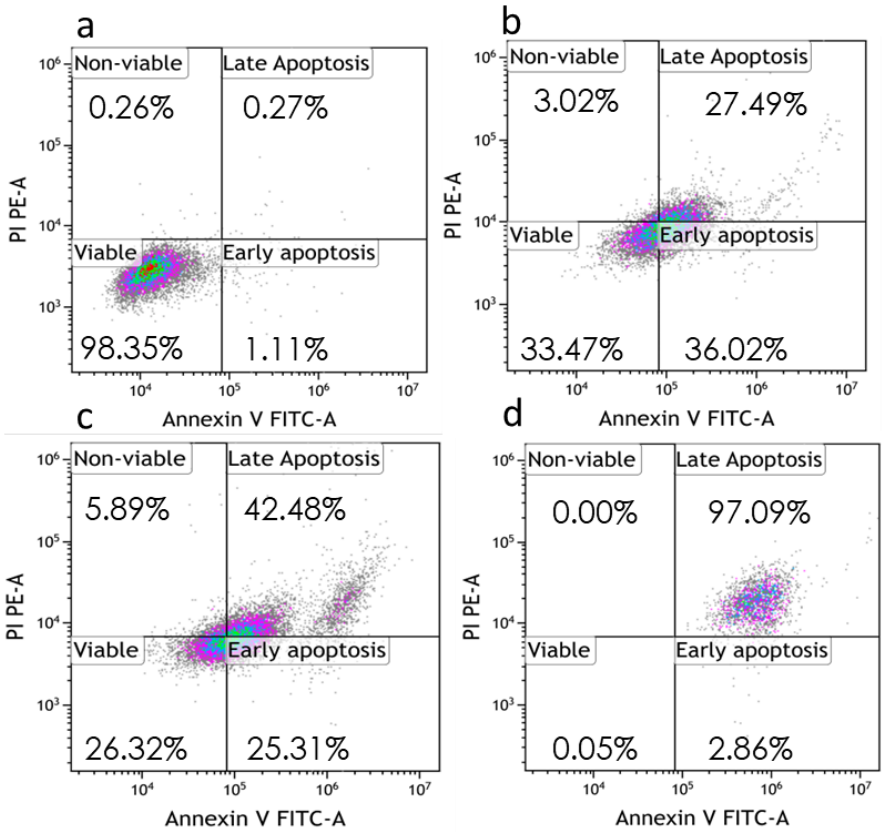

Figure 21: Percentage population of HeLa cells in necrosis (non-viable) and apoptosis (early and late apoptosis) in response to untreated (a) 40.00 µM CAE21 (b), 45.00 µM EGF25 (c) as well as 40.00 µM CAE21 and 45.00 µM EGF25 co-treatment (d). Data was obtained from one repeat, as there were not enough compounds for more repeated experiments. CAE21 and EGF25 combination produced an additive apoptotic response with no necrotic cells compared to individual treatments. Vero cells were not subject to flow cytometric analysis after individual and combined CAE21 and EGF25 treatments.

4.4 RAR2 cytotoxicity with a reduced DMSO solvent

HeLa, Vero and CaSki cells were subject to RAR2 compound treatments at concentrations 150, 100, 75, 50, 25 and 5 µM (DMSO solvent < 1%) in duplicate with 2 repeats in total. Plots of single representative experiments from each cell line are shown (**figure 22**) for visualization. CI values reflect the quality and number of cells attached to the base of each well of the E-plate. HeLa, CaSki and Vero cells did show notable decreases in cell indices after treatment with RAR2 when compared to the untreated control.

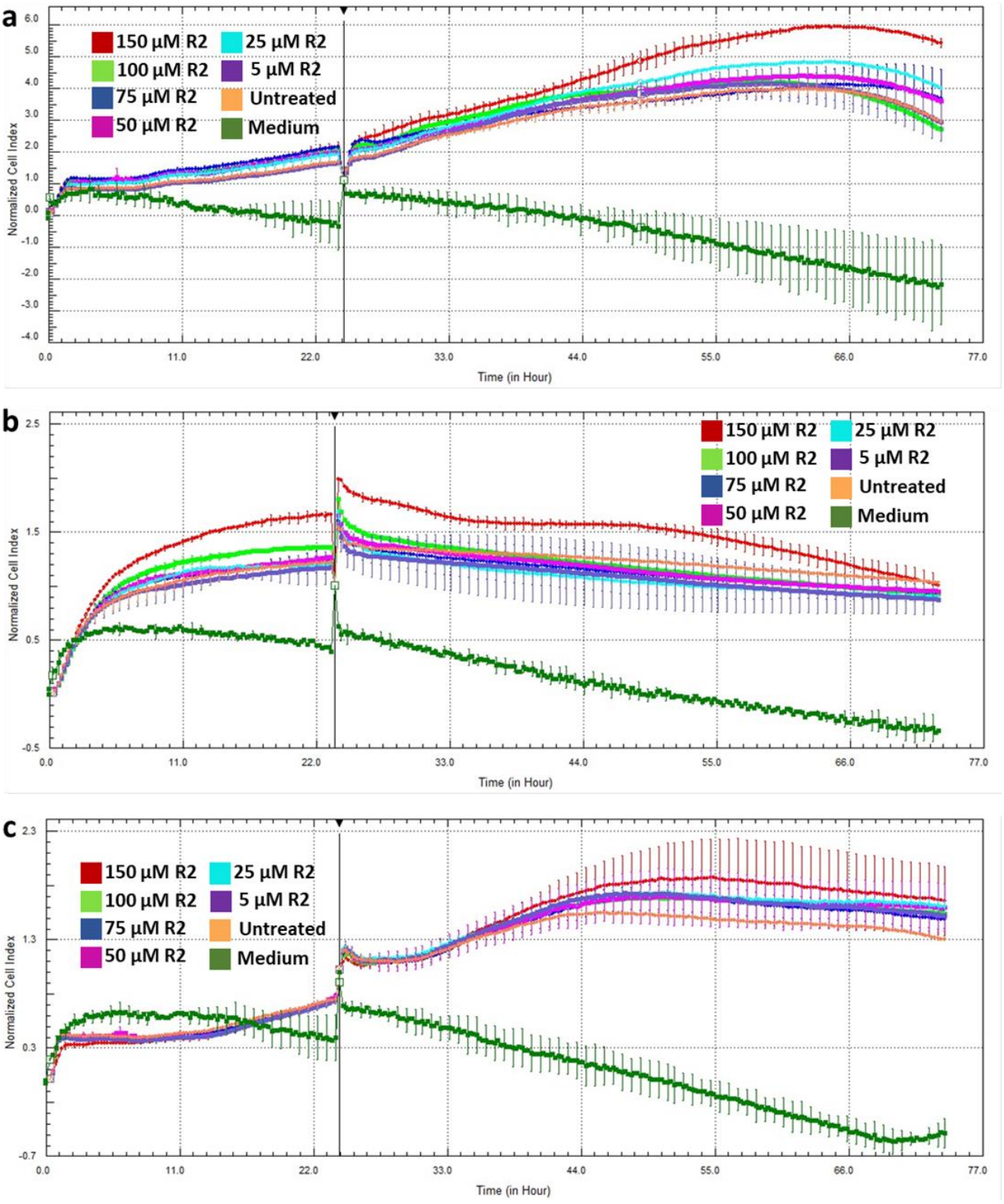

Figure 22: Average cell indices of HeLa (a), CaSki (b) and Vero (c) cells analysed in duplicate in real-time over 72 hours. RAR2 compound was added 24 hours after seeding at 150, 100, 75, 50, 25 and 5 µM. All data was normalized according to this point (indicated by the black line). Each graph is a qualitative representative from single experiments in each cell line. Various treatment conditions are labelled and coded according to colours displayed in the curve. Error bars are used to indicate the standard deviations.

The average IC_{50} doses of RAR2 from all available experiments were also determined using the RTCA software (**table 6**). Using this data, SI values were additionally determined to compare with results gained from MTT cytotoxicity assessments. However, RTCA analysis of RAR2 treatments in HeLa and CaSki cells did not reveal improved cytotoxic effects or cancer cell-selectivity. Therefore, the DMSO solvent did contribute to the cytotoxic effect of RAR2 determined using MTT (**table 3**). Vero cells were most sensitive to RAR2 when compared to both HeLa and CaSki cells after 24- (IC_{50} = 90.09 µM) and 48-hour (IC_{50} = 139.07 µM) treatments. This resulted in HeLa- and CaSki cell selectivity indices < 2.00, suggesting RAR2 does not sufficiently target cancer cells *in vitro*.

Table 6: Table of average RAR2 IC_{50} values from both experimental repeats. Results were represented as IC_{50} ± standard deviations. Thus far, RAR2 with DMSO > 1% yield weak cytotoxicities (IC_{50} > 50 µM) and low HeLa and CaSki cell selectivity (SI < 2).

Time of data collection	IC_{50} in Vero cells (µM)	IC_{50} in HeLa cells (µM)	IC_{50} in CaSki cells (µM)	HeLa selectivity	CaSki selectivity
24h post-treatment	90.09 ± 33.16	121.26 ± 69.17	187.43 ± 34.87	0.74	0.48
48h post-treatment	139.07 ± 14.01	675.59 ± 734.14	121.82 ± 45.32	0.21	1.14

4.5 Molecular properties and receptor target bioactivity

Orally bioavailable drugs may only have one violation to Lipinski's rule of 5.[109] CAE1, RAR2 and camptothecin had no violations to the rule of 5 whereas CAE3, CAE5, CAE8, CAE21 and EGF36 had only one violation (**table 7**). CAE1 and RAR2 also showed optimal TPSA and nrot physiochemical features (TSPA ≤ 120.00 Å, nrot ≤ 10.00). In contrast, CAE3 (log*P* = 7.04), CAE5 (log*P* = 8.29), CAE8 (log*P* = 6.12) and CAE21 (log*P* = 6.22) violated Lipinski's criteria by exceeding the log*P* limit of 5.00. EGF36 had 6.00 H-bond donors, also exceeding Lipinski's restriction of 5.00. DBF4 (MW = 578.52 g/mol, HBAs = 14.00, HBDs = 8.00), EGF4 (MW = 608.56 g/mol, HBAs = 13.00, HBDs = 6.00) and EGF25 (MW = 478.53 g/mol, HBAs = 12.00, HBDs = 6.00) revealed 3.00 violations to Lipinski's rules, in which all compounds had excessive MW, H-bond donor and acceptor values (i.e. MW ≥ 500.00 g/mol, HBAs ≥ 10.00, HBDs ≥ 5.00). From the two anti-cancer compounds chosen for co-treatments, CAE21 demonstrated oral bioavailability while EGF25 did not.

Table 7: Molecular properties of compounds compared to Lipinski's Rule of 5.00 with additional features attributing to drug-likability. Log*P*, HBAs, HBDs and nrot are all unitless values. Units are shown in table headings. In addition to Lipinski's rule of 5, orally bioavailable molecules often each possesses a TPSA ≤ 120.00 Å and nrot ≤ 10.00.[113,181] * CAE21, DBF4 and EGF25 are novel compounds.

Compound	Log*P*	TPSA (Å)	MW (g/mol)	HBAs	HBDs	#Lipinski violations	nrot
CAE1	1.37	110.37	290.27	6.00	5.00	0.00	1.00
CAE3	7.04	57.53	456.71	3.00	2.00	1.00	2.00
CAE5	8.29	20.23	426.73	1.00	1.00	1.00	1.00
CAE8	6.12	94.83	486.69	5.00	3.00	1.00	3.00
CAE21*	6.22	77.75	474.73	4.00	3.00	1.00	2.00
DBF4*	-0.91	228.97	578.52	14.00	8.00	3.00	6.00
EGF4	2.64	205.59	608.56	13.00	6.00	3.00	9.00
EGF25*	2.82	196.35	578.53	12.00	6.00	3.00	8.00
EGF36	0.68	170.05	432.38	10.00	6.00	1.00	4.00
RAR2	1.95	83.58	350.37	6.00	3.00	0.00	2.00
Camptothecin	2.03	81.43	348.36	6.00	1.00	0.00	1.00

Log*P*, lipophilicity; HBA, hydrogen bond acceptor; HBD, hydrogen bond donor; nrot, number of rotational bonds; TPSA, topological polar surface area

In silico QSAR analysis revealed a variety of bioactivity score predictions for six (6) different classes of molecular targets (**table 8**). *C. arereh* compounds CAE1, CAE3, CAE5, CAE8 and CAE21 showed strong bioactivity scores against nuclear receptors with activity values of 0.60, 0.93, 0.85, 0.78 and 0.76 respectively. Although showing weaker bioactivity scores, *C. arereh* compounds also showed sufficient potentials as protease inhibitors with each showing values > 0.00. CAE3, CAE5 and CAE21 were also strongly active against enzymes with scores of 0.55, 0.52 and 0.49. But camptothecin showed the highest bioactivity scoring 1.11 as an enzyme inhibitor. RAR2 showed the highest activity against GPCR receptors with a predicted value of 0.48. CAE1 was the most well-rounded, revealing sufficient bioactivity as all the drug classes with CAE5 and EGF36 showing strong activity in most classes, except as kinase inhibitors and ion channel modulators where they exhibited moderate effects respectively. CAE21 revealed strong activity against targets as GPCR (0.18) and nuclear receptor ligands (0.76), protease (0.22) and enzyme inhibitors (0.49) and moderate effects as ion channel modulators (-0.04) and kinase inhibitors (-0.40). In addition, EGF25 was found to be mildly effective as a GPCR ligand (0.00), ion channel modulator (-0.46), kinase (-0.12) and protease inhibitor (-0.02) and stronger potentials as a nuclear receptor ligand (0.14) and enzyme inhibitor (0.17). To sum up, all compounds showed moderate to high activity against most drug class targets.

Table 8: Bioactivity score predictions of compounds according to 6 main drug classes based on important molecular targets of xenobiotics. Each value is represented as unitless quantities in which values above 0.00 indicate strong activity, between -0.50 and 0.00 suggest moderate activity and below -0.50 shows inactive compounds.[182-183]

Compound	GPCR ligand	Ion channel modulator	Kinase inhibitor	Nuclear receptor ligand	Protease inhibitor	Enzyme inhibitor
CAE1	0.41	0.14	0.09	0.60	0.26	0.47
CAE3	0.31	0.03	-0.50	0.93	0.14	0.55
CAE5	0.27	0.11	-0.42	0.85	0.15	0.52
CAE8	0.21	-0.04	-0.45	0.78	0.18	0.40
CAE21	0.18	-0.04	-0.40	0.76	0.22	0.49
DBF4	0.11	-0.29	-0.03	-0.13	-0.01	0.37
EGF4	-0.11	-0.69	-0.28	-0.06	-0.11	0.00
EGF25	0.00	-0.46	-0.12	0.14	-0.02	0.17
EGF36	0.10	-0.01	0.14	0.31	0.02	0.43
RAR2	0.48	0.03	-0.01	-0.17	-0.01	0.29
Camptothecin	0.46	-0.15	0.27	0.07	-0.10	1.11

5 Discussion

The discovery of highly cytotoxic and selective anti-neoplastic agents that minimize off-target toxicity is the main hurdle in anti-cancer drug discovery.[124] In this study, some of the compounds, namely CAE5, DBF4, EGF4, EGF36 and RAR2, showed to be non-active (IC_{50} > 50 µM) in all cell lines. CAE1, CAE3, CAE8 and EGF36 showed sufficient anti-cancer activity against cervical cancer cells, whereas CAE21 and EGF25 revealed strong cytotoxicity. Interestingly none of the compounds acted selectively on cervical cancer cells as opposed to non-cancer cells. This common trade-off of anti-cancer interventions was observed for the compounds showing therapeutic possibilities.[168,176,184]

In previous studies, various triterpenoids and flavonoids have shown anti-cancer activities in several human cancer cell lines which are listed in **table 4** and **table 5**.[172, 185, 176, 177, 178, 179, 180] Despite the novel pentacyclic triterpenoid, CAE21 (IC_{50} = 42.94 µM), being considered sufficiently bioactive against cervical cancer cells, others with reportedly stronger cytotoxicities in HCT-116- and HeLa cells such as ursolic acid (IC_{50} = 24.00 µM) and hederagenin (IC_{50} = 30.78 µM), a pentacyclic triterpenoid from the evergreen perennial common ivy (*Hedera helix* (*H. helix*)), are described.[172, 176, 186] Betulinic acid and lupeol, known triterpenes that were also included in this study (i.e. CAE3 and CAE5), have shown more optimal anti-cancer activities in literature.[173, 174, 175] A-431- and HeLa tumour cells from these studies were more sensitive to betulinic acid with IC_{50} doses of 3.95 µM and 30.42 µM, respectively. [173, 187] Lupeol was more sensitive to MCF-7, MDA-MB-231 and HeLa cells with IC_{50} concentrations of 2.32, 4.47 and 10.20 µM.[175] These previous findings contradict the results in HeLa cells from this study revealing betulinic acid and lupeol as inactive with IC_{50} doses of 68.32 and 74.88 µM. This is possibly due to evaporation of compound stocks because of repetitive warming from frozen to conduct numerous cell viability experiments.[166] However, there is little accessible data regarding selectivity of terpenoids and flavonoids against human non-cancer cell lines, possibly due to the difficulties in thawing cryopreserved cells and culturing.[188] Hederagenin (**table 4**), yielded more HeLa cell selectivity versus HEK-293 cells (SI = 1.20) than CAE21 against Vero cells (SI = 0.90).[176] Both are insufficient according to standards suggested by Artun, *et al* (SI > 2).[168]

In HeLa cells, EGF25 (IC_{50} = 44.65 µM) is notably more potent than other flavonoids, 2′-hydroxyl neophellamuretin (IC_{50} = 56.10 µM), 2″-O-rhamnosylswertisin (IC_{50} = 69.00 µM) and gallic acid (IC_{50} = 60.00 – 80.00 µM) (**table 5**). However, EGF25 was not potent enough compared to ferulic acid and the recently described 4 H-1-benzopyran-4-one,2-(4-hydroxyphenyl)-3,7-dihydroxy-5-methoxy-8-[5-methyl-2-(1-methylethenyl)-4-hexenyl].[179, 178] The respective IC_{50} values of ferulic acid were 14.00 to 16.00 µM in HeLa and CaSki cells and 4 H-1-benzopyran-4-one,2-(4-hydroxyphenyl)-3,7-dihydroxy-5-methoxy-8-[5-methyl-2-(1-methylethenyl)-4-hexenyl] IC_{50} values were 3.60 and 1.40 µM in A-549 and HCT-116 cells.[179, 178]

Similarly to CAE21, EGF25 showed sub-optimal cancer selectivity in HeLa cells versus Vero cells (SI = 0.64), yet so did another reported flavonoid, gallic acid.[180] According to calculations from reported data in various cervical cancer cell lines, gallic acid revealed selectivity indices of 1.10 to 1.50 in HeLa cells, 1.00 in C-33A cells and 0.70 to 0.80 in SiHa cells against Vero cells.[180] Thus far, the cancer cell targeting ability of terpenoids and flavonoids remain under-reported in literature.

Despite the cancer cytotoxicity of these compounds, not all molecules with strong anti-cancer potential are promoted further in the drug discovery pipeline due to their lack of bioavailability, especially as oral drugs.[107,109] Therefore, Lipinski's rule of 5 was used to identify compounds with sufficient pharmacokinetics for oral absorption and distribution. Most compounds in this study showed sufficient physiochemical properties except for flavonoids DBF4, EGF4 and EGF25, each of which had 3.00 violations to Lipinski's rule of 5. This means that these compounds are not suitable for oral ingestion and may need to be considered for administration via different routes, such as intravenous, inhalation or topical applications.[189]

Natural compounds have an enhanced effect when used in combination as they tend to target more than one cancer cell pathway simultaneously[167], as was seen in the additive cytotoxicity of CAE21 and EGF25 when administered together. This could be the reason why plant extracts containing many plant secondary metabolites together show stronger cytotoxicity than individual compounds.[190] Such additive effects involving combinations of flavonoids and terpenoids have been reported.[191-192] A 16.36 µM concentration of epigallocatechin gallate (IC_{50} = 137.63 µM) combined with various concentrations of terpenoid amarogentin (IC_{50} = 258.14 µM) or clove active ingredient, eugenol (IC_{50} = 1034.10 µM), resulted in reduced IC_{50} values of 148.51 µM and 699.15 µM in HeLa cells.[191]

The increased anti-cancer activity of CAE21 and EGF25 co-treatments in the present study were apoptotic in nature. Triterpenoids are known to induce apoptosis by engaging several molecular targets, including IAPs and anti-apoptotic BCL2 proteins in the mitochondria.[172] Phenolic compounds, which belong to flavonoids, are known to activate anti-cancer pathways through generation of ROS-mediated pathways and oxidative stress, thereby affecting major metabolic pathways of cancer cells.[172] Additional qPCR and western-blots are required to further elucidate the sub-apoptotic or metabolic pathways affected by CAE21 and EGF25. However, combinations of different compound classes may induce more than one insult on cancer cells that increase the likelihood of an apoptotic fate.[167]

Five compounds isolated from *C. arereh* (i.e. CAE1, CAE3, CAE5, CAE8 and CAE21) and EGF25 showed the greatest pharmaceutical potentials as nuclear receptor ligands when analysed *in silico*. Important nuclear and/or cytoplasmic receptors in cervical cancer progression include the estrogen receptors, ERα and ERβ, as they up-regulate E6 and E7 HPV oncogenes on interaction with the estradiol hormone.[16,193-195] This leads to early progression of cervical tumours towards malignancy in murine models.[196] However, estradiol interaction with ERs may be manipulated with selective estrogen receptor modulators (SERMs), such as fulvestrant and raloxifene, which have been used for treatment of hormone receptor-positive breast cancer.[197-199] Although clinical data is lacking, the plant-based SERM hibiscetin, isolated from *Hibiscus sabdariffa* (*H. sabdariffa*), has revealed 5 hydrogen bonds with amino acids proline-324 (*Pro-324*), glutamic acid-353 (*Glu-353*), isoleucine-386 (*Ile-386*) and tryptophan-393 (*Trp-393*) at the ERα active site *in silico*.[200-201] A flavonoid isolated from *Punica granatum* (*P. granatum*, commonly known as pomegranate), 4-coumaric acid methyl ester, was also identified as a lead SERM with optimal pharmacokinetics and strong affinity for ERα and ERβ variants.[200]

Although CAE21 and EGF25 were more strongly predicted as nuclear receptor ligands, they also demonstrated potential bioactivity against GPCRs. Interestingly, a certain GPCR, known as G protein-coupled estrogen receptor (GPER) also acts as cytoplasmic or nuclear receptor of estradiol in HPV-positive cervical cancer cells.[16] In contrast, HPV oncogenes increase quantity and nuclear expression of GPER, similarly to the ERs.[16] Insufficient reports involving the GPER modulation in cervical cancer models are available as current research is still pending, but an *in vitro* study in estrogen-sensitive endometrial cells showed GPER antagonist, G-15, to inhibit cell proliferation.[202] Paradoxically, this was potentiated by combined treatment with a GPER agonist, which would otherwise induce cell growth individually.[202] Therefore, extensive clarification of the anti-cancer ability of SERMs and GPER ligands in cervical cancer is needed.[202]

Quite a few compounds from this study, including CAE21 and EGF25, were predicted to modulate enzymes, suggesting that these compounds have broad specificity to enzyme targets other than kinases and proteases. However, CAE21 and EGF25 did not reveal any potential pharmaceutical potential as kinase inhibitors. CAE21 showed lower yet still sufficient potentials as protease inhibitors than nuclear receptor ligands. This seems counter-intuitive as anti-cancer drugs because caspase enzymes are all proteases, in which their inhibition prevents their apoptotic functions.[25] However, there are many different caspases that can elicit alternative apoptotic and non-apoptotic pathways.[203] For example, caspase-9 inhibition by caspase-9 inhibitor III (Ac-LEHD-cmk) potentiates the apoptotic effects of oridonin, a terpenoid from *Rabdosia rubescens* (*R. rubescens*), which causes oxidative damage to the mitochondrial membrane and disrupts the membrane potential.[203]

The compound solvent, DMSO, showed a confounding cytotoxicity as well as high variability in endpoint data in the cervical cancer model used during compound treatments due to misguided dosing of the compound solvent. However, various concentrations of DMSO, from 0.10 to 3.00%, have been used in *in vitro* cytotoxicity studies in literature,[166, 158, 204, 205] in which concentrations of 0.1 % did not present cytotoxicity in the negative control of this study. This was consistent with a study in a different cell line by Wang *et al*, but rarely reported in literature.[206] Looking back, it would have been optimal to initially analyse the cytotoxicity of various compound solvents in HeLa, Vero and CaSki cells before preparing the compounds. Despite the ability of DMSO to dissolve both polar and non-polar compounds and aid drug penetration into cells, better alternatives, such as hydrogels, liposomes and nano-technology are reported.[207, 208, 209, 210] In addition, these innovations may improve selective cytotoxicity by increasing targeted delivery of higher concentrations to cancer cells.[210]

The choice of MTT assay for compound cytotoxic assessment also posed a limitation in this project, because conversion to the colorimetric product formazan is affected by the number of mitochondria and the metabolic rate of cells in culture.[211] This suggests that the MTT endpoints are very sensitive to slight perturbations in cell culture handling and medium changes. [211] If funding was more abundant, additional real-time cell analysis assays would have been employed to determine cytotoxicity of all compounds. Limited time, compound materials and funding in this case prevented further repetitions with corrected experimental conditions and preparations, especially regarding use of the DMSO solvent.

Terpenoids and flavonoids are powerful phytochemicals than can be combined to potentiate each of their own therapeutic qualities, which is a worthwhile endeavour in anti-cancer drug discovery. However, CAE21 and EGF25 have only entered the pipeline with evidence regarding their additive apoptotic activity in cervical cancer cells. Further study is required to elucidate how CAE21 and EGF25 induce apoptosis, whether they strengthen one response engaging the same molecular pathway or whether they operate via two different molecular pathways. This also raises questions about their apoptotic mechanisms and their anti-angiogenic and anti-metastatic activities in multiple cancer models *in vitro* and *in vivo*. In prospect, CAE21 and EGF25 could potentially be used to stunt cervical cancer progression by targeted modulation of GPCR and nuclear receptors such as GPER and ERs. Despite these possibilities, *in vivo* assessment of CAE21 and EGF25 will more confidently reveal the true bioavailability and bioactivity of these compounds and hence their clinical success should they persist to develop. Despite major hurdles and challenges for the future, the main terpenoid (CAE21) and flavonoid (EGF25) from this study, together, revealed an apoptotic mechanism without necrosis. This proposes additional study of the coincidental anti-inflammatory and anti-cancer effects of CAE21 and EGF25, which suggest chemoprotective and chemo-preventative potentials in cervical cancer treatment.

6 References

1. Jhingran A, Russell AH, Seiden MV, Duska LR, Goodman A, Lee SL, et al. Cancers of the cervix, vulva, and vagina. [Internet] Abeloff's clinical oncology. Sixth edition. ed. Philadelphia, PA: Elsevier; 2020. p. 1468-507.[Available from: https://www.clinicalkey.com/#!/browse/book/3-s2.0-C20150054004.

2. Reich O, Regauer S, McCluggage WG, Bergeron C, Redman C. Defining the cervical transformation zone and squamocolumnar junction: Can we reach a common colposcopic and histologic definition? Int J Gynecol Pathol. 2017; 36(6):517-22. doi:10.1097/PGP.0000000000000381

3. Sung H, Ferlay J, Siegel RL, Laversanne M, Soerjomataram I, Jemal A, et al. Global cancer statistics 2020: Globocan estimates of incidence and mortality worldwide for 36 cancers in 185 countries. CA Cancer J Clin. 2021; 71(3):209-49. doi:10.3322/caac.21660

4. Bray F, Ferlay J, Soerjomataram I, Siegel RL, Torre LA, Jemal A. Global cancer statistics 2018: Globocan estimates of incidence and mortality worldwide for 36 cancers in 185 countries. CA Cancer J Clin. 2018; 68(6):394-424. doi:10.3322/caac.21492

5. South African National Cancer Registry. Cancer in South Africa 2014. Johannesburg.

6. International Agency for Research on Cancer. Population fact sheets: South Africa. Global Cancer Observatory. Lyon, France: World Health Organization; 2018.

7. Egli-Gany D, Spaar Zographos A, Diebold J, Masserey Spicher V, Frey Tirri B, Heusser R, et al. Human papillomavirus genotype distribution and socio-behavioural characteristics in women with cervical pre-cancer and cancer at the start of a human papillomavirus vaccination programme: The CIN3+ plus study. BMC Cancer. 2019; 19(1):111-. doi:10.1186/s12885-018-5248-y

8. Muñoz N, Bosch FX, de Sanjosé S, Herrero R, Castellsagué X, Shah KV, et al. Epidemiologic classification of human papillomavirus types associated with cervical cancer. N Engl J Med. 2003; 348(6):518-27. doi:10.1056/NEJMoa021641

9. Crosbie EJ, Einstein MH, Franceschi S, Kitchener HC. Human papillomavirus and cervical cancer. Lancet. 2013; 382(9895):889-99. doi:10.1016/s0140-6736(13)60022-7

10. Oyervides-Muñoz MA, Pérez-Maya AA, Rodríguez-Gutiérrez HF, Gómez-Macias GS, Fajardo-Ramírez OR, Treviño V, et al. Understanding the HPV integration and its progression to cervical cancer. Infect Genet Evol. 2018; 61:134-44. doi:10.1016/j.meegid.2018.03.003

11. Farmer E, Cheng MA, Hung C-F, Wu TC. Vaccination strategies for the control and treatment of HPV infection and HPV-associated cancer. Recent Results Cancer Res. 2021; 217:157-95. doi:10.1007/978-3-030-57362-1_8

12. Xu H, Egger S, Velentzis LS, O'Connell DL, Banks E, Darlington-Brown J, et al. Hormonal contraceptive use and smoking as risk factors for high-grade cervical intraepithelial neoplasia in unvaccinated women aged 30-44 years: A case-control study in New South Wales, Australia. Cancer Epidemiol. 2018; 55:162-9. doi:10.1016/j.canep.2018.05.013

13. Loopik DL, IntHout J, Melchers WJG, Massuger LFAG, Bekkers RLM, Siebers AG. Oral contraceptive and intrauterine device use and the risk of cervical intraepithelial neoplasia grade iii or worse: A population-based study. Eur J Cancer. 2020; 124:102-9. doi:10.1016/j.ejca.2019.10.009

14. Mignot S, Ringa V, Vigoureux S, Zins M, Panjo H, Saulnier P-J, et al. Pap tests for cervical cancer screening test and contraception: Analysis of data from the constances cohort study. BMC Cancer. 2019; 19(1):317-. doi:10.1186/s12885-019-5477-8

15. Christin-Maitre S, Laroche E, Bricaire L. A new contraceptive pill containing 17β-estradiol and nomegestrol acetate. Womens Health (Lond). 2013; 9(1):13-23. doi:10.2217/whe.12.70

16. Ramírez-López IG, Ramírez de Arellano A, Jave-Suárez LF, Hernández-Silva CD, García-Chagollan M, Hernández-Bello J, et al. Interaction between 17β-estradiol, prolactin and human papillomavirus induce E6/E7 transcript and modulate the expression and localization of hormonal receptors. Cancer Cell Int. 2019; 19:227. doi:10.1186/s12935-019-0935-6

17. Edelstein ZR, Madeleine MM, Hughes JP, Johnson LG, Schwartz SM, Galloway DA, et al. Age of diagnosis of squamous cell cervical carcinoma and early sexual experience. Cancer Epidemiol Biomarkers Prev. 2009; 18(4):1070-6. doi:10.1158/1055-9965.EPI-08-0707

18. Su B, Qin W, Xue F, Wei X, Guan Q, Jiang W, et al. The relation of passive smoking with cervical cancer: A systematic review and meta-analysis. Medicine (Baltimore). 2018; 97(46):e13061-e. doi:10.1097/MD.0000000000013061

19. Campaner AB, Nadais RF, Galvão MA. The effect of cigarette smoking on cervical langerhans cells and T and B lymphocytes in normal uterine cervix epithelium. Int J Gynecol Pathol. 2009; 28(6):549-53. doi:10.1097/PGP.0b013e3181aa232d

20. Poppe WA, Ide PS, Drijkoningen MP, Lauweryns JM, Van Assche FA. Tobacco smoking impairs the local immunosurveillance in the uterine cervix. An immunohistochemical study. Gynecol Obstet Invest. 1995; 39(1):34-8. doi:10.1159/000292372

21. Rossi NM, Dai J, Xie Y, Lou H, Boland JF, Yeager M, et al. Extrachromosomal amplification of human papillomavirus episomes as a mechanism of cervical carcinogenesis. bioRxiv. 2021:2021.10.22.465367. doi:10.1101/2021.10.22.465367

22. Sanchooli A, Aghayipour K, Naghlani SK, Samiee Z, Kiasari BA, Makvandi M. Production of human papillomavirus type-16 l1 vlp in pichia pastoris. Appl Biochem Microbiol. 2020; 56(1):51-7. doi:10.1134/S0003683820010147

23. Shen-Gunther J, Cai H, Zhang H, Wang Y. Abundance of HPV l1 intra-genotype variants with capsid epitopic modifications found within low- and high-grade pap smears with potential implications for vaccinology. Front Genet. 2019; 10 doi:10.3389/fgene.2019.00489

24. Godi A, Bissett SL, Miller E, Beddows S. Relationship between humoral immune responses against HPV16, HPV 18, HPV 31 and HPV 45 in 12-15 year old girls receiving Cervarix® or Gardasil® vaccine. PloS one. 2015; 10(10):e0140926-e. doi:10.1371/journal.pone.0140926

25. Galluzzi L, Vitale I, Aaronson SA, Abrams JM, Adam D, Agostinis P, et al. Molecular mechanisms of cell death: Recommendations of the nomenclature committee on cell death 2018. Cell Death Differ. 2018; 25(3):486-541. doi:10.1038/s41418-017-0012-4

26. Pistritto G, Trisciuoglio D, Ceci C, Garufi A, D'Orazi G. Apoptosis as anticancer mechanism: Function and dysfunction of its modulators and targeted therapeutic strategies. Aging. 2016; 8(4):603-19. doi:10.18632/aging.100934

27. Kang T-W, Yevsa T, Woller N, Hoenicke L, Wuestefeld T, Dauch D, et al. Senescence surveillance of pre-malignant hepatocytes limits liver cancer development. Nature. 2011; 479(7374):547-51. doi:10.1038/nature10599

28. Baar MP, Brandt RMC, Putavet DA, Klein JDD, Derks KWJ, Bourgeois BRM, et al. Targeted apoptosis of senescent cells restores tissue homeostasis in response to chemotoxicity and aging. Cell. 2017; 169(1):132-47.e16. doi:10.1016/j.cell.2017.02.031

29. Zhu L, Xiao F, Yu Y, Wang H, Fang M, Yang Y, et al. Ksp inhibitor sb743921 inhibits growth and induces apoptosis of breast cancer cells by regulating p53, BCL2, and dtl. Anticancer Drugs. 2016; 27(9):863-72. doi:10.1097/CAD.0000000000000402

30. Arakawa S, Tsujioka M, Yoshida T, Tajima-Sakurai H, Nishida Y, Matsuoka Y, et al. Role of ATG5-dependent cell death in the embryonic development of bax/bak double-knockout mice. Cell Death Differ. 2017; 24(9):1598-608. doi:10.1038/cdd.2017.84

31. Orelio C, Harvey KN, Miles C, Oostendorp RA, van der Horn K, Dzierzak E. The role of apoptosis in the development of agm hematopoietic stem cells revealed by BCL2 overexpression. Blood. 2004; 103(11):4084-92. doi:10.1182/blood-2003-06-1827

32. Conradt B, Wu YC, Xue D. Programmed cell death during *Caenorhabditis elegans* development. Genetics. 2016; 203(4):1533-62. doi:10.1534/genetics.115.186247

33. Wallach D, Kang TB, Dillon CP, Green DR. Programmed necrosis in inflammation: Toward identification of the effector molecules. Science. 2016; 352(6281):aaf2154. doi:10.1126/science.aaf2154

34. Rogers C, Fernandes-Alnemri T, Mayes L, Alnemri D, Cingolani G, Alnemri ES. Cleavage of DFNA5 by caspase-3 during apoptosis mediates progression to secondary necrotic/pyroptotic cell death. Nat Commun. 2017; 8:14128-. doi:10.1038/ncomms14128

35. Perry JSA, Morioka S, Medina CB, Iker Etchegaray J, Barron B, Raymond MH, et al. Interpreting an apoptotic corpse as anti-inflammatory involves a chloride sensing pathway. Nat Cell Biol. 2019; 21(12):1532-43. doi:10.1038/s41556-019-0431-1

36. Doran AC, Ozcan L, Cai B, Zheng Z, Fredman G, Rymond CC, et al. CAMKIIγ suppresses an efferocytosis pathway in macrophages and promotes atherosclerotic plaque necrosis. J Clin Invest. 2017; 127(11):4075-89. doi:10.1172/JCI94735

37. Poillet-Perez L, Xie X, Zhan L, Yang Y, Sharp DW, Hu ZS, et al. Autophagy maintains tumour growth through circulating arginine. Nature. 2018; 563(7732):569-73. doi:10.1038/s41586-018-0697-7

38. Cianfanelli V, Fuoco C, Lorente M, Salazar M, Quondamatteo F, Gherardini PF, et al. AMBRA1 links autophagy to cell proliferation and tumorigenesis by promoting c-Myc dephosphorylation and degradation. Nat Cell Biol. 2015; 17(1):20-30. doi:10.1038/ncb3072

39. Cui L, Zhao LP, Ye JY, Yang L, Huang Y, Jiang XP, et al. The lysosomal membrane protein Lamp2 alleviates lysosomal cell death by promoting autophagic flux in ischemic cardiomyocytes. Front Cell Dev Biol. 2020; 8:31. doi:10.3389/fcell.2020.00031

40. Niemann B, Rohrbach S. Chapter 3 - Metabolically Relevant Cell Biology – Role of Intracellular Organelles for Cardiac Metabolism. In: Schwarzer M, Doenst T, editors. The Scientist's Guide to Cardiac Metabolism. Boston: Academic Press; 2016. p. 19-38.

41. Lee SY, Ju MK, Jeon HM, Jeong EK, Lee YJ, Kim CH, et al. Regulation of tumor progression by programmed necrosis. Oxid Med Cell Longev. 2018; 2018:3537471-. doi:10.1155/2018/3537471

42. Dreher MR, Liu W, Michelich CR, Dewhirst MW, Fan Y, Chilkoti A, et al. Tumor vascular permeability, accumulation, and penetration of macromolecular drug carriers. J Natl Cancer Inst. 2006; 98(5)

43. Khaw-On P, Pompimon W, Banjerdpongchai R. Goniothalamin induces necroptosis and anoikis in human invasive breast cancer MDA-MB-231 cells. Int J Mol Sci. 2019; 20(16):3953. doi:10.3390/ijms20163953

44. Petrie EJ, Sandow JJ, Jacobsen AV, Smith BJ, Griffin MDW, Lucet IS, et al. Conformational switching of the pseudokinase domain promotes human MLKL tetramerization and cell death by necroptosis. Nat Commun. 2018; 9(1):2422-. doi:10.1038/s41467-018-04714-7

45. Murai S, Yamaguchi Y, Shirasaki Y, Yamagishi M, Shindo R, Hildebrand JM, et al. A fret biosensor for necroptosis uncovers two different modes of the release of DAMPs. Nat Commun. 2018; 9(1):4457-. doi:10.1038/s41467-018-06985-6

46. Rani M, Nicholson SE, Zhang Q, Schwacha MG. Damage-associated molecular patterns (DAMPs) released after burn are associated with inflammation and monocyte activation. Burns Open. 2017; 43(2):297-303. doi:10.1016/j.burns.2016.10.001

47. Scaffidi P, Misteli T, Bianchi ME. Release of chromatin protein HMGB1 by necrotic cells triggers inflammation. Nature. 2002; 418(6894):191-5. doi:10.1038/nature00858

48. Chen C, Xu Z-Q, Zong Y-P, Ou B-C, Shen X-H, Feng H, et al. CXCL5 induces tumor angiogenesis via enhancing the expression of FOXD1 mediated by the AKT/NF-κB pathway in colorectal cancer. Cell Death Dis. 2019; 10(3):178. doi:10.1038/s41419-019-1431-6

49. Amato J, Cerofolini L, Brancaccio D, Giuntini S, Iaccarino N, Zizza P, et al. Insights into telomeric g-quadruplex DNA recognition by HMGB1 protein. Nucleic Acids Res. 2019; 47(18):9950-66. doi:10.1093/nar/gkz727

50. Tohme S, Yazdani HO, Liu Y, Loughran P, van der Windt DJ, Huang H, et al. Hypoxia mediates mitochondrial biogenesis in hepatocellular carcinoma to promote tumor growth through HMGB1 and TLR9 interaction. Hepatology. 2017; 66(1):182-97. doi:10.1002/hep.29184

51. Ando Y, Ohuchida K, Otsubo Y, Kibe S, Takesue S, Abe T, et al. Necroptosis in pancreatic cancer promotes cancer cell migration and invasion by release of CXCL5. PLoS One. 2020; 15(1):e0228015. doi:10.1371/journal.pone.0228015

52. Elkin ER, Harris SM, Loch-Caruso R. Trichloroethylene metabolite s-(1,2-dichlorovinyl)-l-cysteine induces lipid peroxidation-associated apoptosis via the intrinsic and extrinsic apoptosis pathways in a first-trimester placental cell line. Toxicol Appl Pharmacol. 2018; 338:30-42. doi:10.1016/j.taap.2017.11.006

53. Welsh K, Milutinovic S, Ardecky RJ, Gonzalez-Lopez M, Ganji SR, Teriete P, et al. Characterization of potent Smac mimetics that sensitize cancer cells to TNF family-induced apoptosis. PloS one. 2016; 11(9):e0161952-e. doi:10.1371/journal.pone.0161952

54. Obexer P, Ausserlechner MJ. X-linked inhibitor of apoptosis protein - a critical death resistance regulator and therapeutic target for personalized cancer therapy. Front Oncol. 2014; 4:197-. doi:10.3389/fonc.2014.00197

55. Liang J, Zhao W, Tong P, Li P, Zhao Y, Li H, et al. Comprehensive molecular characterization of inhibitors of apoptosis proteins (IAPs) for therapeutic targeting in cancer. BMC Med Genomics. 2020; 13(1):7-. doi:10.1186/s12920-020-0661-x

56. Lian BSX, Yek AEH, Shuvas H, Abdul Rahman SF, Muniandy K, Mohana-Kumaran N. Synergistic anti-proliferative effects of combination of ABT-263 and MCL-1 selective inhibitor a-1210477 on cervical cancer cell lines. BMC Res Notes. 2018; 11(1):197-. doi:10.1186/s13104-018-3302-0

57. Lee EY, Gong EY, Shin JS, Moon JH, Shim HJ, Kim SM, et al. Human breast cancer cells display different sensitivities to ABT-263 based on the level of survivin. Toxicol In Vitro. 2018; 46:229-36. doi:10.1016/j.tiv.2017.09.023

58. Xu Y, Liao R, Li N, Xiang R, Sun P. Phosphorylation of Tip60 by p38α regulates p53-mediated PUMA induction and apoptosis in response to DNA damage. Oncotarget. 2014; 5(24):12555-72. doi:10.18632/oncotarget.2717

59. Andrysik Z, Galbraith MD, Guarnieri AL, Zaccara S, Sullivan KD, Pandey A, et al. Identification of a core TP53 transcriptional program with highly distributed tumor suppressive activity. Genome Res. 2017; 27(10):1645-57. doi:10.1101/gr.220533.117

60. Narayan G, Xie D, Ishdorj G, Scotto L, Mansukhani M, Pothuri B, et al. Epigenetic inactivation of TRAIL decoy receptors at 8p12-21.3 commonly deleted region confers sensitivity to Apo2l/trail-cisplatin combination therapy in cervical cancer. Genes Chromosomes Cancer. 2016; 55(2):177-89. doi:10.1002/gcc.22325

61. Latchman DS. Gene control. New York, NY: Garland Science, Taylor & Francis Group; 2015.

62. Oakes SA, Scorrano L, Opferman JT, Bassik MC, Nishino M, Pozzan T, et al. Proapoptotic BAX and BAK regulate the type 1 inositol trisphosphate receptor and calcium leak from the endoplasmic reticulum. Proc Natl Acad Sci U S A. 2005; 102(1):105-10. doi:10.1073/pnas.0408352102

63. Chai J, Shiozaki E, Srinivasula SM, Wu Q, Datta P, Alnemri ES, et al. Structural basis of caspase-7 inhibition by XIAP. Cell. 2001; 104(5):769-80. doi:10.1016/s0092-8674(01)00272-0

64. Shiozaki EN, Chai J, Rigotti DJ, Riedl SJ, Li P, Srinivasula SM, et al. Mechanism of XIAP-mediated inhibition of caspase-9. Mol Cell. 2003; 11(2):519-27. doi:10.1016/s1097-2765(03)00054-6

65. Li M, Luo J, Brooks CL, Gu W. Acetylation of p53 inhibits its ubiquitination by MDM2. J Biol Chem. 2002; 277(52):50607-11. doi:10.1074/jbc.C200578200

66. Kocik J, Machula M, Wisniewska A, Surmiak E, Holak TA, Skalniak L. Helping the released guardian: Drug combinations for supporting the anticancer activity of HDM2 (MDM2) antagonists. Cancers (Basel). 2019; 11(7):1014. doi:10.3390/cancers11071014

67. Carabetta VJ, Greco TM, Cristea IM, Dubnau D. YfmK is an n(epsilon)-lysine acetyltransferase that directly acetylates the histone-like protein hbsu in *Bacillus subtilis*. Proc Natl Acad Sci U S A. 2019; 116(9):3752-7. doi:10.1073/pnas.1815511116

68. Li X, Zhao Y, Xia Q, Zheng L, Liu L, Zhao B, et al. Nuclear translocation of annexin 1 following oxygen-glucose deprivation-reperfusion induces apoptosis by regulating bid expression via p53 binding. Cell Death Dis. 2016; 7(9):e2356-e. doi:10.1038/cddis.2016.259

69. Konig SM, Rissler V, Terkelsen T, Lambrughi M, Papaleo E. Alterations of the interactome of BCL2 proteins in breast cancer at the transcriptional, mutational and structural level. PLoS Comput Biol. 2019; 15(12):e1007485. doi:10.1371/journal.pcbi.1007485

70. Lawrence MS, Stojanov P, Mermel CH, Robinson JT, Garraway LA, Golub TR, et al. Discovery and saturation analysis of cancer genes across 21 tumour types. Nature. 2014; 505(7484):495-501. doi:10.1038/nature12912

71. Vervliet T, Lemmens I, Welkenhuyzen K, Tavernier J, Parys JB, Bultynck G. Regulation of the ryanodine receptor by anti-apoptotic BCL2 is independent of its BH3-domain-binding properties. Biochem Biophys Res Commun. 2015; 463(3):174-9. doi:https://doi.org/10.1016/j.bbrc.2015.04.131

72. Márquez-Jurado S, Díaz-Colunga J, das Neves RP, Martinez-Lorente A, Almazán F, Guantes R, et al. Mitochondrial levels determine variability in cell death by modulating apoptotic gene expression. Nat Commun. 2018; 9(1):389-. doi:10.1038/s41467-017-02787-4

73. Schaeffer L. Chapter 14 - The Role of Functional Groups in Drug–Receptor Interactions. In: Wermuth CG, Aldous D, Raboisson P, Rognan D, editors. The Practice of Medicinal Chemistry (Fourth Edition). San Diego: Academic Press; 2008. p. 359-78.

74. Panayotopoulou EG, Müller A-K, Börries M, Busch H, Hu G, Lev S. Targeting of apoptotic pathways by SMAC or BH3 mimetics distinctly sensitizes paclitaxel-resistant triple negative breast cancer cells. Oncotarget. 2017; 8(28):45088-104. doi:10.18632/oncotarget.15125

75. Lim B, Greer Y, Lipkowitz S, Takebe N. Novel apoptosis-inducing agents for the treatment of cancer, a new arsenal in the toolbox. Cancers (Basel). 2019; 11(8):1087. doi:10.3390/cancers11081087

76. Li H, Liu L, Chang H, Zou Z, Xing D. Downregulation of MCL-1 and upregulation of PUMA using mtor inhibitors enhance antitumor efficacy of BH3 mimetics in triple-negative breast cancer. Cell Death Dis. 2018; 9(2):137. doi:10.1038/s41419-017-0169-2

77. Roberts AW, Seymour JF, Brown JR, Wierda WG, Kipps TJ, Khaw SL, et al. Substantial susceptibility of chronic lymphocytic leukemia to BCL2 inhibition: Results of a phase I study of navitoclax in patients with relapsed or refractory disease. J Clin Oncol. 2012; 30(5):488-96. doi:10.1200/jco.2011.34.7898

78. Kipps TJ, Eradat H, Grosicki S, Catalano J, Cosolo W, Dyagil IS, et al. A phase 2 study of the BH3 mimetic BCL2 inhibitor navitoclax (ABT-263) with or without rituximab, in previously untreated B-cell chronic lymphocytic leukemia. Leuk Lymphoma. 2015; 56(10):2826-33. doi:10.3109/10428194.2015.1030638

79. Emer JJ, Claire W. Rituximab: A review of dermatological applications. J Clin Aesthet Dermatol. 2009; 2(5):29-37.

80. Han B, Park D, Li R, Xie M, Owonikoko TK, Zhang G, et al. Small-molecule BCL2 BH4 antagonist for lung cancer therapy. Cancer Cell. 2015; 27(6):852-63. doi:10.1016/j.ccell.2015.04.010

81. Finlay D, Vamos M, González-López M, Ardecky RJ, Ganji SR, Yuan H, et al. Small-molecule IAP antagonists sensitize cancer cells to TRAIL-induced apoptosis: Roles of XIAP and cIAPs. Mol Cancer Ther. 2014; 13(1):5-15. doi:10.1158/1535-7163.MCT-13-0153

82. Darding M, Feltham R, Tenev T, Bianchi K, Benetatos C, Silke J, et al. Molecular determinants of SMAC mimetic induced degradation of cIAP1 and cIAP2. Cell Death Differ. 2011; 18(8):1376-86. doi:10.1038/cdd.2011.10

83. Benetatos CA, Mitsuuchi Y, Burns JM, Neiman EM, Condon SM, Yu G, et al. Birinapant (tl32711), a bivalent SMAC mimetic, targets TRAF2-associated cIAPs, abrogates TNF-induced NF-kappaB activation, and is active in patient-derived xenograft models. Mol Cancer Ther. 2014; 13(4):867-79. doi:10.1158/1535-7163.Mct-13-0798

84. El-Mesery M, Shaker ME, Elgaml A. The SMAC mimetic BV6 induces cell death and sensitizes different cell lines to TNF-α and TRAIL-induced apoptosis. Exp Biol Med (Maywood). 2016; 241(18):2015-22. doi:10.1177/1535370216661779

85. Stad R, Little NA, Xirodimas DP, Frenk R, van der Eb AJ, Lane DP, et al. MDMX stabilizes p53 and MDM2 via two distinct mechanisms. EMBO Rep. 2001; 2(11):1029-34. doi:10.1093/embo-reports/kve227

86. Levy R, Gregory E, Borcherds W, Daughdrill G. P53 phosphomimetics preserve transient secondary structure but reduce binding to MDM2 and MDMX. Biomolecules. 2019; 9(3) doi:10.3390/biom9030083

87. He T, Guo J, Song H, Zhu H, Di X, Min H, et al. Nutlin-3, an antagonist of MDM2, enhances the radiosensitivity of esophageal squamous cancer with wild-type p53. Pathol Oncol Res. 2018; 24(1):75-81. doi:10.1007/s12253-017-0215-5

88. Voon YL, Ahmad M, Wong PF, Husaini R, Ng WT, Leong CO, et al. Nutlin-3 sensitizes nasopharyngeal carcinoma cells to cisplatin-induced cytotoxicity. Oncol Rep. 2015; 34(4):1692-700. doi:10.3892/or.2015.4177

89. Zanjirband M, Edmondson RJ, Lunec J. Pre-clinical efficacy and synergistic potential of the MDM2-p53 antagonists, nutlin-3 and rg7388, as single agents and in combined treatment with cisplatin in ovarian cancer. Oncotarget. 2016; 7(26):40115-34. doi:10.18632/oncotarget.9499

90. Deben C, Wouters A, Op de Beeck K, van Den Bossche J, Jacobs J, Zwaenepoel K, et al. The MDM2-inhibitor nutlin-3 synergizes with cisplatin to induce p53 dependent tumor cell apoptosis in non-small cell lung cancer. Oncotarget. 2015; 6(26):22666-79. doi:10.18632/oncotarget.4433

91. Saxena R, Gupta G, Manohar M, Debnath U, Popli P, Prabhakar YS, et al. Spiro-oxindole derivative 5-chloro-4′,5′-diphenyl-3′-(4-(2-(piperidin-1-yl) ethoxy) benzoyl) spiro[indoline-3,2′-pyrrolidin]-2-one triggers apoptosis in breast cancer cells via restoration of p53 function. Int J Biochem Cell Biol. 2016; 70:105-17. doi:https://doi.org/10.1016/j.biocel.2015.11.003

92. Yuan X, Gajan A, Chu Q, Xiong H, Wu K, Wu GS. Developing TRAIL/TRAILdeath receptor-based cancer therapies. Cancer Metastasis Rev. 2018; 37(4):733-48. doi:10.1007/s10555-018-9728-y

93. Walczak H, Miller RE, Ariail K, Gliniak B, Griffith TS, Kubin M, et al. Tumoricidal activity of tumor necrosis factor-related apoptosis-inducing ligand in vivo. Nat Med. 1999; 5(2):157-63.

94. Kay BP, Hsu C-P, Lu J-F, Sun Y-N, Bai S, Xin Y, et al. Intracellular-signaling tumor-regression modeling of the pro-apoptotic receptor agonists dulanermin and conatumumab. J Pharmacokinet Pharmacodyn. 2012; 39(5):577-90. doi:10.1007/s10928-012-9269-x

95. Ouyang X, Shi M, Jie F, Bai Y, Shen P, Yu Z, et al. Phase III study of dulanermin (recombinant human tumor necrosis factor-related apoptosis-inducing ligand/Apo2 ligand) combined with vinorelbine and cisplatin in patients with advanced non-small-cell lung cancer. Invest New Drugs. 2018; 36(2):315-22. doi:10.1007/s10637-017-0536-y

96. Mantovani A, Locati M, Vecchi A, Sozzani S, Allavena P. Decoy receptors: A strategy to regulate inflammatory cytokines and chemokines. Trends Immunol. 2001; 22(6):328-36. doi:10.1016/S1471-4906(01)01941-X

97. Swers JS, Grinberg L, Wang L, Feng H, Lekstrom K, Carrasco R, et al. Multivalent scaffold proteins as superagonists of TRAIL receptor 2–induced apoptosis. Mol Cancer Ther. 2013; 12(7):1235. doi:10.1158/1535-7163.MCT-12-1107

98. Greer YE, Gilbert SF, Gril B, Narwal R, Peacock Brooks DL, Tice DA, et al. Medi3039, a novel highly potent tumor necrosis factor (TNF)-related apoptosis-inducing ligand (TRAIL) receptor 2 agonist, causes regression of orthotopic tumors and inhibits outgrowth of metastatic triple-negative breast cancer. Breast Cancer Res. 2019; 21(1):27. doi:10.1186/s13058-019-1116-1

99. Fuentes A. Advancements in cervical cancer prevention and management of persistent, recurrent, and metastatic disease: 2016 update. Am J Hematol Oncol. 2017; 12(12)

100. Plissonnier ML, Fauconnet S, Bittard H, Mougin C, Rommelaere J, Lascombe I. Cell death and restoration of trail-sensitivity by ciglitazone in resistant cervical cancer cells. Oncotarget. 2017; 8(64):107744-62. doi:10.18632/oncotarget.22632

101. Kitagawa R, Katsumata N, Shibata T, Kamura T, Kasamatsu T, Nakanishi T, et al. Paclitaxel plus carboplatin versus paclitaxel plus cisplatin in metastatic or recurrent cervical cancer: The open-label randomized phase III trial jcog0505. J Clin Oncol. 2015; 33(19):2129-35. doi:10.1200/jco.2014.58.4391

102. Wedge SR, Kendrew J, Hennequin LF, Valentine PJ, Barry ST, Brave SR, et al. Azd2171: A highly potent, orally bioavailable, vascular endothelial growth factor receptor-2 tyrosine kinase inhibitor for the treatment of cancer. Cancer Res. 2005; 65(10):4389-400. doi:10.1158/0008-5472.CAN-04-4409

103. Symonds RP, Gourley C, Davidson S, Carty K, McCartney E, Rai D, et al. Cediranib combined with carboplatin and paclitaxel in patients with metastatic or recurrent cervical cancer (CIRCCa): A randomised, double-blind, placebo-controlled phase 2 trial. Lancet Oncol. 2015; 16(15):1515-24. doi:10.1016/S1470-2045(15)00220-X

104. Liu L, Wang M, Li X, Yin S, Wang B. An overview of novel agents for cervical cancer treatment by inducing apoptosis: Emerging drugs ongoing clinical trials and preclinical studies. Front Med (Lausanne). 2021; 8 doi:10.3389/fmed.2021.682366

105. Xie Z, Wei Y, Xu J, Lei J, Yu J. Alkaloids from *Piper nigrum* synergistically enhanced the effect of paclitaxel against paclitaxel-resistant cervical cancer cells through the downregulation of MCL-1. J Agric Food Chem. 2019; 67(18):5159-68. doi:10.1021/acs.jafc.9b01320

106. Wang Q, Zheng X-l, Yang L, Shi F, Gao L-b, Zhong Y-j, et al. Reactive oxygen species-mediated apoptosis contributes to chemosensitization effect of saikosaponins on cisplatin-induced cytotoxicity in cancer cells. J Exp Clin Cancer Res. 2010; 29(1):159-. doi:10.1186/1756-9966-29-159

107. Hughes JP, Rees S, Kalindjian SB, Philpott KL. Principles of early drug discovery. Br J Pharmacol. 2011; 162(6):1239-49. doi:10.1111/j.1476-5381.2010.01127.x

108. Chabner BA. NCI-60 cell line screening: A radical departure in its time. J Natl Cancer Inst. 2016; 108(5) doi:10.1093/jnci/djv388

109. Lipinski CA. Lead- and drug-like compounds: The rule-of-five revolution. Drug Discov Today Technol. 2004; 1(4):337-41. doi:10.1016/j.ddtec.2004.11.007

110. Ebhohimen IE, Edemhanria L, Awojide S, Onyijen OH, Anywar G. Chapter 3 - Advances in Computer-Aided Drug Discovery. In: Egbuna C, Kumar S, Ifemeje JC, Ezzat SM, Kaliyaperumal S, editors. Phytochemicals as Lead Compounds for New Drug Discovery: Elsevier; 2020. p. 25-37.

111. Wang S, König G, Roth H-J, Fouché M, Rodde S, Riniker S. Effect of flexibility, lipophilicity, and the location of polar residues on the passive membrane permeability of a series of cyclic decapeptides. J Med Chem. 2021; 64(17):12761-73. doi:10.1021/acs.jmedchem.1c00775

112. Ertl P, Rohde B, Selzer P. Fast calculation of molecular polar surface area as a sum of fragment-based contributions and its application to the prediction of drug transport properties. J Med Chem. 2000; 43(20):3714-7. doi:10.1021/jm000942e

113. Veber DF, Johnson SR, Cheng HY, Smith BR, Ward KW, Kopple KD. Molecular properties that influence the oral bioavailability of drug candidates. J Med Chem. 2002; 45(12):2615-23. doi:10.1021/jm020017n

114. Neves BJ, Braga RC, Melo-Filho CC, Moreira-Filho JT, Muratov EN, Andrade CH. QSAR-based virtual screening: Advances and applications in drug discovery. Front Pharmacol. 2018; 9 doi:10.3389/fphar.2018.01275

115. Paciaroni NG, Norwood VM, Ratnayake R, Luesch H, Huigens RW. Yohimbine as a starting point to access diverse natural product-like agents with re-programmed activities against cancer-relevant GPCR targets. Bioorg Med Chem. 2020; 28(14) doi:10.1016/j.bmc.2020.115546

116. Oh TG, Wang SCM, Acharya BR, Goode JM, Graham JD, Clarke CL, et al. The nuclear receptor, ROR gamma, regulates pathways necessary for breast cancer metastasis. EBioMedicine. 2016; 6:59-72. doi:10.1016/j.ebiom.2016.02.028

117. Monte MJ, Rosales R, Macias RI, Iannota V, Martinez-Fernandez A, Romero MR, et al. Cytosol-nucleus traffic and colocalization with FXE of conjugated bile acids in rat hepatocytes. Am J Physiol Gastrointest Liver Physiol. 2008; 295(1):G54-g62. doi:10.1152/ajpgi.00592.2007

118. Apsel B, Blair JA, Gonzalez B, Nazif TM, Feldman ME, Aizenstein B, et al. Targeted polypharmacology: Discovery of dual inhibitors of tyrosine and phosphoinositide kinases. Nat Chem Biol. 2008; 4(11):691-9. doi:10.1038/nchembio.117

119. Lindenmann U, Brand M, Gall F, Frasson D, Hunziker L, Kroslakova I, et al. Discovery of a class of potent and selective non-competitive sentrin-specific protease 1 inhibitors. ChemMedChem. 2020; 15(8):675-9. doi:10.1002/cmdc.202000067

120. Fouqué A, Lepvrier E, Debure L, Gouriou Y, Malleter M, Delcroix V, et al. The apoptotic members CD95, BCLxl, and BCL2 cooperate to promote cell migration by inducing Ca(2+) flux from the endoplasmic reticulum to mitochondria. Cell Death Differ. 2016; 23(10):1702-16. doi:10.1038/cdd.2016.61

121. Becker V, Hui X, Nalbach L, Ampofo E, Lipp P, Menger MD, et al. Linalool inhibits the angiogenic activity of endothelial cells by downregulating intracellular ATP levels and activating TRPM8. Angiogenesis. 2021; 24(3):613-30. doi:10.1007/s10456-021-09772-y

122. Tamimi NAM, Ellis P. Drug development: From concept to marketing. Nephron Clin Pract. 2009; 113(3):c125-c31. doi:10.1159/000232592

123. Newman DJ, Cragg GM. Natural products as sources of new drugs from 1981 to 2014. J Nat Prod. 2016; 79(3):629-61. doi:10.1021/acs.jnatprod.5b01055

124. Seca AML, Pinto DCGA. Plant secondary metabolites as anticancer agents: Successes in clinical trials and therapeutic application. Int J Mol Sci. 2018; 19(1) doi:10.3390/ijms19010263

125. Justina NN, Akachukwu I, Conrad VS, Fidele N-K. Exploring cancer therapeutics with natural products from african medicinal plants, part ii: Alkaloids, terpenoids and flavonoids. Anticancer Agents Med Chem. 2016; 16(1):108-27. doi:10.2174/1871520615666150520143827

126. Kabera JN, Semana E, Mussa AR, He X. Plant secondary metabolites: Biosynthesis, classification, function and pharmacological properties. J Pharm Pharmacol. 2014; 2:377-92.

127. Cai Y, Zheng Y, Gu J, Wang S, Wang N, Yang B, et al. Betulinic acid chemosensitizes breast cancer by triggering er stress-mediated apoptosis by directly targeting grp78. Cell Death Dis. 2018; 9(6):636. doi:10.1038/s41419-018-0669-8

128. Wang L, Wang C, Tao Z, Zhao L, Zhu Z, Wu W, et al. Curcumin derivative wz35 inhibits tumor cell growth via ros-yap-jnk signaling pathway in breast cancer. J Exp Clin Cancer Res. 2019; 38(1):460. doi:10.1186/s13046-019-1424-4

129. Xu T, Pang Q, Wang Y, Yan X. Betulinic acid induces apoptosis by regulating PI3K/AKT signaling and mitochondrial pathways in human cervical cancer cells. Int J Mol Med. 2017; 40(6):1669-78. doi:10.3892/ijmm.2017.3163

130. Kim B, Kim HS, Jung EJ, Lee JY, B KT, Lim JM, et al. Curcumin induces ER stress-mediated apoptosis through selective generation of reactive oxygen species in cervical cancer cells. Mol Carcinog. 2016; 55(5):918-28. doi:10.1002/mc.22332

131. Lee D, Lee SR, Kang KS, Ko Y, Pang C, Yamabe N, et al. Betulinic acid suppresses ovarian cancer cell proliferation through induction of apoptosis. Biomolecules. 2019; 9(7) doi:10.3390/biom9070257

132. Kouame PB, Jacques C, Bedi G, Silvestre V, Loquet D, Barille-Nion S, et al. Phytochemicals isolated from leaves of *Chromolaena odorata*: Impact on viability and clonogenicity of cancer cell lines. Phytother Res. 2013; 27(6):835-40. doi:10.1002/ptr.4787

133. Watson RR, Preedy VR, Zibadi S Polyphenols : Mechanisms of action in human health and disease. Volume 1. [Internet] London ;: Academic Press; 2018 [cited Access 2018 Access Date]. Available from: https://www.sciencedirect.com/science/book/9780128130063.

134. Block S, Stevigny C, De Pauw-Gillet MC, de Hoffmann E, Llabres G, Adjakidje V, et al. Ent-trachyloban-3beta-ol, a new cytotoxic diterpene from *Croton zambesicus*. Planta Med. 2002; 68(7):647-9. doi:10.1055/s-2002-32903

135. Mohammed MM, Ibrahim NA, Awad NE, Matloub AA, Mohamed-Ali AG, Barakat EE, et al. Anti-HIV-1 and cytotoxicity of the alkaloids of *Erythrina abyssinica* lam. growing in Sudan. Nat Prod Res. 2012; 26(17):1565-75. doi:10.1080/14786419.2011.573791

136. Dzoyem JP, Nkuete AH, Kuete V, Tala MF, Wabo HK, Guru SK, et al. Cytotoxicity and antimicrobial activity of the methanol extract and compounds from *Polygonum limbatum*. Planta Med. 2012; 78(8):787-92. doi:10.1055/s-0031-1298431

137. Ntie-Kang F, Lifongo LL, Mbaze LMa, Ekwelle N, Owono Owono LC, Megnassan E, et al. Cameroonian medicinal plants: A bioactivity versus ethnobotanical survey and chemotaxonomic classification. BMC Complement Altern Med. 2013; 13:147-. doi:10.1186/1472-6882-13-147

138. Missi MB, Evina JN, Zintchem AAA, October N, Bona A, Moela P, et al. Antibacterial and cytotoxic activities of undescribed cassiaric acid and other constituents from *Cassia arereh* stem barks. Nat Prod Res. 2021:1-10. doi:10.1080/14786419.2021.1981313

139. De N, Maori L, Ardo H. A study on antimicrobial effect of extracts of *Cassia arereh* (del.) on some clinical isolates. J Med Plant Res. 2009; 3(3):116-9.

140. National Center for Biotechnology Information. Pubchem compound summary for cid 99615, betulinaldehyde. 2022.

141. William YN, Gilbert A, Shah AJ, Wahid F, Marius M, Yameen MA, et al. Curative effects of *Distemonanthus benthamianus* baillon. Trunk-bark extracts on enteropathogenic *Escherichia coli* 31-induced diarrhea in rats. J Complement Integr Med. 2019; 16(4) doi:10.1515/jcim-2018-0202

142. Matah Marte VM, Ateufack G, Mbiantcha M, Atsamo AD, Adjouzem CF, Djuichou Nguemnang SF, et al. Methanolic extract of *Distemonanthus benthamianus* (caesalpiniaceae) stem bark suppresses ethanol/indomethacin-induced chronic gastric injury in rats. Gastroenterol Res Pract. 2020; 2020:8180323. doi:10.1155/2020/8180323

143. Yousseu Nana W, Ateufack G, Mbiantcha M, Khan S, Majid Rasheed H, Atsamo A, et al. Antidiarrheal potential of *Distemonanthus benthamianus* baillon. Extracts via inhibiting voltage-dependent calcium channels and cholinergic receptors. Asian Pac J Trop Biomed. 2019; 9(11):449-55. doi:10.4103/2221-1691.270977

144. National Center for Biotechnology Information. Pubchem compound 2d-structure for cid 370, gallic acid. 2022.

145. Weyepe Lah FC, Balemaken Missi M, October N, Betote Didoue PH, Nalova Ikome NH, Abdou JP, et al. Antibacterial and antioxidant activities of the extract and some flavonoids from aerial parts of *Echinops gracilis* o. Hoffm. (asteraceae). Nat Prod Commun. 2021; 16(3):1934578X21999151. doi:10.1177/1934578X21999151

146. Bitew H, Hymete A. The genus echinops: Phytochemistry and biological activities: A review. Front Pharmacol. 2019; 10 doi:10.3389/fphar.2019.01234

147. Weyepe Lah FC, Balemaken Missi M, October N, Betote Didoue PH, Nalova Ikome NH, Abdou JP, et al. Antibacterial and antioxidant activities of the extract and some flavonoids from aerial parts of *Echinops gracilis* o. Hoffm. (asteraceae). Natural Product Communications: SAGE Publications Inc; 2021. p. 1934578X21999151.

148. Mbing JN, Missi MB, Ndongo JT, Bayiha ba Njock G, Atchade Ade T, Pegnyemb DE, et al. New flavonoids c-glycosides from *Rhabdophyllum arnoldianum*. Nat Prod Res. 2014; 28(8):539-44. doi:10.1080/14786419.2014.883393

149. Mbing JN, Missi MB, Ndongo JT, Bayiha ba Njock G, Atchade Ade T, Pegnyemb DE, et al. New flavonoids c-glycosides from *Rhabdophyllum arnoldianum*. Nat Prod Res. 2014/02/20 ed2014. p. 539-44.

150. Nakshatri H, Pater MM, Pater A. Ubiquitous and cell-type-specific protein interactions with human papillomavirus type 16 and type 18 enhancers. Virology. 1990; 178(1):92-103. doi:10.1016/0042-6822(90)90382-2

151. Spence RP, Murray A, Banks L, Kelland LR, Crawford L. Analysis of human papillomavirus sequences in cell lines recently derived from cervical cancers. Cancer Res. 1988; 48(2):324.

152. Choo CK, Rorke EA, Eckert RL. Differentiation-independent constitutive expression of the human papillomavirus type 16 E6 and E7 oncogenes in the caski cervical tumour cell line. J Gen Virol. 1994; 75 (Pt 5):1139-47. doi:10.1099/0022-1317-75-5-1139

153. Pattillo RA, Hussa RO, Story MT, Ruckert ACF, Shalaby MR, Mattingly RF. Tumor antigen and human chorionic gonadotropin in CaSki cells: A new epidermoid cervical cancer cell line. Science. 1977; 196(4297):1456-8.

154. Kutwin M, Sawosz E, Jaworski S, Wierzbicki M, Strojny B, Grodzik M, et al. Nanocomplexes of graphene oxide and platinum nanoparticles against colorectal cancer COLO205, HT-29, HTC-116, SW480, liver cancer HepG2, human breast cancer MCF-7, and adenocarcinoma LNCaP and human cervical HeLa B cell lines. Materials. 2019; 12(6):17. doi:10.3390/ma12060909

155. Bowey-Dellinger K, Dixon L, Ackerman K, Vigueira C, Suh YK, Lyda T, et al. Introducing mammalian cell culture and cell viability techniques in the undergraduate biology laboratory. J Microbiol Biol Educ. 2017; 18(2):18.2.38. doi:10.1128/jmbe.v18i2.1264

156. Strober W. Trypan blue exclusion test of cell viability. Curr Protoc Immunol. 2001; Appendix 3:Appendix 3B. doi:10.1002/0471142735.ima03bs21

157. October N, Missi M. Bioactive phenolic and terpenoid compounds as antimicrobial, antioxidant and anticancer agents [Unpublished]. Department of Chemistry, University of Pretoria: Pretoria; 2020.

158. Sowmya PR, Arathi BP, Vijay K, Baskaran V, Lakshminarayana R. Role of different vehicles in carotenoids delivery and their influence on cell viability, cell cycle progression, and induction of apoptosis in HeLa cells. Mol Cell Biochem. 2015; 406(1-2):245-53. doi:10.1007/s11010-015-2442-y

159. Wall ME, Wani MC, Cook CE, Palmer KH, McPhail AT, Sim GA. Plant antitumor agents. I. The isolation and structure of camptothecin, a novel alkaloidal leukemia and tumor inhibitor from *Camptotheca acuminata* 1,2. J Am Chem Soc. 1966; 88(16):3888-90. doi:10.1021/ja00968a057

160. Khaiwa N, Maarouf NR, Darwish MH, Alhamad DWM, Sebastian A, Hamad M, et al. Camptothecin's journey from discovery to who essential medicine: Fifty years of promise. Eur J Med Chem. 2021; 223:113639. doi:10.1016/j.ejmech.2021.113639

161. Martino E, Della Volpe S, Terribile E, Benetti E, Sakaj M, Centamore A, et al. The long story of camptothecin: From traditional medicine to drugs. Bioorg Med Chem Lett. 2017; 27(4):701-7. doi:https://doi.org/10.1016/j.bmcl.2016.12.085

162. Hsiang YH, Hertzberg R, Hecht S, Liu LF. Camptothecin induces protein-linked DNA breaks via mammalian DNA topoisomerase i. J Biol Chem. 1985; 260(27):14873-8. doi:https://doi.org/10.1016/S0021-9258(17)38654-4

163. Goedecke W. Topoisomerases. In: Enna SJ, Bylund DB, editors. Xpharm: The comprehensive pharmacology reference. New York: Elsevier; 2007. p. 1-2.

164. Mosmann T. Rapid colorimetric assay for cellular growth and survival: Application to proliferation and cytotoxicity assays. J Immunol Methods. 1983; 65(1):55-63. doi:https://doi.org/10.1016/0022-1759(83)90303-4

165. Berridge MV, Herst PM, Tan AS. Tetrazolium dyes as tools in cell biology: New insights into their cellular reduction. Biotechnol annu rev: Elsevier; 2005. p. 127-52.

166. Larsson P, Engqvist H, Biermann J, Werner Rönnerman E, Forssell-Aronsson E, Kovács A, et al. Optimization of cell viability assays to improve replicability and reproducibility of cancer drug sensitivity screens. Sci Rep. 2020; 10(1):5798. doi:10.1038/s41598-020-62848-5

167. Boik J. Natural compounds in cancer therapy. First edition ed. Minnesota, USA: Oregon Medical Press, LLC; 2001.

168. Tugba Artun F, Karagoz A, Ozcan G, Melikoglu G, Anil S, Kultur S, et al. *In vitro* anticancer and cytotoxic activities of some plant extracts on HeLa and Vero cell lines. J BUON. 2016; 21(3):720-5.

169. Türker Şener L, Albeniz G, Dinç B, Albeniz I. ICELLigence real-time cell analysis system for examining the cytotoxicity of drugs to cancer cell lines. Exp Ther Med. 2017; 14(3):1866-70. doi:10.3892/etm.2017.4781

170. Adan A, Alizada Gn, Kiraz Ym, Baran Y, Nalbant A. Flow cytometry: Basic principles and applications. Crit Rev Biotechnol. 2017; 37(2):163-76. doi:10.3109/07388551.2015.1128876

171. Visagie M, Jaiswal S, Joubert A. In vitro assessment of a computer-designed potential anticancer agent in cervical cancer cells. Biol Res. 2016; 49(1):1-13. doi:10.1186/s40659-016-0104-5

172. Xie P, Cecchi L, Bellumori M, Balli D, Giovannelli L, Huang L, et al. Phenolic compounds and triterpenes in different olive tissues and olive oil by-products, and cytotoxicity on human colorectal cancer cells: The case of frantoio, moraiolo and leccino cultivars (*Olea europaea* l.). Foods. 2021; 10(11) doi:10.3390/foods10112823

173. Zuco V, Supino R, Righetti SC, Cleris L, Marchesi E, Gambacorti-Passerini C, et al. Selective cytotoxicity of betulinic acid on tumor cell lines, but not on normal cells. Cancer Lett. 2002; 175(1):17-25. doi:10.1016/s0304-3835(01)00718-2

174. Ghosh S, Mukhopadhyay S, Sarkar M, Mandal A, Das V, Kumar A, et al. Biological evaluation of a halogenated triterpenoid, 2α-bromo-dihydrobelulonic acid as inhibitor of human topoisomerase iiα and hela cell proliferation. Chem Biol Interact. 2017; 268:68-76. doi:10.1016/j.cbi.2017.02.015

175. Jafri L, Saleem S, Kondrytuk TP, Haq I-u, Ullah N, Pezzuto JM, et al. Hedera nepalensis k. Koch: A novel source of natural cancer chemopreventive and anticancerous compounds. Phytother Res. 2016; 30(3):447-53. doi:https://doi.org/10.1002/ptr.5546

176. Ozer O, Sarikahya NB, Nalbantsoy A, Kirmizigul S. Increased cytotoxic potential of infrequent triterpenoid saponins of *Cephalaria taurica* obtained through alkaline hydrolysis. Phytochemistry. 2018; 152:29-35. doi:10.1016/j.phytochem.2018.04.015

177. Xu Q-N, Zhu D, Wang G-H, Lin T, Sun C-L, Ding R, et al. Phenolic glycosides and flavonoids with antioxidant and anticancer activities from *Desmodium caudatum*. Nat Prod Res. 2021; 35(22):4534-41. doi:10.1080/14786419.2020.1739044

178. Huang X-B, Yuan L-W, Shao J, Yang Y, Liu Y, Lu J-J, et al. Cytotoxic effects of flavonoids from root of *Sophora flavescens* in cancer cells. Nat Prod Res. 2021; 35(22):4317-22. doi:10.1080/14786419.2020.1712382

179. Luo L, Zhu S, Tong Y, Peng S. Ferulic acid induces apoptosis of HeLa and CaSki cervical carcinoma cells by down-regulating the phosphatidylinositol 3-kinase (PI3K)/AKT signaling pathway. Med Sci Monit. 2020; 26:e920095. doi:10.12659/msm.920095

180. Daduang J, Palasap A, Daduang S, Boonsiri P, Suwannalert P, Limpaiboon T. Gallic acid enhancement of gold nanoparticle anticancer activity in cervical cancer cells. Asian Pac J Cancer Prev. 2015; 16(1):169-74. doi:10.7314/apjcp.2015.16.1.169

181. Van de Waterbeemd H. 5.28 - *In silico* Models to Predict Oral Absorption. In: Taylor JB, Triggle DJ, editors. Comprehensive Medicinal Chemistry II. Oxford: Elsevier; 2007. p. 669-97.

182. Khan T, Dixit S, Ahmad R, Raza S, Azad I, Joshi S, et al. Molecular docking, pass analysis, bioactivity score prediction, synthesis, characterization and biological activity evaluation of a functionalized 2-butanone thiosemicarbazone ligand and its complexes. J Biol Chem. 2017; 10(3):91-104. doi:10.1007/s12154-017-0167-y

183. Husain A, Ahmad A, Khan SA, Asif M, Bhutani R, Al-Abbasi FA. Synthesis, molecular properties, toxicity and biological evaluation of some new substituted imidazolidine derivatives in search of potent anti-inflammatory agents. Saudi Pharm J. 2016; 24(1):104-14. doi:10.1016/j.jsps.2015.02.008

184. Palasap A, Limpaiboon T, Boonsiri P, Thapphasaraphong S, Daduang S, Suwannalert P, et al. Cytotoxic effects of phytophenolics from *Caesalpinia mimosoides* lamk on cervical carcinoma cell lines through an apoptotic pathway. Asian Pac J Cancer Prev. 2014; 15(1):449-54. doi:10.7314/apjcp.2014.15.1.449

185. Wang SR, Fang WS. Pentacyclic triterpenoids and their saponins with apoptosis-inducing activity. Curr Top Med Chem. 2009; 9(16):1581-96. doi:10.2174/156802609789909821

186. Trute A, Gross J, Mutschler E, Nahrstedt A. *In vitro* antispasmodic compounds of the dry extract obtained from *Hedera helix*. Planta Med. 1997; 63(2):125-9. doi:10.1055/s-2006-957627

187. Xu T, Pang Q, Zhou D, Zhang A, Luo S, Wang Y, et al. Proteomic investigation into betulinic acid-induced apoptosis of human cervical cancer HeLa cells. PLoS One. 2014; 9(8):e105768. doi:10.1371/journal.pone.0105768

188. Baust JM, Snyder KK, Van Buskirk RG, Baust JG. Assessment of the impact of post-thaw stress pathway modulation on cell recovery following cryopreservation in a hematopoietic progenitor cell model. Cells. 2022; 11(2):278. doi:10.3390/cells11020278

189. Choy YB, Prausnitz MR. The rule of five for non-oral routes of drug delivery: Ophthalmic, inhalation and transdermal. Pharm Res. 2011; 28(5):943-8. doi:10.1007/s11095-010-0292-6

190. Abdel-Mageed WM, El-Gamal AA, Al-Massarani SM, Basudan OA, Badria FA, Abdel-Kader MS, et al. Sterols and triterpenes from *Dobera glabra* growing in Saudi Arabia and their cytotoxic activity. Plants (Basel). 2021; 10(1) doi:10.3390/plants10010119

191. Pal D, Sur S, Roy R, Mandal S, Kumar Panda C. Epigallocatechin gallate in combination with eugenol or amarogentin shows synergistic chemotherapeutic potential in cervical cancer cell line. J Cell Physiol. 2018; 234(1):825-36. doi:10.1002/jcp.26900

192. Eum DY, Byun JY, Yoon CH, Seo WD, Park KH, Lee JH, et al. Triterpenoid pristimerin synergizes with taxol to induce cervical cancer cell death through reactive oxygen species-mediated mitochondrial dysfunction. Anticancer Drugs. 2011; 22(8):763-73. doi:10.1097/CAD.0b013e328347181a

193. Chung SH, Lambert PF. Prevention and treatment of cervical cancer in mice using estrogen receptor antagonists. Proc Natl Acad Sci U S A. 2009; 106(46):19467-72. doi:10.1073/pnas.0911436106

194. Chung S-H, Franceschi S, Lambert PF. Estrogen and eralpha: Culprits in cervical cancer? Trends Endocrinol Metab. 2010; 21(8):504-11. doi:10.1016/j.tem.2010.03.005

195. Huang X, Wang B, Chen R, Zhong S, Gao F, Zhang Y, et al. The nuclear farnesoid x receptor reduces p53 ubiquitination and inhibits cervical cancer cell proliferation. Front Cell Dev Biol. 2021; 9:583146-. doi:10.3389/fcell.2021.583146

196. Chung S-H, Wiedmeyer K, Shai A, Korach KS, Lambert PF. Requirement for estrogen receptor alpha in a mouse model for human papillomavirus-associated cervical cancer. Cancer Res. 2008; 68(23):9928-34. doi:10.1158/0008-5472.CAN-08-2051

197. André F, Ciruelos EM, Juric D, Loibl S, Campone M, Mayer IA, et al. Alpelisib plus fulvestrant for PIK3CA-mutated, hormone receptor-positive, human epidermal growth factor receptor-2-negative advanced breast cancer: Final overall survival results from SOLAR-1. Ann Oncol. 2021; 32(2):208-17. doi:10.1016/j.annonc.2020.11.011

198. Narayan P, Prowell TM, Gao JJ, Fernandes LL, Li E, Jiang X, et al. Fda approval summary: Alpelisib plus fulvestrant for patients with HR-positive, HER2-negative, PIK3CA-mutated, advanced or metastatic breast cancer. Clin Cancer Res. 2021; 27(7):1842-9. doi:10.1158/1078-0432.Ccr-20-3652

199. Serrano D, Lazzeroni M, Gandini S, Macis D, Johansson H, Gjerde J, et al. A randomized phase II presurgical trial of weekly low-dose tamoxifen versus raloxifene versus placebo in premenopausal women with estrogen receptor-positive breast cancer. Breast Cancer Res. 2013; 15(3):R47. doi:10.1186/bcr3439

200. Usha T, Middha SK, Shanmugarajan D, Babu D, Goyal AK, Yusufoglu HS, et al. Gas chromatography-mass spectrometry metabolic profiling, molecular simulation and dynamics of diverse phytochemicals of *Punica granatum* l. Leaves against estrogen receptor. Front Biosci (Landmark Ed). 2021; 26(9):423-41. doi:10.52586/4957

201. Laskar YB, Mazumder PB, Talukdar AD. *Hibiscus sabdariffa* anthocyanins are potential modulators of estrogen receptor alpha activity with favourable toxicology: A computational analysis using molecular docking, ADME/Tox prediction, 2D/3D QSAR and molecular dynamics simulation. J Biomol Struct Dyn. 2021:1-23. doi:10.1080/07391102.2021.2009914

202. Imesch P, Samartzis EP, Dedes KJ, Fink D, Fedier A. Histone deacetylase inhibitors down-regulate G-protein-coupled estrogen receptor and the GPER-antagonist G-15 inhibits proliferation in endometriotic cells. Fertil Steril. 2013; 100(3):770-6. doi:10.1016/j.fertnstert.2013.05.008

203. Kang N, Cao S-J, Zhou Y, He H, Tashiro S-I, Onodera S, et al. Inhibition of caspase-9 by oridonin, a diterpenoid isolated from *Rabdosia rubescens*, augments apoptosis in human laryngeal cancer cells. Int J Oncol. 2015; 47(6):2045-56. doi:10.3892/ijo.2015.3186

204. Moskot M, Jakóbkiewicz-Banecka J, Kloska A, Piotrowska E, Narajczyk M, Gabig-Cimińska M. The role of dimethyl sulfoxide (DMSO) in gene expression modulation and glycosaminoglycan metabolism in lysosomal storage disorders on an example of mucopolysaccharidosis. Int J Mol Sci. 2019; 20(2) doi:10.3390/ijms20020304

205. Ahmad R, Fatima A, Srivastava AN, Khan MA. Evaluation of apoptotic activity of withania coagulans methanolic extract against human breast cancer and Vero cell lines. J Ayurveda Integr Med. 2017; 8(3):177-83. doi:10.1016/j.jaim.2017.01.001

206. Wang C-C, Lin S-Y, Lai Y-H, Liu Y-J, Hsu Y-L, Chen JJW. Dimethyl sulfoxide promotes the multiple functions of the tumor suppressor HIJ1 through activator protein-1 activation in NSCLC cells. PLoS One. 2012; 7(4):e33772. doi:10.1371/journal.pone.0033772

207. Omtvedt LA, Kristiansen KA, Strand WI, Aachmann FL, Strand BL, Zaytseva-Zotova DS. Alginate hydrogels functionalized with β-cyclodextrin as a local paclitaxel delivery system. J Biomed Mater Res A. 2021; 109(12):2625-39. doi:10.1002/jbm.a.37255

208. Abasalizadeh F, Moghaddam SV, Alizadeh E, Akbari E, Kashani E, Fazljou SMB, et al. Alginate-based hydrogels as drug delivery vehicles in cancer treatment and their applications in wound dressing and 3D bioprinting. J Biol Eng. 2020; 14:8. doi:10.1186/s13036-020-0227-7

209. Fan Y, Marioli M, Zhang K. Analytical characterization of liposomes and other lipid nanoparticles for drug delivery. J Pharm Biomed Anal. 2021; 192:113642. doi:10.1016/j.jpba.2020.113642

210. Kwan HY, Xu QH, Gong RH, Bian ZX, Chu CC. Targeted chinese medicine delivery by a new family of biodegradable pseudo-protein nanoparticles for treating triple-negative breast cancer: *In vitro* and *in vivo* study. Front Oncol. 2021; 10 doi:10.3389/fonc.2020.600298

211. van Tonder A, Joubert AM, Cromarty AD. Limitations of the 3-(4,5-dimethylthiazol-2-yl)-2,5-diphenyl-2h-tetrazolium bromide (MTT) assay when compared to three commonly used cell enumeration assays. BMC Res Notes. 2015; 8:47. doi:10.1186/s13104-015-1000-8